University of Kentucky
UKnowledge

Theses and Dissertations--Physiology | Physiology

2019

PATHOLOGICAL TAU AS A CAUSE, AND CONSEQUENCE, OF CELLULAR DYSFUNCTION

Shelby Meier
University of Kentucky, shelby.meier@uky.edu
Author ORCID Identifier:
https://orcid.org/0000-0003-1946-9004
Digital Object Identifier: https://doi.org/10.13023/etd.2019.368

Right click to open a feedback form in a new tab to let us know how this document benefits you.

Recommended Citation
Meier, Shelby, "PATHOLOGICAL TAU AS A CAUSE, AND CONSEQUENCE, OF CELLULAR DYSFUNCTION" (2019). *Theses and Dissertations--Physiology*. 44.
https://uknowledge.uky.edu/physiology_etds/44

This Doctoral Dissertation is brought to you for free and open access by the Physiology at UKnowledge. It has been accepted for inclusion in Theses and Dissertations--Physiology by an authorized administrator of UKnowledge. For more information, please contact UKnowledge@lsv.uky.edu.

STUDENT AGREEMENT:

I represent that my thesis or dissertation and abstract are my original work. Proper attribution has been given to all outside sources. I understand that I am solely responsible for obtaining any needed copyright permissions. I have obtained needed written permission statement(s) from the owner(s) of each third-party copyrighted matter to be included in my work, allowing electronic distribution (if such use is not permitted by the fair use doctrine) which will be submitted to UKnowledge as Additional File.

I hereby grant to The University of Kentucky and its agents the irrevocable, non-exclusive, and royalty-free license to archive and make accessible my work in whole or in part in all forms of media, now or hereafter known. I agree that the document mentioned above may be made available immediately for worldwide access unless an embargo applies.

I retain all other ownership rights to the copyright of my work. I also retain the right to use in future works (such as articles or books) all or part of my work. I understand that I am free to register the copyright to my work.

REVIEW, APPROVAL AND ACCEPTANCE

The document mentioned above has been reviewed and accepted by the student's advisor, on behalf of the advisory committee, and by the Director of Graduate Studies (DGS), on behalf of the program; we verify that this is the final, approved version of the student's thesis including all changes required by the advisory committee. The undersigned agree to abide by the statements above.

Shelby Meier, Student

Dr. Jose F. Abisambra, Major Professor

Dr. Kenneth S. Campbell, Director of Graduate Studies

PATHOLOGICAL TAU AS A CAUSE, AND CONSEQUENCE, OF CELLULAR DYSFUNCTION

DISSERTATION

A dissertation submitted in partial fulfillment of the
requirements for the degree of Doctor of Philosophy in the
College of Medicine
at the University of Kentucky

By

Shelby Elizabeth Meier

Lexington, Kentucky

Co- Directors: Dr. Jose F. Abisambra, Associate Professor of Physiology

and Dr. Kathryn E. Saatman, Professor of Physiology

Lexington, Kentucky

2019

Copyright © Shelby Elizabeth Meier 2019
https://orcid.org/0000-0003-1946-9004

ABSTRACT OF DISSERTATION

PATHOLOGICAL TAU AS A CAUSE, AND CONSEQUENCE, OF CELLULAR DYSFUNCTION

Tauopathies are a group of neurodegenerative diseases characterized by the abnormal deposition of the protein tau, a microtubule stabilizing protein. Under normal physiological conditions tau is a highly soluble protein that is not prone to aggregation. In disease states alterations to tau lead to enhanced fibril formation and aggregation, eventually forming neurofibrillary tangles (NFTs). The exact cause for NFT deposition is unknown, but increased post-translational modifications and mutations to the tau gene can increase tangle formation.

Tauopathic brains are stuck in a detrimental cycle, with cellular dysfunction contributing to the development of tau pathology and the development of tau pathology contributing to cellular dysfunction. The exact mechanisms by which each part of the cycle contributes to the other are still being explored. To investigate the unique contributions of each part of this cycle we utilized two separate models of tauopathy: one chronic and one acute. Overall this project provides novel insight into the role of pathological tau as both a cause, and a consequence, of cellular dysfunction.

To understand how development of tau pathology contributes to cellular dysfunction we studied chronic disease models. Using human brain tissue we found that under normal conditions tau associates with ribosomes but that this interaction is enhanced in Alzheimer's disease brains. We then used *in vitro* and *in vivo* models of tauopathy to show that this association causes a decrease in protein synthesis. Finally, we show that wild type tau and mutant tau reduce protein translation to similar levels.

To understand how general cellular dysfunction contributes to development of pathology we used an acute model of tauopathy through traumatic brain injury (TBI). We injured rTg4510 tau transgenic mice at different ages to investigate the effect of TBI on tau fibrillization (2 month old) and the effect of TBI on tau already in NFTs (4.5 month old). In 2 month old mice, we found that tau hyperphosphorylation was decreased at 24 hours and increased at 7 days post injury, and that tau oligomerization was decreased at 24 hours post injury. We also found that tau fibrillization was not increased after 24 hours or 7 days post injury. In 4.5 month old mice, we found that TBI did not increase or

decrease tangle counts in the brain, but we did qualitatively observe decreased variability within groups.

Overall these studies contribute novel understanding of tau's role in different disease states. We identified a functional consequence of the interaction between tau and ribosomes, and demonstrated that a single head impact did not increase tau fibril formation within 7 days of injury. While human diseases associated with TBI show neurofibrillary tangle deposition, we have yet to recreate that aspect of the disease in research models of TBI. Our findings support the need for further investigation into the nuances of tau in disease, especially following TBI.

KEYWORDS: tau, protein translation, Alzheimer's disease, traumatic brain injury, neurofibrillary tangles, chronic traumatic encephalopathy

Shelby Elizabeth Meier

(Name of Student)

08/28/2019

Date

PATHOLOGICAL TAU AS A CAUSE, AND CONSEQUENCE, OF CELLULAR DYSFUNCTION

By

Shelby Elizabeth Meier

Jose F. Abisambra, Ph.D.
Co-Director of Dissertation

Kathryn E. Saatman, Ph.D.
Co-Director of Dissertation

Kenneth S. Campbell, Ph.D.
Director of Graduate Studies

08/28/2019
Date

ACKNOWLEDGMENTS

While it is true that this dissertation is considered an individual work, I would be remiss not to acknowledge all the help and support I've received during my time as a student.

First and foremost thank you to my co-Directors, Joe Abisambra and Kathy Saatman. I've been incredibly fortunate to train in both your labs and learn lessons outside the scope of the bench. Thank you for your guidance and wisdom over the past 4 years.

To my advisory committee, thank you for your time and patience over the past 3 years. We've been through many obstacles together, but I wouldn't be where I am today without your guidance. I'll always be grateful that I had a committee that saw my potential and refused to settle for anything less than outstanding.

To the plethora of lab members I've had the absolute honor of working with (Maria, Abe, Max, Matt, Danielle, Alex, Chelsey, Kennedy, Elizabeth, Bhavik, Jennifer, Sarah, Emily, Grant, Blaine, Dealla, Cassidy, Shon, Emad, Chiara, JP, Ryan, Binoy, Anthony, Brad, Nashwa, Lei), let me start by saying thank you. I have learned something from every single interaction we've had, and for that I'm eternally grateful. Thank you all for your guidance, patience, and friendship!

To my family, thank you for supporting me throughout my education. From my first day of kindergarten until today, you've all encouraged me to never settle for anything less than my absolute best. Thank you for listening patiently to my frustrations over the past 8 years of higher and always having my best interests at heart. I love you all!

To Grant, I know you know how thankful I am for you but I'm just going to keep saying it anyway. Thank you for being my rock and for always telling me what I need to hear (whether I like it or not). I love you!

I got lucky in having two academic families: the department of Physiology (PGY) and Sanders-Brown Center on Aging (SBCOA). Thank you to everyone in PGY that has shared in a laugh or offered support throughout the past 4 years (plus a special thank you to Andrew and Tanya for Moe's and planning the best holiday parties in Lexington). To Sanders-Brown Center on Aging, thank you for the unwavering support and kindness. I'm incredibly grateful for the opportunity to have worked alongside all of you.

To my fellow graduate students, thank you all for being the absolute best sounding boards, therapists, lunch partners, drinking buddies, friends, and just all around great people. Ryan, I don't know how I would have survived the past four years without all the memes and pitch-black humor. Also, thanks for forgiving me for always forgetting to invite you to lunch. Laura and Brooke, you two are absolute rays of joy and sunshine. Thank you for always putting a smile on my face! Michael, you've been number one in my book since the very beginning. Thank you (and Molly) for being the friend(s) that became family.

To Sarah Cornett (aka BAE #1) thank you for being the most incredible role model and friend I could ask for. You always take the time to listen and encourage me, despite the fact that talking about science makes you want to claw your eyes out.

To every single person that I didn't mention here but that has encouraged me, made me smile, offered advice, and supported me over the past four years THANK YOU!

TABLE OF CONTENTS

ACKNOWLEDGMENTS ..... **iii**

LIST OF TABLES ..... **vii**

LIST OF FIGURES ..... **viii**

CHAPTER 1. INTRODUCTION **1**

1.1 Overview of tau *1*
1.1.1 Normal physiological role 2
1.1.2 Tau in disease 2
1.1.3 Aggregation 4
1.1.4 Post-translational modifications 7
1.1.5 Mutations 8

1.2 Cellular dysfunction caused by pre-tangle and tangle pathology *9*

1.3 Tau pathology observed after traumatic brain injury (TBI) *11*
1.3.1 Human disease 11
1.3.2 Tau pathology in animal models of TBI 13
1.3.3 TBI as a tool for studying contributions of cellular dysfunction to development of tau pathology 16

1.4 Controlled cortical impact (CC) model of injury *17*

1.5 rTg4510 mouse model of tauopathy *18*

CHAPTER 2. PATHOLOGICAL TAU PROMOTES NEURONAL DAMAGE BY IMPAIRING RIBOSOMAL FUNCTION AND DECREASING PROTEIN SYNTHESIS **24**

2.1 Preface *24*

2.2 Introduction *26*

2.3 Methods *27*

2.4 Results *39*
2.4.1 Tau associates more robustly with ribosomal proteins in AD brains 39
2.4.2 Reduction in protein synthesis is due to impaired translation and not impaired transcription 40
2.4.3 Tau reduces translation *in vitro* and *in vivo* 41
2.4.4 Mutant tau and wild-type tau reduce protein synthesis at similar levels 42

2.5 Discussion *43*

CHAPTER 3. DIFFERENTIAL EFFECTS OF TBI ON PRE-TANGLE AND TANGLE TAU PATHOLOGY **51**

3.1 Introduction *51*

3.2 Materials and Methods *53*

3.3 Results *63*

3.3.1 Prior to overt tangle formation CCI alters tau phosphorylation at 24 hours and 7 days post-injury, but only alters oligomerization at 24 hours post-injury. 65
3.3.2 Prior to overt tangle formation, CCI does not increase tau fibrillization at 24 hours or 7 days post-injury 65
3.3.3 At 4.5 months of age, and with mature tangle deposition, CCI does not significantly increase or decrease tangle counts at 24 hours or 7 days post-injury but it does reduce variability. 67

3.4 Discussion *68*

CHAPTER 4. DISCUSSION **85**

4.1 Summary *85*

4.2 Overall analysis of findings *86*

4.3 Limitations of these studies *88*

4.4 Impact of these data on the field(s) *92*

4.5 Future directions *94*

REFERENCES **98**

VITA **122**

LIST OF TABLES

Table 1.1 Post-translational modifications of tau 21
Table 3.1 Summary of Western blot findings..... 76

LIST OF FIGURES

Figure 1.1 Splicing variants in human tau 20
Figure 1.2 Tau elongation and aggregation 23
Figure 2.1 Tau associates with ribosomes in the brain 47
Figure 2.2 Tau reduces translation of protein, not transcription of mRNA 48
Figure 2.3 Tau reduces translation in vitro and in vivo 49
Figure 2.4 Wild-type and mutant tau reduce translation at similar levels 50
Figure 3.1 Experimental design for data presented in Chapter 3 75
Figure 3.2 Prior to overt tangle formation CCI alters tau phosphorylation at both 24 hours and 7 days post-injury, but only alters oligomerization at 24 hours post-injury 77
Figure 3.3 Prior to overt tangle formation, CCI does not increase tau fibrillization at 24 hours or 7 days post-injury 78
Figure 3.4 Effects of TBI on TBS-soluble and sarkosyl-soluble fractions 79
Figure 3.5 Sectioning and tissue selection for staining and quantification of neurofibrillary tangles by FSB 80
Figure 3.6 At 4.5 months of age, and with mature tangle deposition, CCI does not significantly increase or decrease tangle counts at 24 hours and 7 days post-injury but it does reduce variability observed. 81
Figure 3.7 Comparison of male and female tangle counts in sham and injured mice. 83
Figure 3.8 Fluorojade C staining shows cell death did not affect tangle counts performed. 84
Figure 4.1 Summary of findings presented in this dissertation 97

CHAPTER 1. INTRODUCTION

1.1 Overview of tau

The microtubule associated protein tau (*MAPT)* is primarily characterized as a microtubule stabilizing protein [1]. The *MAPT* gene encoding tau contains 16 exons. Exon 0 contains the promoter region of the gene, which is transcribed in mRNA but is not translated into protein. Exon 1 contains the start codon for protein translation. Exons 2 and 3 comprise the amino terminal inserts and are part of the projection domain [2, 3]. Exons 4a, 6, and 8 are only transcribed and translated in peripheral tissue [4]. Exons 9, 10, 11, and 12 contain the carboxy-terminal repeat domains that function as the microtubule binding domains (reviewed in [4]). Exons 1, 4, 5, 6 9, 11, 12, and 13 are constitutively expressed while exons 2, 3, and 10 undergo alternative splicing events. Because of these alternative splicing events there are a total of six tau isoforms expressed in the adult human brain [5]. Alternatively spliced tau isoforms contain either zero, one, or two amino-terminal inserts (0N, 1N, and 2N, respectively) from exons two and three, and either three or four microtubule binding repeat domains (3R and 4R, respectively; see figure 1.1). In the healthy adult human brain 3R and 4R tau are expressed at a relatively equal ratio [6]. Tau is a hydrophilic and intrinsically disordered protein [7] that undergoes local conformational changes when interacting with other proteins [8, 9]. Tau also has an affinity towards a global conformational change of a paperclip-like shape where the amino-terminus, carboxy-terminus, and microtubule binding domains are in close proximity [10].

1.1.1 Normal physiological role

The primary role of tau as a microtubule stabilizing protein is thoroughly characterized. Other roles of tau in normal physiological conditions are still under investigation, but we currently know of a variety of other functions in which it is involved [11]. A phosphatase activating domain found in amino acid residues 2-18 is involved in inhibition of anterograde axonal transport [12]. The exact function of the amino terminus inserts (0N, 1N, 2N) are not completely understood but they do play a role in cellular distribution of tau [13, 14], the interaction of tau and the plasma membrane [15], and the interaction of tau with dynactin complex [16]. The exact function of the c-terminal region of tau is unknown. One study suggests it could play an influential role in post-translational modifications or protein interactions with other tau domains [17].

1.1.2 Tau in disease

: Tauopathies are a group of neurodegenerative diseases characterized by abnormal deposition of tau in the brain [18]. There are more than 20 known neurodegenerative diseases under this definition [19]. Tauopathies can be further differentiated into primary tauopathies, where tau is the most abundant pathological protein observed, or secondary tauopathies, where tau pathology coincides with other protein pathologies [20]. While the hallmark of tauopathies is fibrillar, insoluble, neurofibrillary tangles (NFTs), other characteristics (such as disruption of the 3R:4R ratio, mislocalization, aberrant post-translational modifications, and mutations) can also be observed [18]. It is unclear whether these observed characteristics are drivers of disease, consequences of disease, or both. Tau is also observed in astrocytes, microglia,

and oligodendrocytes of tauopathic brains [21-23]. Some examples of tauopathies are provided below for context.

Frontotemporal lobar degeneration associated with tau (FTLD-tau, previously termed frontotemporal dementia with parkinsonism linked to chromosome 17 or FTDP-17 [24]) is a term for tauopathies caused by heritable or sporadic mutations to the tau gene [24, 25]. This overarching classification is further separated into five main subtypes of Pick's disease (PiD), corticobasal degeneration (CBD), progressive supranuclear palsy (PSP), globular glial tauopathy (GGT), and argyrophilic grain disease/neurofibrillary tangle predominant dementia (AGD/NFTPD) which includes primary age-related tauopathy (PART). FTLD-tau diseases are primary tauopathies. Clinical presentations of FTLD-tau are broken down into two types [26]: behavioral variant FTD (bvFTD), which includes dementia and/or movement disorders [19], and primary progressive aphasia (PPA), which includes changes in language [26]. Macroscopic neuropathology changes observed include brain atrophy, albeit in different locations depending on specific subtype [18].

Alzheimer's disease (AD) is a neurodegenerative disease that affects an estimated 5.7 million Americans as of 2018 [27]. AD is a secondary tauopathy, as the two hallmarks of AD are amyloid beta plaques and NFTs [28]. Early clinical symptoms include difficulty with short term memory and apathy/depression, while later symptoms include severe memory loss, impaired communication, behavioral changes, and motor skill decline [27]. NFT deposition occurs in a predictable pattern that is described in six stages [28]. Stages I and II show NFT deposition in the entorhinal cortex, stages III and

IV in the limbic region, and stages V and VI in the neocortical regions [28]. AD brains also show extensive atrophy [29].

Chronic traumatic encephalopathy (CTE) is a neurodegenerative disease associated with repeat head traumas [30, 31]. CTE is classified as a primary tauopathy [32, 33]. There is some debate over this classification as other protein pathologies are also observed [34, 35]. Early clinical symptoms include headaches and loss of attention, while late clinical symptoms include cognitive impairment, memory loss, and aggression [36]. The primary neuropathological criterion for post-mortem diagnosis is phospho-tau positive perivascular NFT deposition that occurs at varying depths of the cortical layers [36]. However, CTE brains show other protein abnormalities as well (such as amyloid beta plaques and TDP-43 deposits [32, 37]). In late stages CTE brains show extensive brain atrophy, especially in the cerebrum, ventricles, and cavum septum pellucidum [37].

1.1.3 Aggregation

Under normal physiological conditions, tau is a highly soluble and natively unfolded protein [38]. However, for reasons that are still unclear tau can aggregate into pathological inclusions (paired helical filaments (PHFs) and neurofibrillary tangles (NFTs)) that are a hallmark of tauopathies. Aggregation of tau into PHFs begins with aggregation-competent monomeric tau [39]. This monomeric tau begins to dimerize [40] or oligomerize [41], which is then followed by the rate limiting step of nucleation. Elongation into PHFs occurs following nucleation [39-41] and can be accelerated with the help of anion cofactors such as RNA or heparin [42-46] (Figure 1.2). The formation of beta sheet structures is a major first part of tau aggregation [47-49]. Two hexapeptide

motifs (VQIINK and VQIVYK) are an essential part of forming the beta-sheet structures [39, 50, 51] and are found in the core of PHFs [52, 53]. In fact, when these motifs are disrupted tau is significantly less likely to aggregate [54].

Early data initially suggested that NFT formation was what made tau neurotoxic. Indeed, NFT count in the neocortex is the best correlate to cognitive decline in AD [28, 55-57] and tangle bearing neurons exhibit fewer synaptic connections on their soma [58]. Additionally synaptic signaling and cytoskeletal maintenance are reduced [59, 60], organelle size and placement is disrupted [61], and axonal transport is inhibited in tangle bearing neurons [62]. The presence of extracellular NFTs was also thought to indicate the toxicity of tau, as these extracellular "ghost" or "tombstone" tangles are found after cell death [63]. However, neuronal loss in disease exceeds NFT count [64] and in some brain regions neuronal death and NFT burden don't correlate [65, 66]. Currently the role of NFTs in neuronal toxicity is highly debated. There is an overwhelming wave of evidence showing that non-fibrillar tau species are toxic to cells (further expanded on in the next paragraph. Tthat leaves the field to debate whether NFTs have a toxic chokehold on cells or if tangle formation may actually be a protective way of sequestering toxic tau [67].

Beginning in the 2000's new evidence emerged that the toxicity of tau may not be limited to NFTs, but that non-filamentous (soluble) tau species could contribute to cellular dysfunction and neurodegeneration [68-77]. Additionally, soluble tau was identified as a propagator of tau pathology [78]. Non-filamentous tau can be actively secreted both *in vitro* [79-81] and *in vivo* [82, 83], and that extracellular tau takes on a toxic conformation [84]. The mechanisms of tau secretion are still under investigation,

but there is evidence for a variety of pathways. One mechanism of tau secretion occurs via exosomes and ectosomes [83, 85-87]. Another mechanism is based on formation of nanotubules between neurons to facilitate tau release [88]. Alternatively, other mediators of tau release such as co-chaperones/chaperones [89] and Rab GTPases [90, 91] have been proposed due to much of extracellular tau being membrane free [79, 92]. A recent study showed that tau can also freely translocate across cell membranes and seed aggregation *in vitro [81].* Current understanding of tau uptake by neighbor cells is based on a heparin sulphate proteoglycan (HSPG)-dependent mechanism in which HSPGs trigger the internalization process [93].

The solubility of tau in Sarkosyl, a strong detergent, is a common way to determine the filamentous state of tau. Sarkosyl insoluble tau is fibrillar and composes the NFTs, while Sarkosyl soluble tau is not yet fibrillar and not yet incorporated into NFTs [94]. The method of extracting Sarkosyl soluble and insoluble tau was first published in 1990 by Drs. Greenberg and Davies of Albert Einstein College of Medicine [94]. Using this method, they isolated and analyzed the biochemical properties (antibody reactivity, phosphorylation status, filament morphology, acidity of the proteins, molecular mass) of PHFs [94]. This technique was then standardized for human brain tissue in 1999 by Drs. Lee and Trojanowski [95]. Since the development of the transgenic mouse model for the use of studying disease, the method has been modified and standardized for extracting Sarkosyl soluble and insoluble tau from mouse brains as well [96-99].

1.1.4 Post-translational modifications

Tau undergoes 11 unique types of post-translational modifications (Table 1.1), with many occurring simultaneously (reviewed in [100]). Under normal physiological conditions, some of these post-translational modifications serve as regulatory mechanisms for tau function and degradation [101-103]. However, in tauopathies many of these post-translational modifications enhance tau pathology development. The best characterized of these modifications is phosphorylation.

Normal phosphorylation events at specific serines, threonines, and tyrosines reduce tau's affinity for microtubules, thereby regulating tau-microtubule binding interactions and allowing microtubule breakdown or stabilization as needed [101-103]. There are 85 potential sites for tau to be phosphorylated, of which 75 have been proven to be phosphorylated *in vitro* or *in vivo* [100]. We currently know of at least 41 kinases that can phosphorylate tau [104]. Dephosphorylation of tau occurs through 5 main phosphatases [105] with the key phosphatase being protein phosphatase 2a (PP2a) [106, 107]. In human adult brains, tau has an average of two phosphates per molecule under normal physiological conditions [4, 108]. In AD brains, tau becomes hyperphosphorylated with an estimated eight phosphates per molecule [101, 109-111]. A highly debated topic currently is the role of phosphorylation in tau aggregation. It is unclear as to whether phosphorylation enhances the propensity of tau to aggregate, as hyperphosphorylation precedes aggregation [112] but phosphorylation at specific sites actually protects against aggregation [113]. Two other types of post-translational modifications, glycosylation and prolyl-isomerization, reduce hyperphosphorylation and aggregation [114-122]. Additionally, hyperphosphorylation of tau occurs during

hibernation and anesthesia-induced hypothermia but does not result in tangle formation [123, 124]. As such, hyperphosphorylated tau alone should not be equated with aggregation or NFT formation.

1.1.5 Mutations

Mutations in the tau gene can be broadly categorized into two groups by their primary effects: changing pre-mRNA splicing of exon 10 or changing tau-protein interactions. Of the 107 experimentally studied tau mutants listed on AlzForum only 3 mutations affect both protein interactions and splicing events [125]. About half of the known tau mutations affect the alternative splicing events at exon 10 [126]. Changes to the splicing of exon 10 by these mutations cause a shift in the ratio of 3R to 4R tau. Typically these mutations increase the amount of 4R tau [127-137], although there is evidence that three mutations reduce 4R tau levels [130, 138]. The other half of known tau mutations primarily cause changes in tau-protein interactions. The majority of these mutations occur in the microtubule binding domain found in the C-terminal repeats and reduce the stabilization of microtubules [139, 140]. The one known exception is the missense mutation Q336R, which actually promotes microtubule assembly and enhances tau's function as a microtubule stabilizing protein [141]. Secondarily, missense mutations such as R5H [142], A152T [143, 144], I20V [145], N296del [146], P301L [127, 147-149], Q336H [150], Q336R [141], V337M [151, 152], S352L [153], P364S [154], and N410H [155] enhance tau aggregation and NFT formation. These mutations are also linked to increased risk for development of the neurodegenerative disorders termed FTLD-tau.

1.2 Cellular dysfunction caused by pre-tangle and tangle pathology

Neurofibrillary tangles are the strongest correlate to cognitive decline in AD [55-57]. However the toxicity of these mature tangles has been called into question in recent years [156]. Currently, it is believed that the major method by which NFTs contribute to cellular dysfunction is through physically impeding normal functions such as axonal transport [157]. Filamentous tau aggregates fill the cellular soma and recruit more tau to enlarge the tangle formation [158], which further impairs normal cellular function by sequestering functional protein in these aggregates. Additionally, NFT-bearing neurons show increased transcription of senescence-related RNA and irregular bioenergetics [159]. Senescence in the short term triggers anti-apoptotic intracellular mechanisms [160] (which supports the findings that NFT-bearing neurons survive [161]). However, chronically senescent cells take on the senescence-associated secretory phenotype which increases pro-inflammatory cytokines and may actually accelerate disease progression [162].

As previously discussed, pathological tau is not limited to aggregated tau found in NFTs. In-depth analysis of all cellular dysfunction caused by pre-tangle tau pathology is outside the scope for this dissertation; however references for other commonly studied types of tau-driven cellular dysfunction are given to provide perspective: synaptic dysfunction [69, 163-178], mitochondrial dysfunction [179-183], calcium dyshomeostasis [172, 184-186], impaired axonal transport: [187-195]. Of particular importance for this dissertation is the interaction of tau with critical components of protein translation including RNA, RNA-binding proteins, and ribosomes.

The interaction of tau with RNA was first reported in 1996 [42]. The negatively charged RNA interacts with the positively charged C-terminal repeat domains in tau and functions as a cofactor to enhance (but not initiate) PHF formation [42]. While 4R tau is naturally resistant to PHF formation due to disulfide bridge formation from the additional repeat domain [196], interaction with RNA allows fibrillization to occur in 4R as well as 3R tau [42, 197]. Additionally, this interaction with RNA allows tau to become part of a complex coacervate in which the coacervate is densely packed with tau but tau still remains soluble [198]. Extended time in this coacervate induces fibril formation [198]. RNA is also found sequestered within NFTs in human tauopathic brains [199, 200].

Tau also interacts with RNA-binding proteins [201, 202]. Of particular interest in recent years is the interaction of tau with T-cell antigen 1 (TIA1), a ribosomal binding protein associated with stress granule formation [203]. TIA1, as well as multiple other ribosomal binding proteins, associate with less condensed tau as observed through immunofluorescent imaging [202]. The association of tau with TIA1 in stress granules accelerates misfolding events, mislocalization, and enhances overall pathology development [175]. Additionally, TIA1 helps to regulate the cellular response to oligomeric forms of tau and enhances propagation of oligomeric tau [204].

Although tau interacts directly with ribosomes, the specific tau-ribosomal protein interactions are different in tauopathic and non-tauopathic brains [201, 202, 205, 206]. Additionally, ribosomal dysfunction is an early event in AD brains [205] but the cause for this dysfunction is unclear. The direct effect of tau's association with ribosomal proteins is also still unclear.

1.3 Tau pathology observed after traumatic brain injury (TBI)

The link between neurodegeneration and TBI has been researched since World War I [207]. Frequent bouts of explosive blasts left soldiers experiencing headache, amnesia, inability to concentrate, difficulty sleeping, depression, and suicidal thoughts [207]. Tau pathology is observed in human brain tissue after TBI [208, 209] and elevated tau levels in serum and cerebrospinal fluid after injury correlate with worsened outcomes [210, 211]. Utilizing both animal models of injury and human diseased brains, the role of TBI in development of tau pathology is slowly being uncovered.

1.3.1 Human disease

One of the first diseases linked to TBI was dementia pugilistica [31], now known as CTE [30, 31]. As previously stated, CTE is a primary tauopathy with the main microscopic neuropathological feature being phospho-tau positive NFTs [32, 33, 36]. Criteria for post-mortem diagnosis of CTE include perivascular phospho-tau immunoreactive NFTs in the neocortex, at the depths of cerebral sulci, and in the superficial layers of the crests of the cerebral cortex [32]. Phospho-tau positive astrocytic tangles are also observed in CTE in cortical sulci and occasionally near vessels [37]. The neuropathological staging of CTE is broken down into four levels [36]. Stage 1 is restricted to discrete foci in the cerebral cortex sulci typically around blood vessels [36]. Stage 2 shows multiple epicenters of pathology in the cortical sulci, but NFT deposition also spreads to the superficial layers of the adjacent cortex [36]. Stage 3 shows widespread NFT deposition, including in the entorhinal cortex and hippocampus [36]. Stage 4 shows pathology deposition throughout most of the cerebral cortex [36]. The specific phospho-tau antibodies used to show phospho-tau immunoreactive NFTs are

AT8 (serine 202/threonine 205) and CP-13 (only serine 202) [36]. In 2016, the National Institute on Neurological Disorders and Stroke and the National Institute on Biomedical Imaging and Bioengineering came to a consensus for the neuropathological diagnosis of CTE [32]. This consensus established CTE as a unique neurodegenerative disorder, separate from other tauopathies (especially Alzheimer's disease). Although CTE and AD show similar tau pathology on some levels (all six tau isoforms are present in both, 3R and 4R tau are present in both, both have NFTs), there are some obvious differences between them. For example, the distribution of tangle pathology is very different between AD and CTE. Early stages of AD show tau pathology in the entorhinal cortex [28] while early staging of CTE shows tau pathology in the frontal lobe [36]. Late stages also show differences in distribution (AD = uniform [28], CTE = irregular [36]) and location of pathology (CTE = brainstem and white matter show heavy NFT deposition [36], AD = brainstem and white matter show minimal NFT deposition [28]). Additionally, the pathological folding of tau filaments in CTE includes a hydrophobic cavity that is absent in AD tau filaments [212].

TBI has also been speculated to be a driver of Alzheimer's disease development, but the link between TBI and AD is still poorly understood. In 1985 the first study linking TBI as a risk factor for AD showed a significantly higher odds ratio of developing AD after TBI in instances of self-reported TBI with loss of consciousness [213]. Six years later, a meta-analysis of original data from 11 case-controlled studies by Mortimer *et al.* showed a significant association between head trauma and AD in self-reported TBIs with loss of consciousness in pooled data analyses [214]. When stratified to look at relative risk in males compared to females, they found that only males had an increased

relative risk of developing AD after TBI [214]. After that, multiple studies showed conflicting results on whether TBI increased the risk of developing AD [215-223], decreased time to onset of AD [224, 225], or had no effect on the risk of developing AD [226-231]. One particular study performed 12 years after Mortimer *et al.* sought to replicate those findings while expanding on the meta-analysis by performing a systemic review of all findings in the literature [221]. They partially replicated the findings that TBI increased risk of AD in males; however, in the analysis of studies published after the original Mortimer *et al.* the overall association between TBI and AD was not significantly increased [221]. Another systematic literature review of studies linking TBI to AD shows that the conflict may be driven by methodological differences and failure to have standardized reporting methods [232].

TBI has also been shown to increase the risk of developing FTLD [233-235], of which there are three neuropathological subtypes: FTLD-tau, FTLD-TDP (where TDP-43 is the major pathology observed) and FTLD-FUS (where FUS is the major pathology observed) [236]. As these studies looked at living patients clinical diagnoses of FTLD, they were unable to describe changes in tau pathology. Therefore, it is still unclear if TBI increases the risk of developing FTLD through tau, TDP-43, or FUS.

1.3.2 Tau pathology in animal models of TBI

The heterogeneity of factors contributing to tau pathology development in humans confounds our understanding of the mechanistic link between development of tauopathies and TBI. To better study the effects of TBI on tau in an isolated, controlled fashion researchers turned to animal models. In depth reviews of other commonly used TBI

models are outside the scope of this dissertation and can be found elsewhere [237, 238]. Even with highly reproducible models, reported changes in tau pathology after injury seem to be highly dependent on injury severity and time after injury.

Changes in total tau levels have been investigated alongside changes in post-translationally modified tau. In lateral fluid percussion injury and rotational acceleration injury of rats, total tau levels are increased in serum as early as one hour post-injury [239, 240]. In brain tissue from a transgenic mouse model expressing human mutations in APP, presenilin, and tau the changes in total tau levels after CCI are conflicting. One report shows an increase [241] while another report from the same group shows no change [242]. When total tau did increase in this model, the increase was dependent on injury severity [241]. Other groups looking at total tau levels after CCI injury show an increase [243]. Total tau levels in the cortex and hippocampus of weight-drop injured rats also show an increase in total tau levels out to 71 days post-injury [244]. After blast injury, there is an initial decrease in total tau levels at 6 hours post-injury; however, by 24 hours post-injury there is a significant increase [245].

Phosphorylated tau is the most frequently reported tau-based outcome in animal models of TBI. While tau phosphorylation should not be equated to the NFT pathology observed in human TBI-diseased brains, it is still an important outcome to measure in TBI models. There is not a singular common phosphosite reported by all, and as such many models report on a variety of phosphosites observed after injury. Generally speaking, tau phosphorylation levels are increased after injury [246-248].

The level of tau phosphorylated at serine 202 and threonine 205, as detected by the AT8 antibody, is increased after closed [248-250] and open [241, 251, 252] head injury in mice [241, 249-251] and rats [252]. Increased tau phosphorylation at these sites have been reported as early as 7 days post-injury in the cortex [248] and 24 hours post-injury in the hippocampus [251]. The level of tau phosphorylated at only serine 202, as detected by the antibody CP-13, is increased in closed [248, 253, 254] and open [243] head injury of mice. After blast injury, CP-13 levels are increased at 24 hours post-injury but they are not increased at 30 days post-injury [248]. The level of tau phosphorylated at threonine 205 is increased in closed [255] and open [256] head injury in mice [256] and rats [257]. The level of tau phosphorylated at threonine 181, as detected by the antibody AT270, is increased in mice after blast injury [248, 253, 255]. The level of tau phosphorylated at threonine 212 and serine 214, as detected by the antibody AT100, is increased after blast injury in mice [248]. The level of tau phosphorylated at threonine 231 is increased in closed [258-260] and open [258, 261] head injury in mice. The effect of TBI on tau phosphorylation at serine 396 and serine 404 as detected by the antibody known as PHF1 is unclear. Some studies show no change in PHF1 levels in mice following single and repeat closed head injury [248, 254, 262] while one study shows repeat head injury increasing PHF1 levels [263]. Interestingly levels of tau only phosphorylated at serine 396, but not serine 404, is increased after closed head injury in mice at 24 hours and 30 days post-injury [248] and rats at 24 hours, 3 days, and 7 days post-injury [264].

While tau phosphorylation has been documented extensively in TBI studies (as demonstrated above) there is a significant lack of research in understanding how TBI

affects tau fibrillization. As previously stated, hyperphosphorylation does not equate to aggregation and fibrillization. As such the individual effects of TBI on fibrillar and non-fibrillar tau are unclear, as is the ability of TBI to accelerate tau fibrillization.

To date only four studies have been performed that questioned the effect of TBI on tau oligomerization. All four studies showed an increased in oligomeric tau levels after injury [252, 265-267]. Using the blast model of injury, tau oligomers were shown to be increased acutely after injury [265, 267] while repeat closed head injury with mechanical impactor showed increased levels of tau oligomers six months after injury [266]. The parasagittal lateral fluid percussion model of injury showed increased hippocampal tau oligomers 4 hours, and up to 24 hours, after injury [252].

Interestingly, NFT formation has not been observed in models of TBI using mice that only express endogenous tau [268]. The only study to date that investigated NFT formation, not tau phosphorylation as a non-equivalent surrogate, showed results that weren't entirely conclusive. This study used a transgenic mouse model expressing the shortest isoform of human tau (Figure 1.1) that underwent repeat CHI [268]. Out of 12 mice that underwent the injury paradigm, only one mouse showed increased NFT deposition 9 months after sustaining injuries [268].

1.3.3 TBI as a tool for studying contributions of cellular dysfunction to development of tau pathology

TBI results in both primary and secondary injuries. Primary injuries result explicitly from the impact during TBI, while secondary injuries are due to activation of physiological responses after the primary injury [269]. Many of the secondary injury

responses observed after TBI are similar to the cellular dysfunction observed in neurodegenerative diseases that cause tau pathology [74, 270-300]; however, the responses observed in TBI typically occur more acutely than the ones observed in tauopathies. An in depth analysis of each type of cellular dysfunction observed after TBI is outside the scope of this dissertation, but for perspective references on some examples are provided: neuroinflammation [301], calcium dyshomeostasis [302], impaired axonal transport [303, 304], abnormal kinase and phosphatase activity [305], and cell death [306].

1.4 Controlled cortical impact (CC) model of injury

As mentioned before, TBI highly heterogeneous. To properly study different classifications of TBI, multiple *in vivo* models are used to recapitulate what is observed in humans. As the CCI model was used for experimental procedures in chapter three, a brief explanation of the model is provided.

The CCI model is an open head, contusion model of injury. With the head secured, a craniotomy is performed at midline [307] or lateral from the midline [308] to expose the intact dura [307]. A pneumatic [307] or electromagnetic [308] impactor with a metal [307, 308] or silicone [309] tip is used to impact the exposed cortical tissue. Severity of the injury depends heavily on tip material [309] and shape [310], velocity [308], and impact depth [311]. This model is primarily a focal model of injury with some diffuse effects observed [312].

Widespread cell death drives lesion development at the impact site throughout the penumbra over the 2-week post-injury period [308, 313, 314]. Injury also causes

disruption in the blood-brain barrier that peaks around 24 hours post-injury and is restored by 9 days post-injury [310]. Hippocampal cell loss is also observed after injury, especially in the dentate gyrus as early at 24 hours post-injury [315]. Axonal degeneration [316] and glial activation (both astrocyte and microglia) [317] are observed after injury as well. Multiple secondary injury responses are observed after CCI including apoptosis [318, 319], neuroinflammation [320], and calcium dyshomeostasis [321, 322].

This model was originally developed in ferrets [307] but has since been adapted to rodents [323, 324], pigs [325], and non-human primates [326]. In mice, there are no overt sex-specific differences observed in neurodegeneration [327, 328] or microglial response after injury [328]. There are sex-specific differences in cortical vasculature alterations and astrocyte reactivity, with males showing more complex cortical vascular network 7 days after injury and females showing greater astrocyte reactivity at 1 day post-injury [328].

1.5 rTg4510 mouse model of tauopathy

There are currently over 30 transgenic mouse models used to study tauopathies (reviewed in [329]). The rTg4510 tau transgenic mouse model is of particular importance for this dissertation. The rTg4510 was developed in 2005 through a collaborative effort at the University of Minnesota Medical School, Massachusetts General Hospital, and Mayo Clinic in Jacksonville. These mice have two transgenes: the first is a tetracycline responsive element placed upstream from the human P301L tau transgene (tetO-MAPT*P301L), and the second is an activator transgene with a tet-off open reading frame downstream from the CAMKII promoter (Camk2a-tTA) [70]. This model

expresses human P301L tau at approximately thirteen times endogenous mouse tau levels, which accelerates tau pathology deposition.

The rTg4510 mouse was used due to its early onset of tau pathology and its easily controllable transgene expression through a doxycycline diet. Changes in tau pathology are age dependent. Conformational changes in tau (as detected by the antibody MC-1) and phosphorylation of tau at serine 202 (as detected by the antibody CP-13) are detected as early as 1.3 months of age in both the hippocampus and the cortex [330]. Phosphorylation of tau at threonine 231, as detected by the antibody TG-3, is detectable in the hippocampus as early as 1.3 months but isn't detectable in the cortex until 2.5 months [330]. By 2.5 months of age phosphorylation of tau at serine 202/threonine 205, serine 396/404, and serine 409 is detectable in the hippocampus and the cortex [330]. NFT deposition begins at 2.5 months of age in the cortex [70, 330] and is observed in the hippocampus by 4 months of age [330]. Prominent tau phosphorylation and tangle deposition is observed by 4-5.5 months of age and continues to worsen with age [330]. Suppression of tau expression by doxycycline does not clear the brain of NFT deposits already present [70].

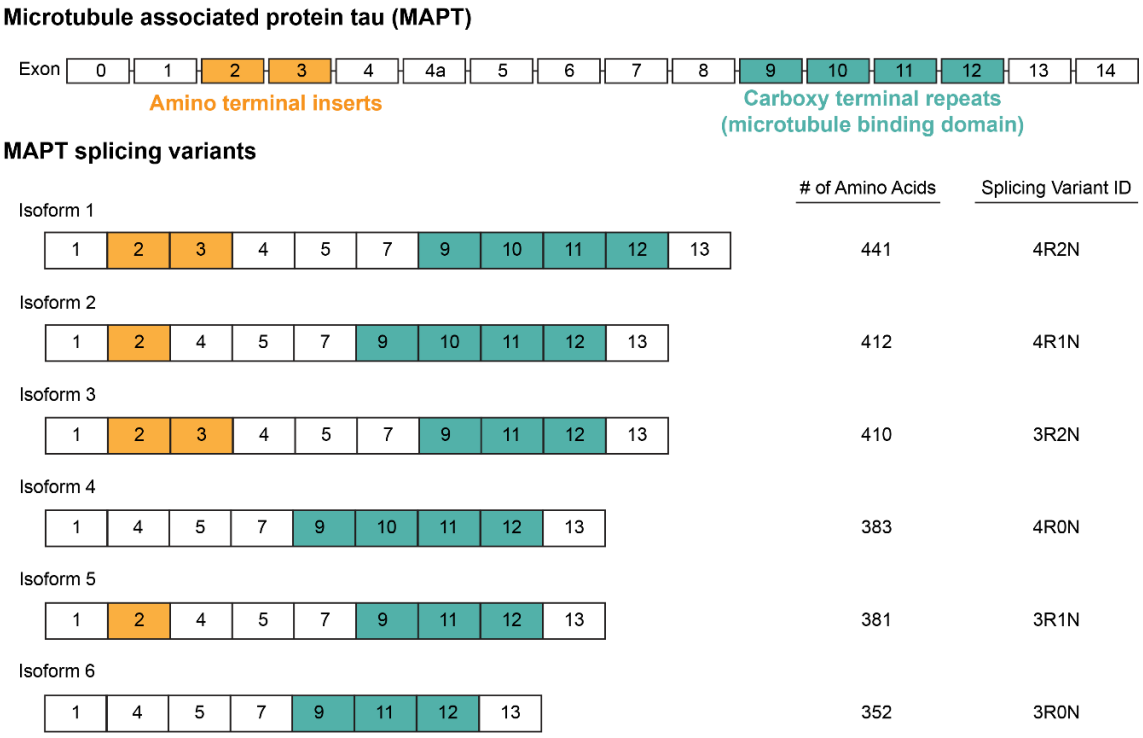

Figure 1.1: Splicing variants in human tau. The microtubule associated protein tau (MAPT) has six different isoforms that occur due to alternative splicing events at exons 2, 3, and 10

Table 1.1: Post-translational modifications of tau

Modification type	Site	Outcome of modification
Phosphorylation	T17, Y18, Y29, Y39, S46, T50, T52, S56, S68, T69, T71, T95, T101, T102, T111, S113, T123, S131, S135, T139, T153, T169, T175, T181, T184, S185, S191, S195, Y197, S198, S199, S202, T205, S208, S210, T212, S214, T217, T220, T231, S235, S237, S238, S241, T245, S258, S262, S263, S285, S289, S293, S305, S316, S320, S324, S341, S352, S356, T361, T373, T386, Y394, S396, S400, T403, S404, S409, T414, S412, S413, S416, S422, T427, S433, S435	Decreased affinity for microtubule binding under normal conditions; aggregation and development of pathology under abnormal conditions
Truncation	D13, E45, R230, E391, D421	Enhanced aggregation and neuronal apoptosis
Nitration	Y18, Y29, Y197, Y394	Promotes polymerization and aggregation
Glycosylation	T181, S199, S202, T205, T212, S214, T217, S262, S356, S404, S422	Protection from hyperphosphorylation and reduced aggregation potential
Glycation	K87, K132, K150, K163, K174, K225, K259, K280, K281, K347, K353, K369	Blocks degradation; promotes polymerization, stabilization, and aggregation
Polyamination	Q6, K24, Q88, Q124, K163, K174, K180, K190, K225, K234, K240, Q244, Q276, Q288, Q351, K383, K385, Q424	Promote NFT formation
Prolyl-isomerization	T231	*Cis* to *trans* conformational change; promotes Dephosphorylation and microtubule binding

Ubiquitination	K254, K311, K353,	Promotes proteolysis under normal conditions; indirectly involved in pathology development in abnormal conditions
Sumoylation	K340	Suggested to counteract ubiquitination
Oxidation	C322	Promotes PHF assembly
Acetylation	L280	Auto-acetylation can occur at all lysine residues; Promotes or reduces aggregation and/or degradation depending on lys

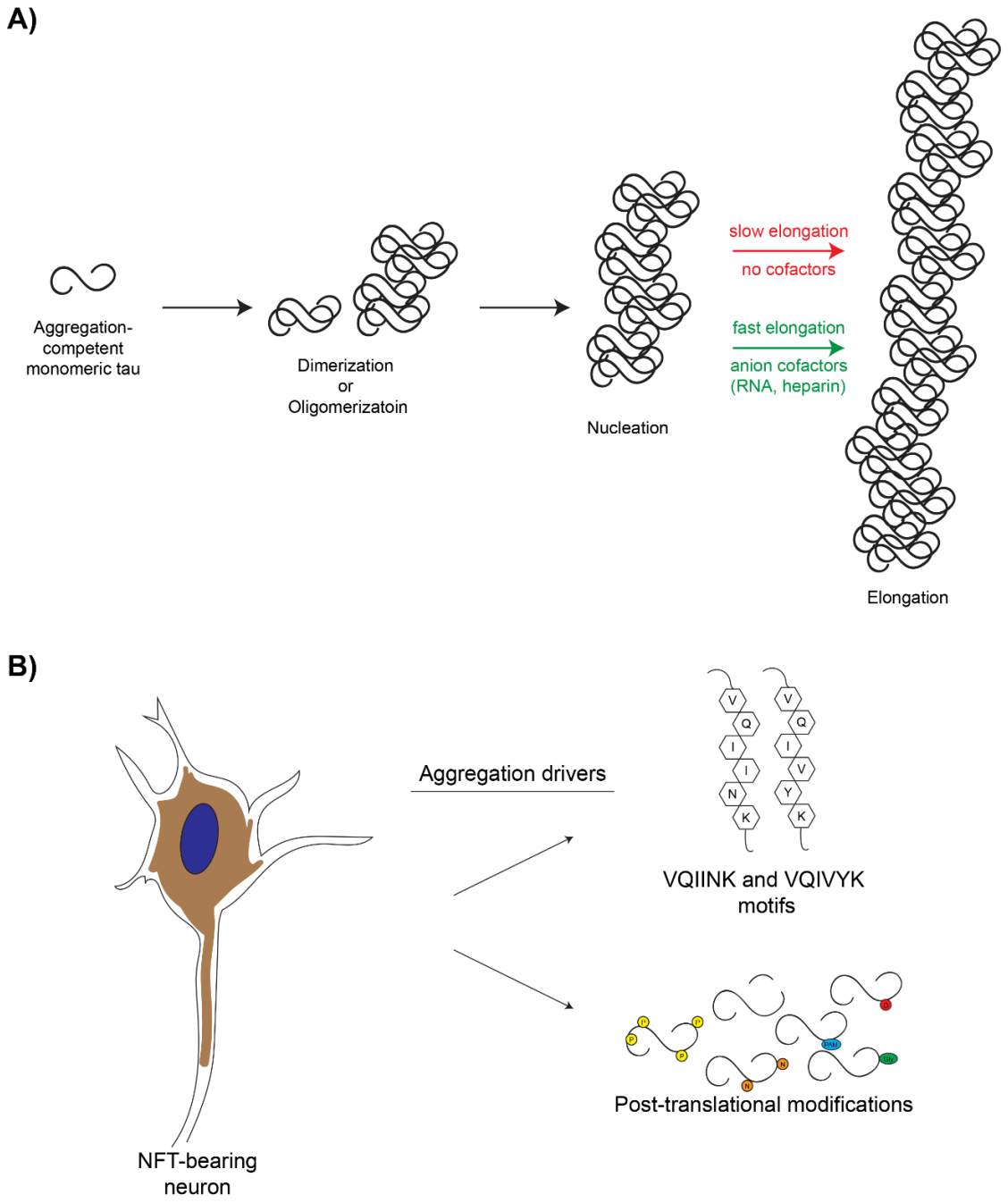

Figure 1.2: Tau elongation and aggregation. (A)Aggregation-competent tau elongates to form paired helical filaments (PHFs). (B) Tau aggregation is driven by two main factors: VQIINK and VQIVYK motifs and post-translational modifications. Hyperphosphorylation as a factor for aggregation is still debated, and should not be equated to aggregation. Abbreviations: P = phosphorylation, N = nitration, PAM = polyamination, Gly = glycation, O = oxidation.

CHAPTER 2. PATHOLOGICAL TAU PROMOTES NEURONAL DAMAGE BY IMPAIRING RIBOSOMAL FUNCTION AND DECREASING PROTEIN SYNTHESIS

2.1 Preface

Chapter 2 is modified from the published article "Pathological tau promotes neuronal damage by impairing ribosomal function and decreasing protein synthesis" written by Shelby Meier, Michelle Bell, Danielle N. Lyons, Jennifer Rodriguez-Rivera, Alexandria Ingram, Sarah N. Fontaine, Elizabeth Mechas, Jing Chen, Benjamin Wolozin, Harry LeVine, Haining Zhu, and Jose F. Abisambra. Under the CC-BY 4.0 license this work (Meier *et al.*, 2016 *J Neurosci* 36(3):1001-7.) became public material 6 months after publication and permission from the Journal of Neuroscience is not needed to reproduce this work.

The text and figures of the manuscript have been edited to highlight the research performed primarily by Shelby Meier as part of her dissertation. However, a number of collaborators and colleagues contributed to the data in this chapter and in Meier *et al.* (2016). Specific contributions are acknowledged below.

Figure 2.1A: Western blots were performed by Maria Bodero.

Figure 2.1C: Sample homogenates were created by Maria Bodero and subjected to mass spectrometry by Jing Chen and Haining Zhu.

Figure 2.2B: PSD-95 Western blots were performed by Danielle Lyons. RT-PCR was performed by Jennifer Rodriguez-Rivera.

Figure 2.3B: Primary neuronal cell culture was performed by Danielle Lyons.

Figure 2.3C: Puromycin immunostaining and imaging was performed by Blaine Weiss and Juan Pablo Arango; image analysis was performed by Shon Koren.

Figure 2.4A: Transfection of tau plasmids into cells was performed by Sarah Fontaine.

We acknowledge the University of Kentucky Alzheimer's Disease Center (UK-ADC) and its Neuropathology Core, which is supported by NIH/NIA P30 AG028383. We also acknowledge the University of Kentucky Proteomics Core that is partially supported by grants from the NIH/NIGMS (P20GM103486) and the NIH/NCI (P30CA177558). This work was also supported in part by NIH R01NS077284 (to H.Z.). The LC-MS/MS instrument was acquired with a High-End Instrumentation Grant S10RR029127 (to H.Z.) from the National Institutes of Health. We further acknowledge NIH/NINDS P30NS051220 for support and maintenance of the microscopy core used for imaging. J.F.A., D.L., and S.M. were supported by NIH/NINDS 1R01 NS091329-01, Alzheimer's Association NIRG-14-322441, NIH/NCATS 5UL1TR000117-04, NIH/NIGMS 5P30GM110787, GlaxoSmithKline, Department of Defense AZ140097, UK-ADC Pilot Award 8.1 supported by NIH/NIA P30 AG028383, the University of Kentucky Epilepsy Center (EpiC) and NIH/NIMHD L32 MD009205-01. We thank Dr. Pedro Vera and the Lexington VA Medical Center for support. We also thank Dr. Peter Davies for his generous contribution of the PHF1 antibody. We thank Dr. Chad Dickey for developing and sharing the iHEK cell lines and the tau plasmids. We thank Ms. Ela Patel and Ms. Sonya Anderson with their assistance accessing the human brain tissue. We also thank Dr. Fred Schmitt for insightful discussions and crucial intellectual

contributions to this study. Finally, this work was possible thanks to the generous contribution of oligomers and T22 antibodies from Dr. Rakez Kayed and Ms. Urmi Sengupta.

2.2 Introduction

Aberrant accumulation of tau is associated with the etiology of more than eighteen known neurodegenerative diseases collectively termed tauopathies. Alzheimer's disease (AD), the most common tauopathy, affects over 36 million people world-wide [331]. A common and early symptom in tauopathic patients is progressive memory loss. There is no cure for tauopathies, and current therapeutics stave off symptoms only temporarily. This is partly due to limited understanding of the molecular mechanisms linking tau and disease onset.

Synaptic function depends on constant protein synthesis; therefore, neurons are especially vulnerable to chronic attenuation of RNA translation [332]. Although transient suppression of translation is an adaptive cellular response to endoplasmic reticulum (ER) stress [333], chronic inhibition of RNA translation contributes to the pathogenesis of multiple neurodegenerative disorders, including tauopathies [334-336]. Pronounced ribosomal deficiencies appear in regions where tau pathology is evident [205], yet the link between tau and ribosomal function has not been established

Protein synthesis is necessary for memory formation [337]. The fact that progressive memory loss is common to virtually all tauopathies suggests that ribosomal dysfunction could be an underlying mechanism leading to clinical symptoms. Indeed, tau binds to ribosomes in the brain, and this interaction is enhanced in tauopathic brains [206,

338]. Additionally, we determined ER-bound proteins associate with tau with the most robust association being found between tau and RNA-binding proteins [334, 339].

Here we show that ribosomes associate with pathological and non-pathological tau. Consequently, ribosomal function becomes impaired and global protein synthesis is reduced. These data suggest that tau-mediated ribosomal dysfunction is a common pathogenic process that affects synapses leading to cognitive impairment.

2.3 Methods

Human brain samples: Human samples were obtained from the University of Kentucky (UK) Alzheimer's disease Center. Sample collection and experimental procedures involving human tissue were in compliance with the UK Institutional Review board (IRB). Samples from Brodmann areas 21/22 were used. AD tissues were scored as Braak V (female, 93-year-old), VI (male, 88-year-old), and VI (female, 80-year-old); samples from non-demented controls were Braak I (male, 79-year-old), II (female, 94-year-old), and II (female, 88-year-old). The average PMI was 3h.

Microsomal isolation: This preparation was used as an enrichment method to isolate the rough endoplasmic reticulum from homogenized human brain tissue. The unique buoyancy of rough microsomes in concentrated sucrose solutions allows for easy separation using simple centrifugation. The microsomal preparation technique used is as follows: 200 mg of human brains were homogenized with a Dounce homogenizer using homogenization buffer (0.25M Sucrose, 1:100 Protease Inhibitor Cocktail Set III (EMD Millipore, Cat# 539134), 1:100 Phophatasearrest Phosphatase Inhibitor Cocktail 2 (GBiosciences, cat#786-451),), 1:100 Phophatasearrest Phosphatase Inhibitor Cocktail 3

(GBiosciences, cat#786-452), 1:100 100mM PMSF) using gentle strokes while keeping the homogenization tube in ice. Samples were then centrifuged at 16,000 x g for 15 minutes at 4 degrees celsius. The supernatant was collected, transferred to a new tube, and then centrifuged at 100,000 *x g* in specialized tubes with reinforced bottoms for 60 minutes at 4 degrees celsius. The supernatant and microsomal pellet were separated and the microsomal pellet was resuspended in RIPA buffer with 1:100 Protease Inhibitor Cocktail Set III, 1:100 Phophatasearrest Phosphatase Inhibitor Cocktail 2, 1:100 Phophatasearrest Phosphatase Inhibitor Cocktail 3, 1:100 100mM PMSF. This method was utilized previously in our lab and was published in previous work that provided preliminary data guiding the work performed in this chapter [201]. Microsomal isolation was performed on one AD brain and one control brain.

Co-immunoprecipitation (co-IP) and liquid-chromatography tandem mass spectrometry (LC-MS/MS): Co-immunoprecipitation and LC-MS/MS were utilized to determine if, and which, ribosomal proteins interacted with full length tau. For co-immunoprecipitation, microsomal samples were incubated with Tau46 antibody (Cell Signaling, cat#4019) or Actin (Sigma, cat#A2228) overnight at 4 degrees Celsius on rotating shaker. Protein G dynabeads (Thermo Fisher, cat#10003D) we then added and samples were incubated at 4 degrees Celsius on rotating shaker for 5 hours. Tubes were placed on a magnetic rack. As dynabeads are magnetic, the beans with bound antibody (and proteins of interest) remained on the side of the tube while the rest of the sample was vacuumed out. Beads were washed twice with buffer 1 (10mM Tris, 50mM NaCl, 0.2% Tween-20, at final pH 7.5) and twice with buffer 2 (10mM Tris, 50mM NaCl, at final pH 7.5). For protein retrieval from the beads, beads were resuspended in 25uL of

2x Laemmli buffer with beta-mercaptoethanol and boiled at 100 degrees for 10 minutes. Samples were then ran on SDS-PAGE gel. The gel was stained with coomassie blue dye to visualize protein bands. Gels were then sent to the laboratory of Dr. Haining Zhu for LC-MS/MS. A total of four samples were used for the analysis: one AD microsomal sample co-immunoprecipitated with Tau46, one AD microsomal sample co-immunoprecipitated with Actin, one control brain microsomal sample co-immunoprecipitated with Tau46, and one control brain microsomal sample co-immunoprecipitated with Actin.

Samples were co-immunopreciptated with Tau46 antibody over other full length tau antibodies because Tau46 detects and bind to the final 37 amino acids of the tau protein. By using a c-terminus tau antibody, we maximized detecting mature tau and minimized detecting immature tau that was interacting with ribosomal proteins because it was actively being translated. Actin was used as a control for random protein interaction, as actin is a ubiquitous protein. Proteins that were identified in the Actin LC-MS/MS fraction and the Tau46 LC-MS/MS fraction were removed from the list as they were not tau specific interactions.

Protein complexes binding with Tau46 and Actin were identified using LC-MS/MS and UniProtKB, an online database containing functional information on proteins. For LC-MS/MS, each lane in the gel was excised into 12 major portions and subjected to dithiothreitol reduction, iodoacetamide alkylation, and in-gel trypsin digestion using a standard protocol as previously reported [340, 341]. The resulting tryptic peptides were extracted, concentrated to 15 µl each using a SpeedVac, and 5 µl

was injected for nano-LC-MS/MS analysis. LC-MS/MS data were acquired on an LTQ Velos Orbitrap mass spectrometer (Thermo Fisher Scientific, Waltham, MA) coupled with a Nano-LC Ultra/cHiPLC-nanoflex HPLC system (Eksigent, Dublin, CA) through a nanoelectrospray ionization source. The tryptic peptides sample was injected by an autosampler, desalted on a trap column, and subsequently separated by reverse phase C18 column (75 mm i.d. × 150 mm) at a flow rate of 250 nL/min. The HPLC gradient was linear from 5% to 60% mobile phase B for 30 min using mobile phase A (H2O, 0.1% formic acid) and mobile B (90% acetonitrile, 0.1% formic acid). Eluted peptides were analyzed using data-dependent acquisition: peptide mass spectrometry was obtained by Orbitrap with a resolution of 60,000. The seven most abundant peptides were subjected to collision induced dissociation and MS/MS analysis in LTQ linear trap. The LCMS/MS data were submitted to a local MASCOT server for MS/MS protein identification search via the ProteomeDiscoverer software. The mass error tolerance was 5 ppm for peptide MS and 0.8 Da for MS/MS. All peptides were required to have an ion score greater than 30 ($p < 0.05$). The false discovery rate in each LC-MS/MS analysis was set to be less than 1%.

The raw data provided by Dr. Haining Zhu in the form of an excel sheet identified all the proteins that co-immunoprecipitated with Tau46 or Actin. In this list, a unique accession number was give. This accession number was used on UniProtKB to identify the functional role of that specific protein. Proteins that were associated with RNAs, ribosomes, or protein translation were grouped into the RNA-binding protein category,

In vitro translation assay: 1-Step IVT Kit (Thermo, cat#88881) was used as directed by the kit instructions with minor modifications: a black bottom 96-well plate was loaded with IVT-kit components and 10ng of recombinant proteins. GFP (ex-482nm/em-512nm) was measured every 15min in a BioTek Synergy HT at 30ºC for 6h. Each sample was run in triplicate and raw values were plotted using GraphPad Prism. The plots were then analyzed by linear regression using GraphPad Prism.

Cell culture: Cell culture was used to better understand the effect of tau on translation, and to further confirm that tau reduced translation. Cell culture experiments for Figure 2.3B used a stably transfected inducible human embryonic kidney cell line that expressed wild type 4R0N human tau (iHEK-Tau). Cell culture experiments for Figure 2.4A used the same iHEK-Tau cells as Figure 2.3B for the WT Tau, but they also sued the stably transfected inducible human embryonic kidney cell line that expressed mutant human ΔK280 tau. Stable transfection of the human tau gene in these cells is maintained by addition of Zeocin (for the tau plasmid) and Blasticidin (for the tetracycline repressor) antibiotics to the cell culture media. These cells use a tetracycline on system, meaning that expression of tau is induced when tetracycline is present in cell culture media. For these experiments, tetracycline was added to the cell culture media at 1 μg/mL for the specified amount of time.

Cell culture experiments for Figure 2.4B used human embryonic kidney 293 (HEK293) cells that were transiently transfected with wild type and mutant tau plasmids. HEK293 cells come from a neuronal lineage, and are easily maintained in the laboratory, making them ideal for these transient transfections.

Plasmid preparation for these transfections was performed in *E. Coli* cells. In a 50uL aliquot of cells (Lucigen, E. cloni chemically competent cells, cat# 60108), 1uL of WT, P301L, or ΔK280 tau DNA was added. These tau plasmids are similar to the 4R0N WT tau plasmids mentioned above as they also are under zeocin selection. Cells were then incubated on ice for 30 minutes. Cells were then heat shocked at 42 degrees Celsius for two minutes, followed by immediate transfer to ice for 2 minutes, to increase acceptance of DNA into the cells. Under flame, 400uL of LB broth was added to the cells and the samples were incubated on horizontal shaker at 200rpm at 37 degrees Celsius for 1 hour. After this and under flame, 65uL of sample was pipetted onto LB agar plates containing zeocin. LB agar plates were incubated at 37 degrees Celsius ove night. The plates were removed the next day and a single colony from each plate was isolated and incubated in 4mL of LB broth overnight. DNA was isolated using the Qiagen Mini Prep kit (Qiagen, cat#27106) as directed. Final DNA concentration was measured using the BioTek EPOCH plate reader and the Gen5 software. The 260nm/280nm ratio was used to determine purity of DNA. A 260/280 ratio of between 1.9 and 2 shows approximately 95-100% nucleic acid concentration.

Once the plasmid was prepared and DNA was isolated, the DNA was transfected into the HEK cells. For each 10cm dish containing HEK cells, 10ug of DNA total was transfected using Lipofectamine 2000 (Thermo Fisher, cat#12566014) in serum free media. Plates were kept in the incubator for 4 hours and then the serum free media was replaced with complete media containing zeocin. All cells underwent SUnSET as described below and were harvested as described below.

Primary Neurons: Primary neuronal cultures were used to study the effects of tau on protein translation in neurons specifically. Isotonic buffer was prepared (in 500mL: 4.0g of NaCl, 2.7mL of 1M KCl, 1mL of 100mM Na_2HPO_4, 1mL of 100mM KH_2P0_4, 0.695g glucose, 10.1g sucrose) and placed in 4 degree Celsius refrigerator. It is critical that this is chilled before harvesting neurons. While the buffer was chilling, 10cm dishes were coated with poly-L lysine to optimize final cell adhesion when plating neurons and allowed to sit for 2-4 hours in a sterile cell culture hood. The poly-L lysine solution was then aspirated off and plates were allowed to fully dry in sterile cell culture hood. For primary neuron harvesting, P1 pups were decapitated into a 10cm dish filled with chilled isotonic buffer. Using curved forceps, the skull was peeled off to remove the brain. The cortices and hippocampi were separated from the rest of the brain and placed in a new 10cm dish with fresh isotonic buffer. Meninges were removed from both the cortex and the hippocampi. Meninges-free brain regions were then moved to a fresh 10cm dish with clean isotonic buffer. This plate and the isotonic buffer glass bottle were then sterilized with 70% ethanol and moved into the cell culture hood.

Prior to beginning neuron isolation on the P0 pups, complete media (DMEM, 10% fetal bovine serum, 1% penicillin-streptomycin, 1% Glutamax) was placed in a 37 degree Celsius water bath to warm. In the 10cm dish containing the brains, isotonic buffer was aspirated out and replaced with fresh isotonic buffer. This was repeated 3 times. After the final aspiration, all brain pieces were moved to the center of the dish and finely chopped into small pieces with a brand new razor blade. Chopped up brains were then moved to 50mL conical and 6mL of Trypsin was added to the conical. Conical was incubated in the 37 degree Celsius water bath for 10 minutes. The volume inside the

conical was then pipetted up and down to break up the chunks of brain. Complete media was then added to the conical until it reached the 50mL line. The conical was then centrifuged at 1000rpm for 10 minutes at 22 degrees Celsius to pellet the cells. The media was vacuumed out of the conical and 25mL of fresh complete media was added to resuspend the cells. The conical was centrifuged again at 1000rpm for 10 minutes at 22 degrees Celsius to pellet the cells. The media was vacuumed out and cells were resuspended in 5mL of complete media. Cells were counted using a hemocytometer. Cells were then plated using complete media on the 10cm dishes with poly-L lysine at a concentration of 1.5-5 million cells/plate.

Twenty-four hours after plating the cells, the complete media was switched out for neurobasal media (50mL Neurobasal media, 1mL B27 supplement, 125uL Glutamax) for optimal neuronal growth without glial cell growth as well. Neurobasal media was supplemented every 3-4 days, as complete change of the media removed adhesion/growth factors the neurons had secreted. Primary neuronal cultures underwent SUnSET as described below and were harvested as described below

Surface sensing of translation (SUnSET): The SUnSET method was original published as a non-radioactive way of measuring protein translation [342]. The originally published method was applied as written in all cell culture experiments performed. For cell culture, cells were incubated with 5μg/mL of puromycin in cell culture media for 1h prior to harvest. One hour post-puromycin application, cell culture media was removed and cells were gently rinsed with cold 1X PBS to remove any residual puromycin. Cells were then harvested as described below.

Administration of puromycin into animals occurred 30 minutes before euthanasia and tissue collection. Puromycin was administered intraperitoneal injection at 225mg/kg. Mice were then euthanized as described below. Puromycin powder was purchased from Research Products International (cat# P33020) and resuspended in water. Proteins were analyzed using immunoblots or immunohistochemistry.

Cell culture harvest: Cell were then harvested with cell scrapers and 100 µl of MPER complete (96uL MPER, 1uL 100mM PMSF, 1uL Protease Inhibitor Cocktail Set III, 1 uL Phophatasearrest Phosphatase Inhibitor Cocktail 2, and 1 uL Phophatasearrest Phosphatase Inhibitor Cocktail 3). The total volume was transferred to a 1.5mL microcentrifuge tube, briefly vortexed, and incubated on rotational shaker at 4 degrees Celsius for 10 minutes. Samples were then spun down at 13,000 *x g* at 4 degrees Celsius for 10 minutes. The supernatant was transferred to new tubes and was used for western blotting.

Mouse euthanasia: Mice were euthanized in a method approved by the University of Kentucky IACUC. Mice were placed in an isolation chamber and were then administered 5% isoflurane by vaporizer. After five minutes, the toe was pinched and if the there was no response the animal was moved to the perfusion setup to begin transcardial perfusion. Mice were perfused with cold 0.9% NaCl solution until liquid flowing out of the right atrium was clear. At this point, mice were immediately decapitated and the brain was removed from the skull. The brain was cut into the left and right hemispheres. The left hemisphere was drop fixed in 4% paraformaldehyde in PBS for immunohistochemistry experiments. The right hemisphere was separated into neocortex, hippocampus, and

cerebellum and snap frozen using liquid nitrogen. Snap frozen samples were stored at -80 degrees Celsius until used for experiments.

Tissue sectioning: Human and mouse brains were drop-fixed in 4% para-formaldehyde in PBS and were cryoprotected by incubating in sequential concentrations of sucrose (10%, 20%, and 30%) sucrose for 24 h each. Samples were frozen on a temperature-controlled freezing stage, sectioned (25 µm) on a sliding microtome in the coronal plane, and stored in a solution of PBS containing 0.02% sodium azide at 4 degrees celsius.

Western blotting (WB): Protein concentration of samples for western blotting was performed using a BCA kit (Pierce, cat# 23225)) and BioTek EPOCH plate reader. For all western blots 10ug of protein was loaded per well. Protein samples were incubated with 4X Laemmli Buffer+beta mercaptoethanol and boiled at 100 degrees Celsius. Samples were then loaded into tris-glycine gels (Invitrogen, WT0102) and ran at 150V until dye front was roughly 1cm from bottom of gel cassette. Samples were then transferred to PVDF membranes, blocked in 5% milk at room temperature for 1 hour, and incubated in primary antibodies overnight. The primary antibodies used were anti-tau h-150 (1:1000; SantaCruz), actin (1:1000; Sigma), RPL28 and RPP0 (1:1000; GeneTex), PHF1 (1:500), Hsp70 (1:1000; ENZO), PSD-95 (1:1000; Cell Signaling), and Puromycin (1:1000; EMD Millipore). Bands were detected using horse radish peroxidase secondary and film, or infrared secondary and the Licor Odyssey Imaging system. Image analysis was performed using ImageJ. Bands of the protein of interest were normalized to a

loading control. Normalized values were plotted in GraphPad prism and analyzed using Student's t-test in GraphPad Prism.

Immunofluorescence (IF): IF was performed visualize the interaction between oligomeric tau and ribosomal protein S6. Briefly, fixed human brain sections from the superior/medial temporal gyrus (SMTG) were mounted on slides using 30% ethanol. Tissue was adhered to the slide by allowing slides to dry at room temperature overnight. Slides were framed using a hydrophobic pen, and tissue was incubated in blocking buffer at room temperature for one hour. Primary antibodies were diluted in blocking buffer and tissue was incubated in this solution overnight at 4 degrees Celsius. Primary antibodies used for staining were T22 (1:100, gift from Rakez Kayed) and RPS6 (1:250; SantaCruz Biotech.). Tissue was then washed and incubated in fluorescent secondary antibodies (AlexaFluor, Rabbit 596 for T22 and Mouse 488 for RPS6) at room temperature for one hour. Slides were washed and then coverslipped. Tissues were also stained with Sudan black and Neurotrace (1:200). Slides with AD and control sections were stained omitting primary antibodies to establish non-specific background signal.

Immunohistochemistry (IHC): Free-floating tissue was treated with 3% (v/v) hydrogen peroxide + 10% (v/v) methanol in Tris-buffered saline (TBS, pH 7.4) to quench endogenous peroxidase activity. The Mouse on Mouse (MOM) Detection Kit (Vector Labs, BMK-2202) was used for blocking and staining procedures, with buffers prepared as described in standard protocol supplied with the kit. Sections were then incubated in Mouse Ig blocking buffer for 1 hour at RT. Sections were incubated overnight at 4 °C with puromycin monoclonal antibody at 1:100 (EMD Millipore, MABE343) in MOM

Diluent. Sections were washed with TBS and incubated with biotinylated anti-mouse IgG (Vector Laboratories) for 10 min at RT. Sections were washed again and incubated in ABC solution (Vector Laboratories) for 10 min at RT. Sections were washed again and incubated in diaminobenzidine (DAB) (Sigma–Aldrich) and hydrogen peroxide in TBS. Sections were washed, mounted, and cover-slipped using Depex mounting media (Electron Microscopy Science). Images of the cortex (specifically somatosensory cortex, SSp) were taken and quantified together for analysis. All values were normalized to signal in non-transgenic control mice.

Microscopy: A Nikon Eclipse Ti laser-scanning confocal microscope was used to capture images in Figure 2.1B. Fields of view was established at 20X and images were taken a using 40x objective. Areas imaged included areas of tau staining with morphological distribution in agreement with Neurotrace labeling. All acquisition intensities, field sizes, and settings were kept consistent across all images. Images were prepared using the NIS Elements 4.20 (Nikon) and Photoshop Cs6 (Adobe) software. No quantification data was collected from these images as we were investigating the qualitative interaction between tau oligomers and ribosomal protein S6 (namely, if there was any obvious special overlap).

A BioTek Cytation5 automated microscope and multi-mode plate reader was used to capture images in Figure 2.3C. Areas imaged included areas of puromycin staining in the neocortex dorsal to the hippocampus. All acquisition intensities, field sizes, and settings were kept consistent across all images. Images were prepared using the BioTek Gen5 software and Photoshop Cs6 (Adobe). Quantification of these images

was performed using FIJI (Fiji Is Just ImageJ) software. The integrated density was measured per mouse (3-4 mice per condition). The 4.5 month and 7 month non-transgenic measurements were averaged respectively and all samples (rTg4510 and non-transgenic) were normalized to their age-matched non-transgenic average. These normalized values were then plotted in GraphPad prism. Values were then analyzed by standard two-way ANOVA using GraphPad prism.

Quantitative Real-Time PCR: Total RNA was extracted from rTg4510 tau transgenic and littermate control primary neuronal cultures using EZNA total RNA Kit II according to manufacture instructions (Omega Bio-tek Cat#: R6934-01). RNA was quantified using a BioTek spectrophotometer and cDNA was produced using SuperScript IV (Invitrogen). Q-RT-PCR was performed using TaqMan Gene Expression probes for PSD-95 and GAPDH using a ViiA^{TM} 7 Real Time PCR System (Applied Biosystems). 95 expression was evaluated by normalizing to GAPDH as an internal control. The real-time values for each sample were average and evaluated using the comparative CT method.

2.4 Results

2.4.1 Tau associates more robustly with ribosomal proteins in AD brains

To identify tau-associated ribosomal proteins in AD, microsomes were isolated from non-demented control and AD brain tissues. Full-length tau (or actin as control) was co-IP from microsomes, and tau-associated peptides were identified using LC-MS/MS. Proteins were grouped into functional categories based on UNIPROT. A striking

difference was that tau associated with more RNA-binding proteins in AD than in control (Fig. 2.1C).

To further characterize the tau-ribosome association, we compared tau levels in AD and control subcellular fractions (Fig. 2.1A). While tau levels were similar between the fractions lacking ribosomes, tau was significantly increased in the AD ribosomal fraction (Fig. 2.1A). We also detected a PHF1-positive smear in the AD ribosomes (Fig. 2.1A). PHF1 recognizes pS396/S404, which is associated with late stage tangles in AD [343]. Additionally, we immunofluorescently labeled ribosomal protein S6 and oligomeric tau in human AD brain tissue (Fig. 2.1B). We noticed a qualitative relationship in that positive signal from tau oligomers overlapped with positive signal from ribosomal protein S6 (Fig 2.1B). These data all support previous findings in the literature that tau associates with ribosomes.

2.4.2 Reduction in protein synthesis is due to impaired translation and not impaired transcription

The consequences of the tau-ribosome association are unknown. We hypothesized that the aberrant interaction between pathological tau species and ribosomes impairs translation and not transcription. To test this, we measured the impact of tau on ribosomal function in an *in vitro* translation cell free assay. We added recombinant tau oligomers or bovine serum albumin (BSA) as control with *in vitro* translation assay components and a GFP plasmid reporter. The rate of translation, measured by GFP, was significantly decreased in the presence of tau oligomers (Fig. 2.2A). To determine whether this effect was specific to tau oligomers, we tested the impact of oligomeric α-synuclein and insulin

on translation (Fig. 2.2A). We found no significant change in GFP with addition of α-synuclein and insulin, suggesting that this effect is specific to tau.

To further confirm that the effect we were seeing in reduced GFP signal was due to impaired translation and not reduced transcription, we measured the levels of the PSD-95 mRNA in rTg4510 and non-transgenic littermate primary neurons. We found that PSD-95 mRNA levels were increased by two-fold in rTg4510 primary neurons compared to controls while PSD-95 protein levels were reduced in rTg4510 neurons (*p=0.049) (Fig.2.2B). These data suggest that tau impairs RNA translation, and that this pathological mechanism directly affects translation without impairing gene expression.

2.4.3 Tau reduces translation *in vitro* and *in vivo*

We next measured the effect of pathological tau on the rate of translation in human embryonic kidney cells using a technique called surface sensing of translation (SUnSET) [342]. This technique is a puromycin-based pulse assay. Puromycin acts as a tRNA analog and is attached to proteins as they are being synthesized (Fig. 2.3A). These puromycin tagged proteins can then be detected using a commercially available antibody for puromycin. For cell culture experiments puromycin was added to medium 1h before harvesting cells at 5ug/mL. For *in vivo* experiments puromycin was administered through an intraperitoneal injection at 225mg/kg 30 minutes before tissue harvest.

We used iHEK-Tau cells, an inducible HEK line that overexpresses wild-type human 4R0N tau upon addition of tetracycline [334], to study the effects of tau overexpression on translation. Use of tetracycline allowed control over the start and overall duration of tau expression. We first performed a time-course experiment in which

tetracycline was added to iHEK-Tau cells over 72 hrs. One hour before harvesting these cells we treated them with puromycin at 5ug/mL. We found that increased PHF1 and total tau levels correlated with decreased puromycin signal (Fig. 2.3B). We then performed a rescue experiment in which tau was expressed for 96h and then tau expression was turned off for 24h or 96h (Fig. 2.3B). We found that puromycin levels were restored to normal once PHF1 levels were reduced. We also measured changes in the rate of translation in primary neurons derived from rTg4510 tau transgenic and control mice using SUnSET on primary neuronal cultures. The rTg4510 model overexpresses human P301L mutant tau [70]. At DIV14, puromycin was added to the medium and primary neurons were harvested. Puromycin-tagged proteins were significantly decreased in rTg4510 neurons (*p=0.0111) compared to nons (Fig. 2.3B).

Using the intraperitoneal injection of puromycin into rTg4510 and non-transgenic littermates, we observed the changes in translation *in vivo.* We saw that there was a significant decreased in overall translation in the rTg4510 mice compared to non-transgenic littermates (Fig. 2.3C). The difference in puromycin-positive signal did not significantly differ over time. Taken together, these *in vitro* and *in vivo* data demonstrate the ability of disease-associated tau to significantly reduce translation.

2.4.4 Mutant tau and wild-type tau reduce protein synthesis at similar levels

Since mutations on tau are associated with risk for many tauopathies, we sought to determine whether mutant tau variants inhibited protein synthesis differently than wild-type tau. To this end, we performed SUnSET in iHEK cells that overexpress the disease-associated ΔK280 tau [344]. We found that expression of WT or ΔK280 tau

decreased protein synthesis (Fig. 2.4A), and that this reduction was not significantly different between the two cell lines (Fig. 2.4A). We then compared translation levels between mutant forms of tau by transiently transfecting HEK293 cells with WT, ΔK280, or P301L tau plasmids. We found no significant difference in protein synthesis levels between WT, ΔK280, or P301L expressing cells (Fig. 2.4B). These data suggest that tau expression and accumulation of hyperphosphorylated tau impairs protein synthesis, but that mutations in tau do not make this interaction between tau and ribosomes any more problematic.

2.5 Discussion

This study couples cellular and biochemical approaches with proteomics to expand the understanding of the ER-specific tau interactome. The unbiased proteomics approach (Fig. 2.1C) reported the largest change corresponded to an increase in the association of ribosomal proteins with tau in AD. Using three *in vitro* models we show that protein synthesis was significantly decreased as a consequence of the aberrant tau-ribosome association. While it has been previously reported that tau interacted with ribosomes [206, 345], the functional consequences of this interaction was unknown until now. We identified a dysfunctional consequence of tau-ribosome association that impairs protein synthesis, providing the first steps to understanding the mechanism delineating cognitive decline symptoms in tauopathic patients.

LC-MS/MS results comparing the RNA-binding proteins that associate with tau show that elongation or initiation factors do not associate with tau in AD samples (Fig. 2.1C). These data suggest that the association of pathological tau with ribosomes

abrogates the recruitment of translation factors to the tau-ribosome complex, and this could lead to reduced translation.

To avoid false positive results from the LC-MS/MS, we implemented rigorous exclusion criteria [339], which omitted well-known tau-associated proteins, but increased confidence in these interactions. Our co-IP focused on identifying mature, and not nascent, tau. We used a tau antibody (Tau46) that recognizes the carboxy-terminal tau sequence (404-441). As such, this approach obviates truncated tau species. Future efforts to identify truncated tau-associated ER proteins might determine novel pathological mechanisms.

In these LC-MS/MS studies, we only isolated a specific portion of ribosomes bound to the endoplasmic reticulum using microsomal fractionation [346]. There are additional free ribosomes found in the cell that carry out protein synthesis for proteins primarily used within the cell [347]. While membrane bound and free ribosomes are functionally extremely similar and only differ in location, their location could have a large impact on interactions with other proteins. Membrane bound ribosomes are directly [348] and stably [349] bound to the endoplasmic reticulum. This could reduce the pool of proteins that are able to interact with these ribosomes by directly blocking a potential binding site. Future experiments should be conducted comparing tau-associated ribosomal proteins in free and bound ribosomes to determine overlap between the two. Additionally, determining the sites where tau binds to ribosomes could also clarify this.

Although tau mutations are not typically associated with risk for AD, there are 48 tau mutations that are associated with onset of other tauopathies (reviewed in [350]). The

defining pathological hallmark of tangles in AD is hyperphosphorylated tau [188]. Interestingly, using *in vitro* models, we found that protein synthesis was impaired equally by WT and two disease-associated mutant tau variants: P301L and ΔK280. P301L tau is most commonly associated with frontotemporal dementia and Parkinsonism linked to chromosome 17 (FTDP-17) [148]. Expression of this form of tau in the rTg4510 transgenic mice leads to earlier onset and robust neurofibrillary tangle formation [70]. The ΔK280 tau mutant is also associated with FTDP-17 [344], as well as AD [351]. The presence of this mutation decreases tau's ability to bind to microtubules [352], and leads to increased tau aggregation [353]. Our findings indicate that tau-mediated impairment of protein synthesis could be a common mechanism of neuronal dysfunction between tauopathies.

Interestingly, oligomers of other proteins (α-synuclein and insulin) did not alter ribosomal function. This finding suggests that there is a mechanism of ribosomal downregulation that specifically implicates tau, but not all other oligomeric and pathologically altered proteins. However, it is possible that proteins involved in the pathogenic mechanisms of other neurodegenerative disorders such as Aβ, poly-glutamines, and TDP-43 could also inhibit *de novo* protein synthesis.

Characterization of this ribosome-directed molecular mechanism of tauopathies could provide novel therapeutic opportunities. For instance, therapeutic strategies aiming to uncouple pathological tau from the ribosome might restore RNA translation and prove effective to treat AD and other tauopathies. To do this, specific ribosomal proteins that associate with tau need to be identified as well as the discreet regions where tau binds to

these proteins. This would guide the proof-of-concept use of peptides resembling these amino acid stretches to outcompete tau from associating with the ribosome and thereby restore protein synthesis.

This work suggests a direct effect of tau on translation by its association with ribosomes; however, there is also an indirect relationship between tau and translation. One of these is the chronic activation of the protein kinase RNA-like endoplasmic reticulum kinase (PERK). Accumulation of tau impairs ER-associated degradation (ERAD), which then activates the unfolded protein response (UPR) and subsequently the PERK pathway [334]. The prolonged activation of the PERK pathway leads to a reduction in RNA translation through phosphorylation of the initiation factor eIF2α [354]. This alteration could be a cumulative result of tau's direct and indirect effects on translation. Our study provides further evidence that tau's involvement in disease is multi-faceted, that pathological tau heavily affects translation of proteins, and that the tau-ribosome complex could serve as a key therapeutic target for tauopathies.

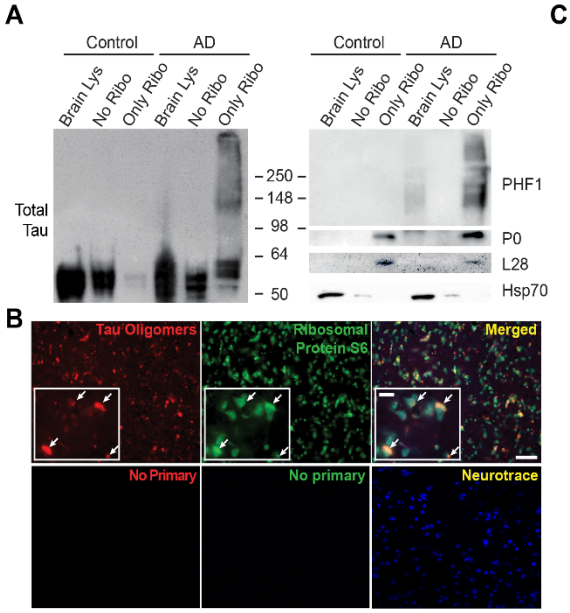

C

Tau Associated RNA-Binding proteins		
Unique to AD samples	***Common in AD and Control***	***Unique to Control samples***
60S ribosomal protein L23	60S ribosomal protein L19	60S ribosomal protein L18
60S ribosomal protein L24	60S ribosomal protein L14	60S ribosomal protein L15
60S ribosomal protein L35	60S acidic ribosomal protein P2	60S ribosomal protein L29
60S ribosomal protein L10	60S acidic ribosomal protein P1	60S ribosomal protein L17
60S ribosomal protein L13a	60S ribosomal protein L26-like	60S ribosomal protein L26
60S ribosomal protein L21	40S ribosomal protein S17	60S ribosomal protein L23a
40S ribosomal protein S23	40S ribosomal protein SA	Phenylalanyl-tRNA synthetase α-chain
40S ribosomal protein S3a	40S ribosomal protein S25	
40S ribosomal protein S13	40S ribosomal protein S7	
60S acidic ribosomal protein P0	Eukaryotic translation initiation factor 4H	
60S acidic ribosomal protein P0-like	Eukaryotic translation initiation factor 5A-1	
Putative 60S ribosomal protein L13a-like	Elongation factor 2	
WD repeat-containing protein 33	Elongation factor Tu	
Kinesin heavy chain isoform 5C	Phenylalanyl-tRNA synthetase β-chain	

Figure 2.1: Tau associates with ribosomes in the brain. (A) Representative immunoblot showing association of tau with sub-cellular fractions from human brain samples. While some tau is found in the ribosomal fraction of control brains, the interaction is much stronger in AD brains. Ribosomal proteins P0 and L28, and cytosolic protein Hsp70, were used to confirm that the fractionation was successful. (B) Representative IF of human AD brains showing overlap of oligomeric tau with ribosomal protein S6. (C) Table of tau associated RNA-binding proteins found to interact in human AD and control brains using co-immunoprecipitation followed by LC-MS/MS.

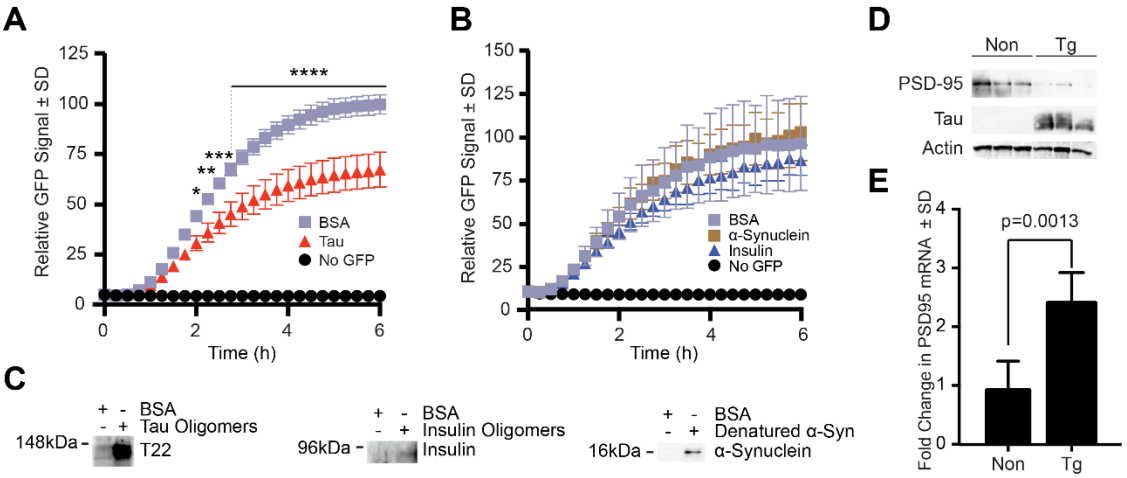

Figure 2.2: Tau reduces translation of protein, not transcription of mRNA. (A) IVT graph showing reduction of translational output as measured by GFP fluorescence (after 6h) in wells with tau oligomers compared to BSA control. Each sample was run in triplicate and each point on the graph is the average of those triplicates. (B) IVT graph showing no reduction in GFP fluorescence in wells with oligomeric α-synuclein and insulin compared to BSA. Each sample was run in triplicate and each point on the graph is the average of those triplicates. (C) Immunoblots confirm the presence of oligomers in the translation assay; α-synuclein samples were denatured to yield monomers because high molecular weight oligomeric conformers are not detectable with anti-α-synuclein antibodies. (D) Representative immunoblot and (E) quantification of RT-PCR of transgenic and non-transgenic homogenates from primary neuronal cultures. The levels of PSD-95 mRNA were significantly increased, but the levels of PSD-95 protein were significantly reduced in the rTg4510 mice compared to non-transgenic controls (p=0.0013 by t-test). N=3 for both non-transgenic and transgenic analyses.

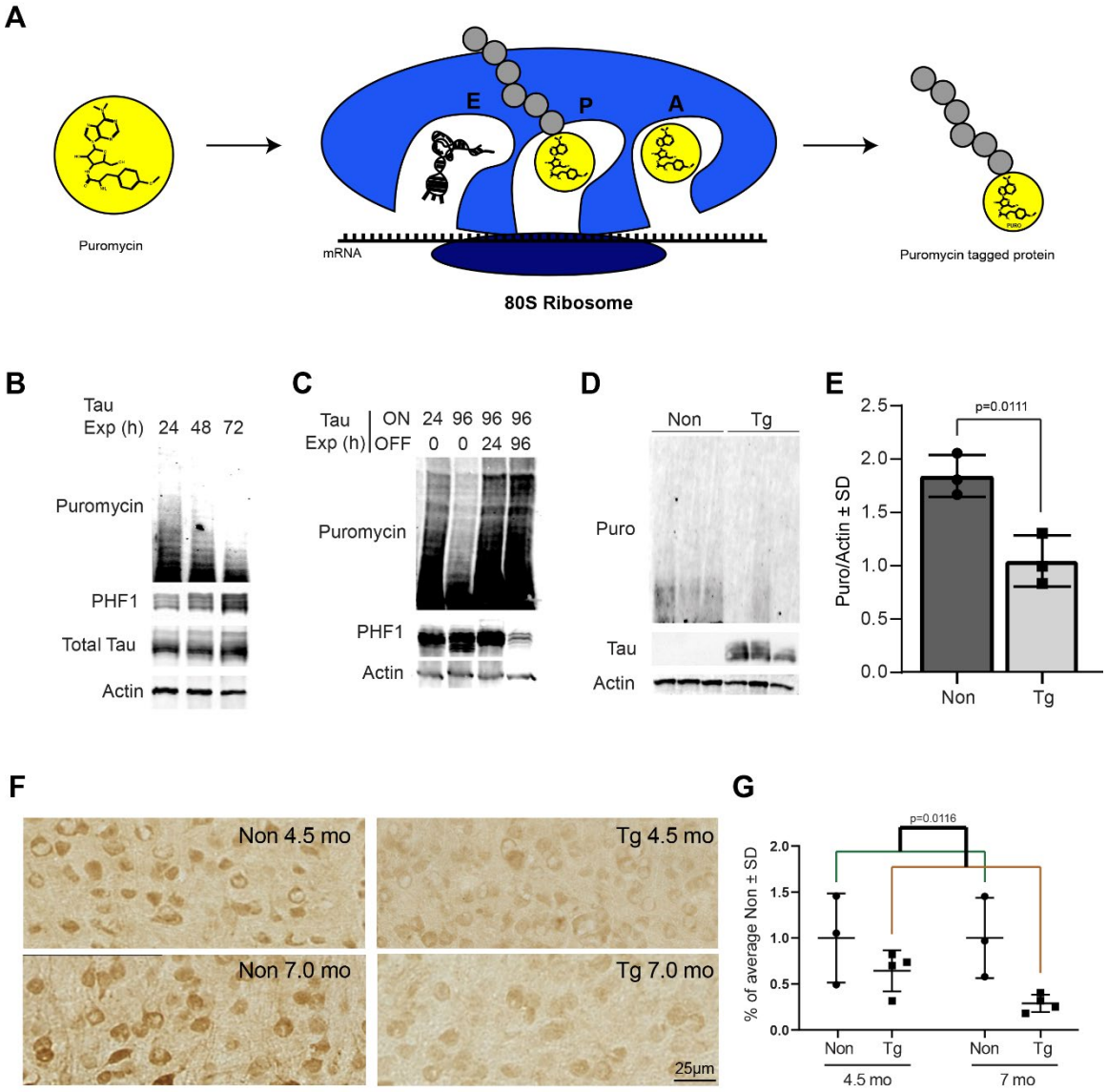

Figure 2.3: Tau reduces translation in vitro and in vivo. (A) Schematic demonstrating the basic mechanism of action for the SUnSET puromycin-based assay. (B) Immunoblot showing total and PHF1 tau are inversely proportional to the rate of protein synthesis. iHEK-Tau cells stimulated with tetracycline to express tau increasing levels of tau over time show a decrease in protein translation as measured by puromycin levels. (C) Immunoblot showing that removal of tetracycline and subsequent cessation of tau expression restores protein synthesis. (D) Immunoblot showing puromycin and total tau levels in primary neuronal cultures from non-transgenic and transgenic mice. (E) Quantification of immunoblot showing significant reduction of protein synthesis in transgenic primary neurons compared to non-transgenic primary neurons (p=0.0111 by t-test). N=3 for primary neuronal culture analysis. (F) IHC staining of puromycin in non-transgenic and rTg4510 transgenic mice. (G) Quantification of IHC staining showing a significantly different amount of puromycin positive signal between non-transgenic mice and transgenic mice (p=0.0116). Puromycin positive signal is not affected by age (p=0.3297). Analysis of puromycin positive signal in IHC by standard two-way ANOVA.

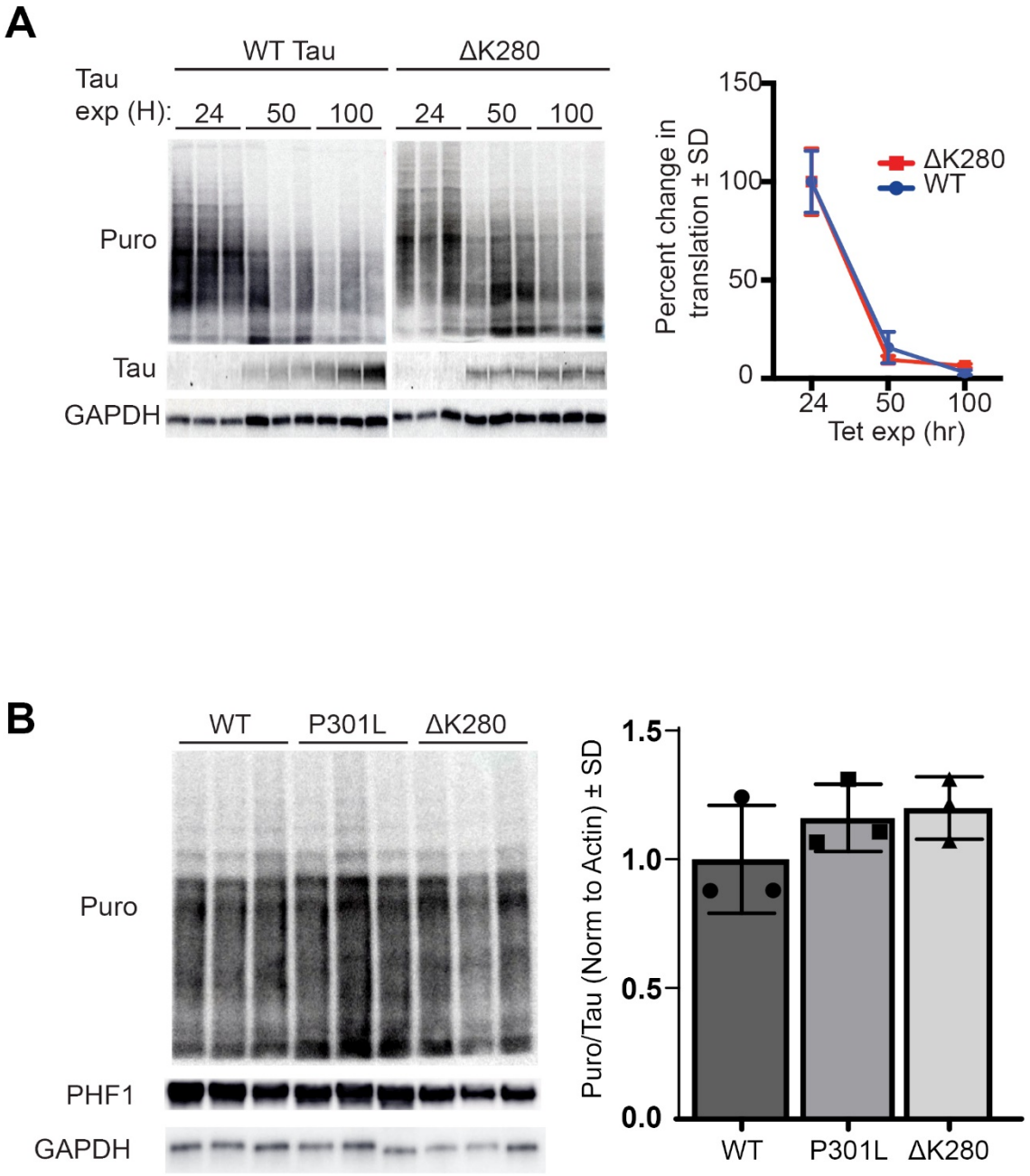

Figure 2.4: Wild-type and mutant tau reduce translation at similar levels. (A) Representative immunoblot showing reduction in protein translation over time in WT and ΔK280 cells. Quantification of puromycin signals at each time point show no significant difference between wild-type or ΔK280. (B) Representative immunoblot showing reduction in protein translation is similar between wild-type, P301L, and ΔK280 cells. Quantification shows no significant difference of puromycin signals between cell types (p=0.3328 by One-way ANOVA).

CHAPTER 3. DIFFERENTIAL EFFECTS OF TBI ON PRE-TANGLE AND TANGLE TAU PATHOLOGY

3.1 Introduction

According to the CDC, TBI is a major health concern. Data from 2014 show 2.87 million emergency department visits were related to TBI [355]. The link between TBI and development of tau pathology is an intensely researched topic, with investigators from many different backgrounds and specialties coordinating research efforts. Following injury, tau becomes phosphorylated in both animal models of TBI and in human diseases associated with TBI like CTE [269]. Additionally, phospho-tau positive NFTs are found in the brains of people diagnosed post-mortem with CTE [36], and the definitive diagnostic criteria for CTE are tau centric [32] as described in Chapter 1. As head trauma is a risk factor for CTE, there is increasing interest in understanding how TBI affects NFT formation.

Primary injuries to the brain from TBI cause activation of physiological response mechanisms that lead to widespread cellular dysfunction and secondary injuries [269]. Some types of cellular dysfunction observed after TBI, such as neuroinflammation [74, 271, 273-277, 356, 357] and oxidative stress [294-300], can cause tau hyperphosphorylation and aggregation in models of chronic tauopathies. However, it is still unknown if this cellular dysfunction contributes to the development of tau pathology in TBI.

Current understanding of the link between TBI and tau pathology is limited to how TBI affects post-translational modifications of tau. The vast majority of reports in

rodent models of TBI that investigate tau phosphorylation after injury show changes [269, 358, 359]; however, as phosphorylation of tau does not always lead to development of neurofibrillary tangles [113, 123, 124] we still do not understand how tangles develop after TBI. One of the possible reasons why our knowledge is lacking is because endogenous mouse tau does not form tangles. To date, the only study to report any NFT deposition after injury utilized a transgenic mouse model expressing the shortest isoform of human tau that underwent multiple closed head injuries [268]. Out of the 12 mice that underwent the injury paradigm, only one mouse showed increased NFT deposition 9 months after sustaining injuries [268]. Since the transgenic mouse model in that study did not show robust increase in tangle deposition after injury [268], and no other reports of tangle deposition in any other model have been reported, we chose to use the rTg4510 mouse model of tauopathy for experiments in this chapter. This model expresses a human mutant form of tau (P301L) [70] that is naturally prone to aggregation and NFT development [360]. Additionally, expression of tau in this model can be suppressed with doxycycline [70]. NFT deposition begins at 2.5 months of age and progresses in an age dependent manner [70, 330]. Suppression of tau expression by doxycycline does not clear the brain of NFTs that are already present [70].

The goal of this study was to investigate the isolated effects of TBI on pre-fibrillar tau and fibrillar tau in NFTs. To study the effect of brain injury on pre-fibrillar tau we used mice at the age of 2 months. At this age, abnormal conformational and phosphorylation changes are observed but mature tangle deposition is extremely rare [70, 330]. To study the effect of brain injury on fibrillar tau in NFTs we used mice that were placed on a doxycycline diet at 3 months of age and injured at 4.5 months of age.

Administration of doxycycline for six weeks allowed the tau that was not already included in mature tangles to be cleared or recruited into existing tangles [70, 158]. Suppression of tau using doxycycline was especially important during this experiment, as it minimized the possibility of detecting non-fibrillar tau that was not originally from a tangle. In both groups, tissue was collected 24 hours and 7 days post-injury.

We hypothesized that TBI would increase tau phosphorylation (as previously reported [241, 251]) and would accelerate tau fibrillization in the 2 month old rTg4510 mice. We found that TBI affects tau phosphorylation but does not lead to fibrillization within the first 7 days after injury. We also hypothesized that TBI would cause breakdown of NFTs in the cortex, which would lead to an increase in levels of non-fibrillar tau. We also hypothesized that TBI would decrease NFT numbers in 4.5 month old rTg4510 mice. We were unable to discern if NFTs were broken down in to non-fibrillar tau due to technical limitations, but we found that TBI does not significantly decrease tangle counts.

3.2 Materials and Methods

rTg4510 tau transgenic mice: To minimize repetitiveness, a detailed explanation of the rTg4510 model can be found in Chapter 1. For experiments in this chapter the rTg4510 mice were used because of the ability to control tau expression and the rapid onset of extreme tau pathology. This mouse model is a double transgenic model on an FVB background carrying a tetracycline responsive element upstream of human 4R0N P301L tau cDNA that express human tau at 13 times higher levels than endogenous mouse tau [70, 330]. Administration of doxycycline to these mice suppresses tau expression. These

mice show abnormal conformational changes in tau as early as 1 month of age, abnormal tau phosphorylation occurring as early as 2 months of age, and mature tangle deposition occurring as early as 2.5 months of age [70, 330]. Pathology progression is age-dependent and sex-dependent differences have been reported as early as 5.5 months of age with female pathology being worse than male [361].

Male and female rTg4510 mice were used for this study. A total of 54 mice were used in this study, of which 24 mice did not receive doxycycline. The 24 male and female mice that did not receive doxycycline diet were used study the effects of TBI on pre-fibrillar tau ($n_{24hrSham}$=6, $n_{24hrCCI}$=7, $n_{7daySham}$=6, $n_{7dayCCI}$=5). The 30 mice that did receive doxycycline diet were used to study the effects of TBI on fibrillar tau in NFTs ($n_{24hrSham}$=8, $n_{24hrCCI}$=8, $n_{7daySham}$=8, $n_{7dayCCI}$=6). These mice received 0.625 g/kg doxycycline feed (Envigo, Teklad Cusom Diet, #TD.01306) *ad libitum.* Doxycycline feed was started at 3 months of age, and continued on until they were euthanized. This study was approved by the University of Kentucky Institutional Animal Care and Use Committee and conformed to the National Institutes of Health Guide for the Care and Use of Animals in Research.

Controlled cortical impact (CCI) injury: Male and female mice underwent sham or CCI injury at 2 or 4.5 months of age. Mice were anesthetized with vaporized isoflurane in a closed chamber at 5% v/v until they no longer responded to toe pinch reflex. Mice were then secured in a stereotactic frame and anesthesia was maintained at 3% v/v for the duration of the surgery (approximately 30 minutes per mouse). Artificial tears were applied to the eyes to prevent drying. Mice were kept on a heating pad to maintain body

temperature throughout the surgery. To remove fur on top of the head, hair removal cream (Nair) was applied to the top of the head for roughly two minutes. Hair removal cream was wiped off with a paper towel and remaining cream was cleaned off using a wet paper towel. The surgical site was sterilized by alternating applications, starting with Betadine and ending with 70% ethanol. After sterilization, a midline incision was made to expose the skull. A roughly 5mm in diameter craniotomy was performed lateral from the midline suture and centered between lambda and bregma. An electromagnetic impactor (Leica, ImpactOne) was used to injure the animal. The injury was delivered at 1.0mm depth, 100ms dwell time, 5.0 m/s and was centered in the craniotomy. These injury parameters were intended to yield a mild to moderate injury as previously published [241]. The injury site was covered with a cranioplasty created from dental mold material and the cranioplasty was secured with super glue. The incision was sutured closed with 4-0 Nylon sutures. Immediately after surgery completion, mice received 1mL intraperitoneal injection of sterile saline to aide in recovery. Mice recovered in an empty animal cage situated so that half the bottom was touching a heating pad and half the bottom was not. After surgery, mice were placed in a clean animal housing cage with moistened chow on the floor. Sham animals underwent all procedures except impact. To ensure scientific rigor, surgeries were randomized by surgery type (sham vs CCI) and time point (24 hours and 7 days).

Euthanasia and tissue harvest: Mice were anesthetized with vaporized isoflurane in a closed chamber at 5% v/v until they no longer responded to toe pinch reflex. Mice then underwent cardiac perfusion using a perfusion pump. For staining analyses, mice were perfused with 0.9% saline for 5 minutes followed by ice-cold 4% PFA for roughly 2

minutes. Mice were decapitated and whole heads were placed in 50mL conicals with 4% PFA for 48 hours. After this fixation period, skulls were removed and whole brains were placed in 4% PFA for an additional 24 hours. Brains were then cryoprotected in 30% sucrose for 24 hours and then sectioned at 25µm thick on a freezing stage sliding microtome. Sectioned tissue was stored at 4 degrees Celsius in PBS plus sodium azide. For western and dot blot analyses, mice were perfused with 0.9% saline only for approximately 7 minutes. Mice were decapitated and brains were removed from the skull. Brains were separated into ipsilateral (craniotomy/injured side) and contralateral (non-craniotomy/impacted side) cortex, hippocampus, and cerebellum. The rest of the brain was then collected in a separate tube. All regions were then flash frozen in liquid nitrogen.

Immunofluorescent staining: Tissue was mounted onto ColorFrost Plus slides using a solution of 30% ethanol in water and allowed to dry at room temperature for approximately 1 hour. Slides were then framed with a hydrophobic pen and allowed to dry at room temperature for an additional 15 minutes. Slides were blocked with immunofluorescent blocking buffer (IFBB: 10% normal goat serum, 0.2% Triton-X100, 0.02% sodium azide in 1X TBS). at room temperature for 2 hours on a horizontal shaker. Primary antibodies were diluted in IFBB and slides were incubated in IFBB with primary antibody (HT7, 1:1000, Thermo, cat#MN1000) overnight at 4 degrees Celsius on rotating shaker. The following day slides were rinsed with TBS twice for 5 minutes per rinse. Slides were then incubated in IFBB + secondary antibody (Alexafluor, Rabbit 594, 1:1500) at room temperature for 2 hours. Slides were washed in TBS four times for 5 minutes per wash. Slides were then incubated in 0.1% Sudan Black B in 70% ethanol and

washed with TBS + 0.1% Tween-20 four times for 5 minutes per wash. Slides were then incubated in 100mM 1-Fluoro-2,5-bis(3-carboxy-4-hydroxystyryl)benzene (FSB) at room temperature on horizontal shaker for 30 minutes. Slides were then washed with TBS + 0.1% Tween-20 four times for 5 minutes per wash. Slides were then coverslipped using Fluoromount-G and edges were sealed with nail polish. Nail polish was allowed to dry at room temperature for 1 hour and then slides were kept at 4 degrees Celsius until imaging.

In these experiments the biochemical dye FSB (Dojindo Molecular Technologies, cat#F308-10), a fluorescent Congo red derivative, was used to detect the beta sheet structures found in tau tangles. This dye is particularly important in isolating tangle formations as typical antibody staining methods are unable to differentiate between non-tangle and tangle tau.

Fluorojade C staining was performed as previously described [362] with modifications. After imaging the HT7 and FSB stain, coverslips were removed from the slides and slides were washed in TBS-T to remove mounting media. Slides were quickly dipped in 95% ethanol to remove previous Sudan Black B stain. Slides were then reframed with the hydrophobic pen and washed in TBS for 5 minutes. To quench nonspecific reactivity to fluorojade C stain, slides were incubated in DAB prepared according to the manufacturer's instructions (Vector Laboratories, DAB peroxidase Substrate Kit, cat# SK-4100) for 5 minutes. Slides were washed in TBS for 5 minutes and then allowed to dry on slide warmer set at 40-45 degrees Celsius for 20 minutes. After drying, slides were incubated for 5 miinutes in 1% NaOH in 80% ethanol Slides were then incubated for 2 minutes in 70% ethanol. Slides were then incubated for 2 minutes in

deionized water, followed by an incubation for 10 minutes in 0.06% potassium permanganate. Slides were then rinsed in deionized water four times. Slides were then incubated for 10 minutes in 0.01% Fluorojade C in deionized water. Slides were then rinsed 5 times in deionized water. Slides were kept from light and air dried at room temperature for 5 minutes. Slides were additionally dried for 30 minutes at 50 degrees Celsius on slide warmer. Slides were then incubated twice in xylene for 10 minutes per incubation. Slides were then coverslipped with Cytoseal (Thermo, cat# 831016) and kept from light.

Imaging: Slides were imaged using Nikon TiE and C2+ Confocal. Images of the FSB and HT7 stain were taken using the 20X and 100X objective. Images of the Fluorojade C staining were taken using the 10X objective on a bright field microscope. All acquisition intensities, field sizes, and settings were kept consistent across all images.

Image quantification and analysis: To quantify non-fibrillar tau levels after injury, we utilized the Imaris software developed by Oxford Instruments. The proprietary ND2 files taken at 100X on the Nikon TiE and C2+ confocal microscope were uploaded into the Imaris software. The positive signals from the HT7 stain and the FSB stain were rendered into separate 3D objects. The total volume of the HT7 channel was the value for fibrillar and non-fibrillar tau. The FSB channel was set as the mask channel (this measurement was only fibrillar tau) and the volume of overlap between the FSB channel and the HT7 channel was calculated. The overlap volume was then subtracted from the total HT7 volume to determine the non-fibrillar tau volume. Final measurements obtained were the total fibrillar tau (FSB channel volume only), the total fibrillar and non-fibrillar tau

volume (HT7 channel volume only), and the total non-fibrillar tau volume (HT7/FSB overlap subtracted from the HT7 alone).

To calculate the number of NFTs after injury proprietary ND2 files were converted to maximum projection PNG files using FIJI software. Max projection images of the FSB stain were compiled into a single folder and tangle counts were performed using MatLab. The MatLab script written to analyze tangle counts filtered out background staining by setting the threshold for stain intensity. It also filtered out objects (like tissue edge fragments or speckles) by size exclusion criteria that were set based on tangle size. Tangle counts were averaged across 3-4 pieces of tissue, with each piece of tissue being roughly 500µm apart.

Tissue homogenization and biochemical separation of tau: Separation of sample into different fractions is especially useful and one of the few ways to investigate the biochemical states of tau. The whole neocortex homogenate contains all types of tau observed in the sample (fibrillar and non-fibrillar) and provides a general, nonspecific overview of protein status. The sarkosyl-insoluble fraction contains only sarkosyl-insoluble tau which is biochemically characterized as beta sheet enriched, fibrillar tau. This form of tau seeds non-filamentous tau and develops into neurofibrillary tangles [158]. This fraction does not differentiate between straight filaments or paired helical filaments. This method of fractionation has been previously characterized in this mouse line [98]. The protocol performed here is referred to as “Protocol A” in this publication [98].

A master conical of homogenization buffer was prepared buffer (Homogenization buffer: 10µL phosphatase inhibitor, 10µL Protease Inhibitor Cocktail 2 (EMD Millipore, 535140), 10µL Protease Inhibitor Cocktail 3 (EMD Millipore, 539132), and 10µL 100mM PMSF for every 1mL of Hsiao TBS (50mM Tris Base, 274mM NaCl, 5mM KCl at pH8.0)) and kept on ice. Neocortical tissue was weighed and a volume of homogenization buffer was added to the tube at ten times the weight of the tissue. Tissue was homogenized for 30 seconds using a mounted tissue homogenizer. Samples were then ultracentrifuged at 13,000*xg* for 15 minutes at 4 degrees Celsius. The supernatant was then transferred to a new tube and labeled as "Whole Neocortex homogenate". Protein concentration of the whole neocortex homogenate was determined by BCA. After this, 400µg of protein from this supernatant was taken to begin biochemical fractionation steps. Sample volumes were brought to the same volume using Hsiao TBS. Samples were ultracentrifuged at 100,000*xg* for 23 minutes at 4 degree Celsius. The supernatant was transferred to a new tube and labeled "S1". The pellet was then homogenized with 300µL of Buffer B (Buffer B: 10mM Tris pH7.4, 0.8M NaCl, 10% sucrose, 1mM EGTA, 1mM PMSF) using a handheld pestle homogenizer until pellet was completely resuspended. Samples were then ultracentrifuged at 100,000*xg* for 23 minutes at 4 degrees Celsius. The supernatant was transferred to another tube and incubated on a rotating shaker at 225 rpm with 1% v/v sodium lauroyl sarcosinate (sarkosyl) at 37 degrees Celsius for 1 hour. After incubation, samples were ultracentrifuged at 100,000*xg* for 45 minutes at 4 degrees Celsius. The supernatant was transferred to another tube and labeled the sarkosyl-soluble fraction while the pellet was resuspended in 50µL of 2X Laemmli buffer with 62.5mM DTT and labeled the sarkosyl-insoluble fraction.

Western blotting: Whole neocortex homogenate sample was prepared by adding 4X Laemmli buffer with beta mercaptoethanol to 7.5µg of sample. For gels analyzing the sarkosyl-insoluble samples, 10µL of final sarkosyl-insoluble fraction was taken. All samples were boiled at 100 degrees Celsius for 15 minutes. Samples were run in a 7.5% Tris-Glycine gel (Bio-Rad) and were wet transferred onto PVDF membrane. The membranes were blocked in 5% milk or bovine serum albumin in TBS+0.1% Tween-20 at room temperature for 1 hour. Membranes were then incubated overnight in primary antibodies at 4 degrees Celsius. Primary antibodies used were AT8 (Thermo, cat# MN1020) at 1:500, HT7 (Thermo, cat# MN1000) at 1:1000, and Actin (Cell Signaling, cat# 4970) at 1:2000. Bands were detected using horse radish-peroxidase conjugated secondary (Rabbit - Southern Biotech, cat# 4055-05, Mouse – Thermo, cat#G-21040), ECL kit (Thermo, cat#32106), and film. All samples from each isolated fraction (whole neocortical homogenates, cytosolic S1, sarkosyl-soluble, and sarkosyl-insoluble) were run on the same blot and transferred to the same membrane.

AT8 and HT7 antibodies were developed on the same membrane. The membrane was incubated in AT8 first, then stripped using a gentle stripping buffer (0.015% Glycine, 0.001% SDS, 0.01% Tween-20 in 500mL distilled water, pH 2.2). The membrane was incubated in the stripping buffer on a horizontal shaker for two 7 minute washes. The membrane was then washed twice in TBS + 0.01% Tween-20 for 5 minutes. The membrane was then blocked in 5% milk at room temperature for 1 hour and incubated overnight in HT7 antibody.

Western blot quantification and analysis: Films were digitized using an Epson Perfection V800 Photo Color Scanner at 300dpi and saved as .tif files to minimize data loss through scanning. Bands of interest were quantified using ImageJ software to find the area under the curve. Raw values were copied into Excel where they were then normalized to the actin loading control values. To quantify tau phosphorylation levels, AT8 was normalized to HT7 after both values had been individually normalized to actin. This method gave us a ratio of phospho-protein to total protein. These values were then plotted in GraphPad Prism and analyzed using Student's t-test.

Dot blotting: The dot blot apparatus was set up according to manufacturer's instructions (Whatman, Minifold-I Dot Blot System, cat# 10447900). A dot blot was used to investigate tau oligomerization due to the antibody's ability to detect only oligomers that were not significantly denatured. For the whole neocortex homogenate and TBS-soluble fractions, 7.5ug of sample was used. For the sarkosyl-soluble and sarkosyl-insoluble fractions 3uL of sample was used. Samples were vacuumed through a nitrocellulose membrane, which was then blocked in 5% milk at room temperature for 1 hour. Total protein load for whole neocortex homogenate and TBS-soluble fractions was measured for the whole neocortex homogenate using the LICOR ReVERT Total Protein Stain (Licor, Cat#926-11011) prior to blocking. Membrane was then incubated with primary antibody overnight at 4 degrees. The primary antibody used was T22 (EMD Millipore, cat# ABN454) at 1:500. Whole neocortex homogenate dot blot signal was detected using the infrared conjugated Licor secondary (Licor, IRDye 800CW, cat#926-32211). TBS-soluble, sarkosyl-soluble, and sarkosyl-insoluble dot blot signals were detected using

horse radish-peroxidase conjugated secondary (Rabbit - Southern Biotech, cat# 4055-05, Mouse – Thermo, cat#G-21040), ECL kit (Thermo, cat#32106), and film.

Dot blot quantification and analysis: Quantification of dot blot intensities was performed using the Licor Image Studio Lite software. Background intensity was subtracted from sample intensity to give the final intensity of each experimental data point. These values were copied to Excel where T22 was normalized to the ReVERT loading control. These normalized values were then plotted in GraphPad Prism and analyzed using Student's t-test.

3.3 Results

The overall objective of this chapter was to understand the effects of TBI on pre-tangle and tangle-only pathology. We hypothesized that TBI would increase tau phosphorylation (as previously reported [241, 251]) and would accelerate tau fibrillization in the 2 month old rTg4510 mice. We also hypothesized that in 4.5 month old rTg4510 mice with only tangle pathology, TBI would cause breakdown of NFTs into non-fibrillar tau in the cortex. Finally, we hypothesized that TBI would reduce overall NFT numbers in 4.5 month old rTg4510 mice.

Male and female rTg4510 mice that were 2 months of age were used to study the effects of TBI on pre-tangle tau. At this age, abnormal conformation and phosphorylation of tau are present but mature tangle formation is extremely rare [330]. These mice were subjected to CCI injury and euthanized 24 hours or 7 days after injury. The 24 hour time point was chosen based on previously published work showing an increase in AT8 and

total tau levels in the hippocampus after CCI at these time points [241, 251]. The 7 day time point was chosen as it was the earliest time point we believed we would be able to detect tau fibrillization.

We also chose to study the effects of TBI on isolated tangle pathology. One group at particularly high risk of receiving a TBI according to the CDC are people ≥ 75 years old [363]. NFT deposition is observed in 98% of brains aged 75 years or older at time of autopsy [364]. As that is an overwhelming majority of people showing tangle pathology that are at a high risk for TBI, we believed it was important to investigate the effects of TBI on tangles pathology alone as well.

To study the effects of TBI on NFT pathology 3 month old male and female rTg4510 mice were placed on a doxycycline diet until time of euthanasia. In this model tangle deposition has started at 3 months of age but it is not yet overt. The administration of doxycycline to these mice suppresses additional production of human P301L tau for as long as they are kept on the diet [70]. Six weeks of doxycycline administration at this concentration is the minimum amount of time to allow suppression of new tau production and to allow any non-tangle tau to be recruited into tangle or cleared from the brain [158, 330]. Suppression of tau using doxycycline was especially important during this experiment, to minimize identification of non-fibrillar tau that did not come from a tangle. At 4.5 months of age these mice were subjected to CCI injury and euthanized 24 hours or 7 days after injury.

3.3.1 Prior to overt tangle formation CCI alters tau phosphorylation at 24 hours and 7 days post-injury, but only alters oligomerization at 24 hours post-injury.

For clarity on findings from all fractions, a table is provided (Table 3.1). Using the whole neocortex homogenate (Figure 3.3A – red box) we investigated changes in total tau phosphorylation and oligomerization after injury. At 24 hours post-injury, tau phosphorylation was decreased in the ipsilateral cortex of injured mice compared to shams. Interestingly, at 7 days post-injury tau phosphorylation was increased in the ipsilateral cortex of injured mice compared to shams. At both time points total tau levels were not significantly different between sham and injured mice (Figure 3.2A). At 24 hours post-injury, tau oligomerization was decreased in the ipsilateral cortex of injured mice compared to shams but by 7 days we found no significant difference between sham and injured mice (Figure 3.2B).

3.3.2 Prior to overt tangle formation, CCI does not increase tau fibrillization at 24 hours or 7 days post-injury

To identify changes in fibril formation after injury, the ipsilateral neocortex homogenates from sham and injured 2 month old rTg4510 mice were subjected to fractionation. The fibrillar state of tau can be determined using sarkosyl, a detergent, and high speed centrifugation. The final fraction obtained after incubation with sarkosyl and centrifugation is known as sarkosyl-insoluble tau (Figure 3.3A – P3 pellet, blue box). This fraction contains beta sheet-enriched, fibrillar tau that seeds non-fibrillar tau and develops into neurofibrillary tangles [47, 158]. This fraction does not differentiate the types of fibrils found (straight or paired helical filaments). For this fraction we only

looked at total tau, as that would provide insight to all tau rather than a specific subset of tau.

At 24 hours post-injury, total tau levels in the sarkosyl-insoluble fraction of injured mice were significantly decreased compared to shams while at 7 days post-injury they were not significantly different (Figure 3.3B). Sarkosyl-insoluble oligomeric tau levels were not significantly different at 24 hours or 7 days post-injury (Figure 3.3C). Taken with the data from Figure 3.2, these data suggest that fibril formation does not increase within 7 days of injury even though post-translational modifications of tau are occurring.

As the results showing no tau fibrillization after injury were unexpected, we decided to investigate the other two fractions obtained in the sarkosyl fractionation process. The S1 fraction (Figure 3.3A – orange box) contains the TBS-soluble tau found in the cytosol. The S2 fraction (Figure 3.3A – green box) contains the sarkosyl-soluble tau. It is suggested that these two fractions contain toxic soluble forms of tau discussed in chapter 1 [68, 98]. At both the 24 hour and 7 day post-injury time points, TBS-soluble phosphorylated, oligomerized, and total tau levels were not significantly different between sham and injured mice (Figure 3.4A-B). At 24 hours post-injury sarkosyl-soluble total tau levels were significantly decreased but at 7 days post-injury they were not significantly different (Figure 3.4C-D) while sarkosyl-soluble oligomeric tau levels were not significantly different at 24 hours post-injury, but at 7 days post-injury they were significantly decreased (Figure 3.4 C-D).

3.3.3 At 4.5 months of age, and with mature tangle deposition, CCI does not significantly increase or decrease tangle counts at 24 hours or 7 days post-injury but it does reduce variability.

To study the effects of TBI on only fibrillar tau in NFTs, the fixed brains of sham and injured 4.5 month old rTg4510 mice were stained with HT7 and FSB. For quantification, four sections of tissue roughly 500µm apart were imaged to find the average tangle count per mouse (Figure 3.5).

We proposed to investigate the breakdown of NFTs into non-fibrillar tau after injury as part of these experiments. We theorized that we could calculate the total volume of fibrillar and non-fibrillar tau (HT7 stain) and the total volume of only fibrillar tau (FSB stain) from 100X images taken on a Nikon confocal microscope. We then theorized that we could find the volume of non-fibrillar tau by subtracting the fibrillar tau volume from the total tau volume. To do this we proposed to use the Imaris image analysis software. We were unable to successfully complete this experiment as the negative control brains reacted with the fluorescently labeled mouse secondary. This indicated that the brains had not been properly perfused and there was still endogenous IgG left behind. As the FSB was a biochemical dye, and not a mouse specific antibody, we continued with counting tangles.

At both 24 hour and 7 days post-injury, there was no significant increase or decrease in tangle count. However, we did observe a decrease in the variability of injured mice compared to shams (Figure 3.6). To confirm that there wasn't a sex-based dimorphism in the data, we separated the males and females in each group. We observed no significant difference between tangle counts in males and females in sham and injured

mice (Figure 3.7). We also performed Fluorojade C (FJC) staining to investigate the effect of cell death on tangle counts. We observed more positive signal in injured brains compared to shams; however, the increased signal was observed adjacent to the cortical regions were tangle counts were performed (Figure 3.8). This indicated that cell death did not affect tangle numbers. To ensure changes in pathology weren't occurring elsewhere we also performed count analysis in the hippocampus of sham and injured animals. Tangle numbers in injured animals were not significantly different from sham animals in the hippocampus.

3.4 Discussion

The primary purpose of this study was to investigate the effect of TBI on biochemical characteristics of tau. We used rTg4510 mice at different ages to isolate the effects on pre-fibrillar tau (2.5 month old mice) and primarily tangle pathology (4.5 month old mice on a doxycycline diet) (Figure 3.1). Following CCI injury on 2.5 month old mice, the sarkosyl-insoluble fraction was separated from the whole neocortex homogenate (Figure 3.3A). Injury caused changes in tau phosphorylation (Figure 3.2A) but it did not increase tau fibrillization (Figure 3.3B). Following CCI injury on 4.5 month old mice that had been administered doxycycline, we stained fixed tissue using FSB to detect beta sheet enriched structures in neurofibrillary tangles. We observed no significant increase or decrease observed in tangle count after injury, but sample variability was reduced after injury (Figure 3.5).

This study is the first to investigate the effects of a single injury on the biochemical characteristics of tau. The studies published to date have reported on total tau and post-

translationally modified tau in rodents after TBI through immunohistochemistry and whole sample homogenates, similar to the data in Figure 3.2. A detailed explanation of these findings based on injury model and tau type can be found in chapter 1.

The studies by Dr. David Brody's group in the 3xTg mouse model (expressing the APP KM670/671NL, MAPT P301L, and PSEN1 M146V mutations) heavily influenced this project. These studies subjected mice to single CCI injury to evaluate changes in tau and amyloid β at multiple injury severities up to 24 hours post-injury [251]. These studies only reported total tau changes by immunohistochemical staining in the ipsilateral fimbria and amygdala, and the contralateral CA1 regions [241, 251]. In the mild-moderate injured group (which most closely resembled the cavitation observed in our injured mice) total tau levels were increased in the fimbria, but not significantly different in the amygdala and contralateral CA1 at 24 hours post-injury [251]. It is unclear whether these studies investigated changes in tau in other regions as the ipsilateral fimbria and amygdala, and the contralateral CA3 were the only regions discussed in the publication. The effect of this mild-moderate CCI on total tau levels remains unclear, as reports from Dr. Brody's group using the same CCI severity and mouse model are conflicting [241, 242, 251, 365]. Additionally, changes in tau phosphorylation as measured by Western blotting of AT8 was only reported in the ipsilateral hippocampus of mice with moderate injuries (a more severe injury than our own). These injuries showed AT8 levels were increased compared to sham at 24 hours post-injury [251]. It is unclear if AT8 levels were investigated in any other region, as the ipsilateral hippocampus was the only region reported on. While this provides useful insight and information into tau changes on a general level, it does not offer specific insight into neuropathological development of tau

into tangles. These changes in tau were not observed in wild-type sham or injured mice [251].

Our experimental findings in this chapter expand upon the work previously published by Dr. Brody's group by reporting on cortical findings, effects of TBI on tau fibrilization, and effects of TBI on NFTs. Our work investigates tau in a more isolated fashion, as we used transgenic mice expressing only human tau rather than the triple transgenic model. The cortical homogenate analysis by Western blot shows that total tau levels are not significantly different from shams at 24 hours or 7 days after mild-moderate injury, but tau phosphorylation levels are different. Additionally, our findings provide insight into the question of TBI causing tau fibrillization after injury. At least in the relatively acute time frame of 24 hours to 7 days we find that it does not.

Interestingly, we found that tau fibrillization was not increased at 24 hours or 7 days after injury (Figure 3.3B). This was contrary to our original hypothesis that fibrillization would be increased after injury. As previously mentioned, this is the first study investigating the effects of a single injury on tau fibrillization. However, one study was performed to investigate the effects of repeat head injury in the T44 mouse model of tauopathy expressing the shortest isoform of human tau at 5 times endogenous mouse tau levels. In this study, mice received two injures on each side of the skull (a total of four injuries a day) once a week for four weeks (a total of 16 injuries per mouse). Out of the twelve mice subjected to injury, only one mouse showed increased neurofibrillary tangle pathology and increased fibrillar tau using biochemical separation [268]. Both our data and data from *Yoshiyama et al*. do not demonstrate a robust link between TBI and CTE;

however there are limitations to these findings. The major limitation of both these studies is time, which could be the driving factor as to why we didn't observe fibril formation. In diseases like CTE repeat TBI exposure typically occurs over 5 to >25 years [366]. Single injury mouse models and even repeat injury mouse models for a relatively short time (compared to lifetime exposure) may not be enough to induce the fibrillar changes observed in humans. Additionally, our study was limited to single injury exposure.

One of the more interesting findings we observed was that tau phosphorylation at 24 hours post-injury was decreased while tau phosphorylation at 7 days was increased (Figure 3.2A). There have been no other reports of a decrease of AT8 at 24 hours post-injury. Three different groups, all investigating the effects of blast injury, show that in rat, transgenic mouse, and wild-type mouse models there is no significant difference between AT8 levels in sham and injured rodents at 24 hours post-injury [248, 367, 368]. These studies specifically looked at cortical [248] and hippocampal tissue [367, 368]. Differences observed between our study and these studies could be due to the model of TBI used (open head CCI vs. closed head blast), as pathology changes in blast injury are usually more mild than CCI. Another group, investigating the effects of lateral fluid percussion injury on AT8 levels, reported no significant difference in AT8 levels at 3 days post injury between naïve, sham, and injured genotype-control mice in the both the ipsilateral and contralateral cortices [369]. Difference observed between our study and this study could also be attributed to TBI model differences or differences in transgenic mouse models, as this study used a genotype-control of CCR2-depleted transgenic mouse model. Additional studies show increased levels of AT8 at 7 days post- injury or later [248-250, 252], in agreement with our findings.

In speculation of what might be driving the decrease observed in AT8 at 24 hours post-injury, we can discuss major tau kinases and phosphatases. GSK3β is a major tau kinase [370] that is known to phosphorylate tau at the epitopes detected by AT8 [371]. Inhibitory phosphorylation of GSK3β at serine 9 peaks at 24 hours post-CCI injury [372]. While activation of GSK3β by phosphorylation at tyrosine 216 following injury has not been extensively studied, at least one publication reports no change in GSK3β activation at 24 hours post-injury [365]. Phosphatase activity is generally decreased after injury, with inhibition not occurring until 24 hours post-injury [373-375]. Since GSK3β (a major tau kinase) is inhibited within the first 24 hours post-injury (with no evidence that activation occurs simultaneously at that time), and phosphatase activity isn't significantly inhibited until 24 hours post-injury, it is reasonable to suspect that the decreased AT8 levels could be driven by activity of phosphatase within the 24 hours acute window. The increase in phosphorylation observed at the later time point of 7 days post-injury could be due to the switch from kinase inhibition/phosphatase activation to kinase activation/phosphatase inhibition.

Our findings on tau oligomerization (Figure 3.2B) also differ from the findings of other publications. However, detailed understanding of oligomeric tau after TBI is extremely limited as there are only 4 publications showing changes in tau oligomerization after injury. Following lateral fluid percussion injury in rats, tau oligomerization is increased in the hippocampus but not the cortex at 24 hours post-injury [252]. Following blast injury in wild-type mice, tau oligomerization is increased in the hippocampus at 24 hours post-injury [265] and 72 hours post-injury in the cortex [267]. Following repeat closed head injury of 2 weekly impacts for 3-4 months, tau oligomerization is increased

at 6 months post-injury [266]. It is possible that we found a decrease in tau oligomers at the 24 hour time point because the blood brain barrier breakdown peaks around 24 hours after CCI but is restored by 9 days post-injury [310]. The relatively leaky blood brain barrier at 24 hours post-injury could allow more oligomers to leak into the CSF and blood stream after injury, which would cause fewer oligomers to be present and detectable in the cellular homogenates used in our studies. We believe that as the 7 day time point is much closer to the 9 day reported time point where barrier integrity is restored, the detection of oligomers in the cellular homogenates is not significantly decreased. Tau oligomers have not explicitly been observed in CSF or blood after injury; however, oligomeric tau has been detected in the sera and CSF of AD patients [376].

In investigating the effect of TBI on NFTs, we utilized the rTg4510 model by placing 3 month old mice on doxycycline diet for 6 weeks. At this age mice show tangle deposition and, by placing them on a doxycycline diet, tau expression is suppressed. Any tau not already in a tangle is recruited into a tangle or cleared from the brain [70, 158]. Three months of age is the earliest we chose to place the mice on doxycycline as that is the earliest age they start to consistently show tangle deposition. This age was chosen as to allow tangle deposition to occur, but to minimize the risk of death by injury due to older age. In analyzing the tangle counts at the 24 hour and 7 day time point (Figure 3.5) we saw no significant increase or decrease from the injured mice compared to sham, but we did see a reduction in variability. It is possible that there is a floor effect on these data, as many of the CCI data points are approaching zero but the sham animals also have a spread of zero to eighty tangles. In future experiments this would be corrected by aging the mice to 4.5 months (when significant cortical tangle deposition has occurred) and

then placing them on a doxycycline diet for 6 weeks. This would allow for higher baseline tangle counts in the sham animals, and a more accurate view of what injury does to tangles without the floor effect. It is also possible that TBI does not have any effect on NFTs (as we saw neither an increase nor a decrease in tangle counts after injury). This could mean that in terms of tau pathology after TBI, NFTs are relatively inert.

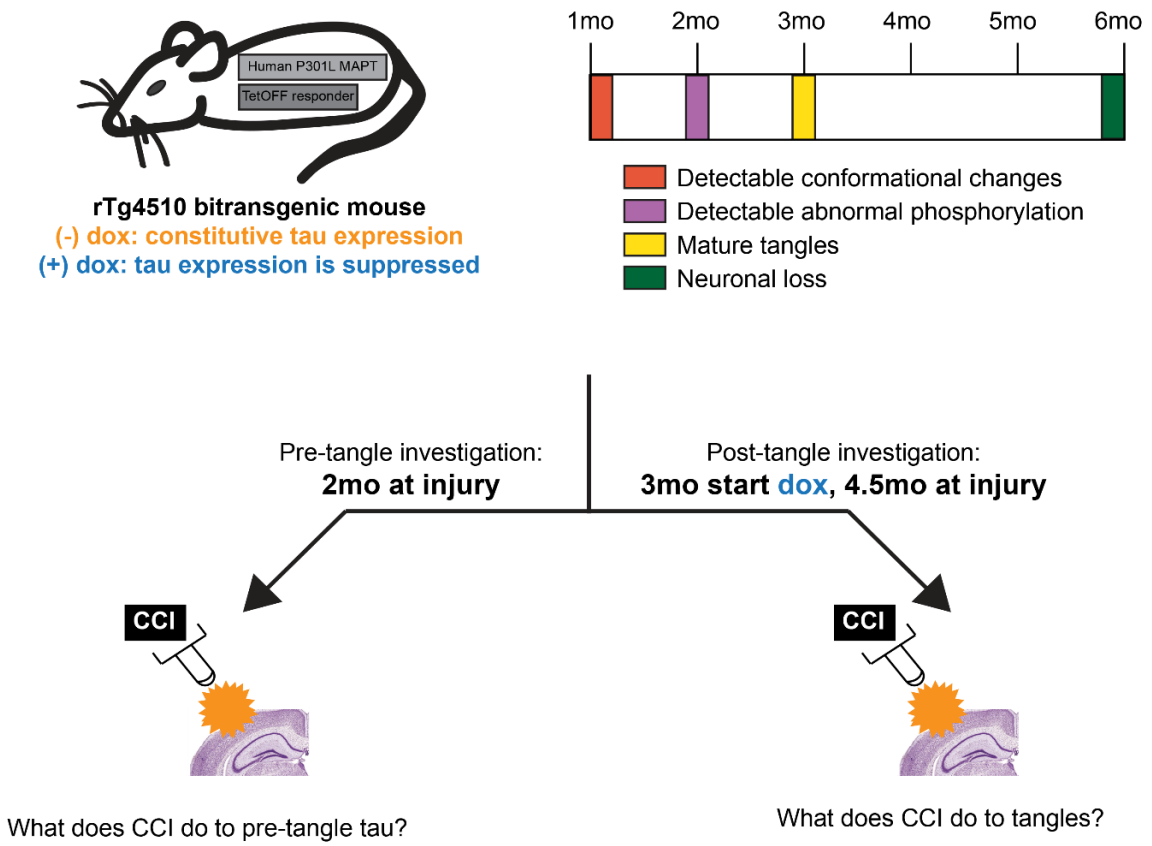

Figure 3.1: Experimental design for data presented in Chapter 3. Male and female rTg4510 mice that were 2 months of age were used to study the effects of TBI on pre-tangle tau. At this age, abnormal conformation and phosphorylation of tau are present but mature tangles are not present. To study the effects of TBI on predominantly tangle pathology male and female rTg4510 mice were placed on a doxycycline diet at the age of 3 months and kept on this diet until time of euthanasia. In this model tangle deposition has started at 3 months of age but it is not yet overt. Six weeks of doxycycline administration is the minimum amount of time suppress new tau production and allow any non-tangle tau to be recruited into tangle or cleared from the brain

Table 3.1: Summary of Western blot findings.

24 HOURS POST-INJURY COMPARED TO SHAM			
	Phospho-tau (AT8)	**Oligomeric tau (T22)**	**Total tau (HT7)**
Whole Neocortex Homogenate	Decreased	Decreased	No change
Sarkosyl-insoluble	N/A	No change	Decreased
TBS-soluble	No change	No change	No change
Sarkosyl-soluble	N/A	No change	Decreased
7 DAYS POST-INJURY COMPARED TO SHAM			
	Phospho-tau (AT8)	**Oligomeric tau (T22)**	**Total tau (HT7)**
Whole Neocortex Homogenate	Increased	No change	No change
Sarkosyl-insoluble	N/A	No change	No change
TBS-soluble	No change	No change	No change
Sarkosyl-soluble	N/A	Decreased	No change

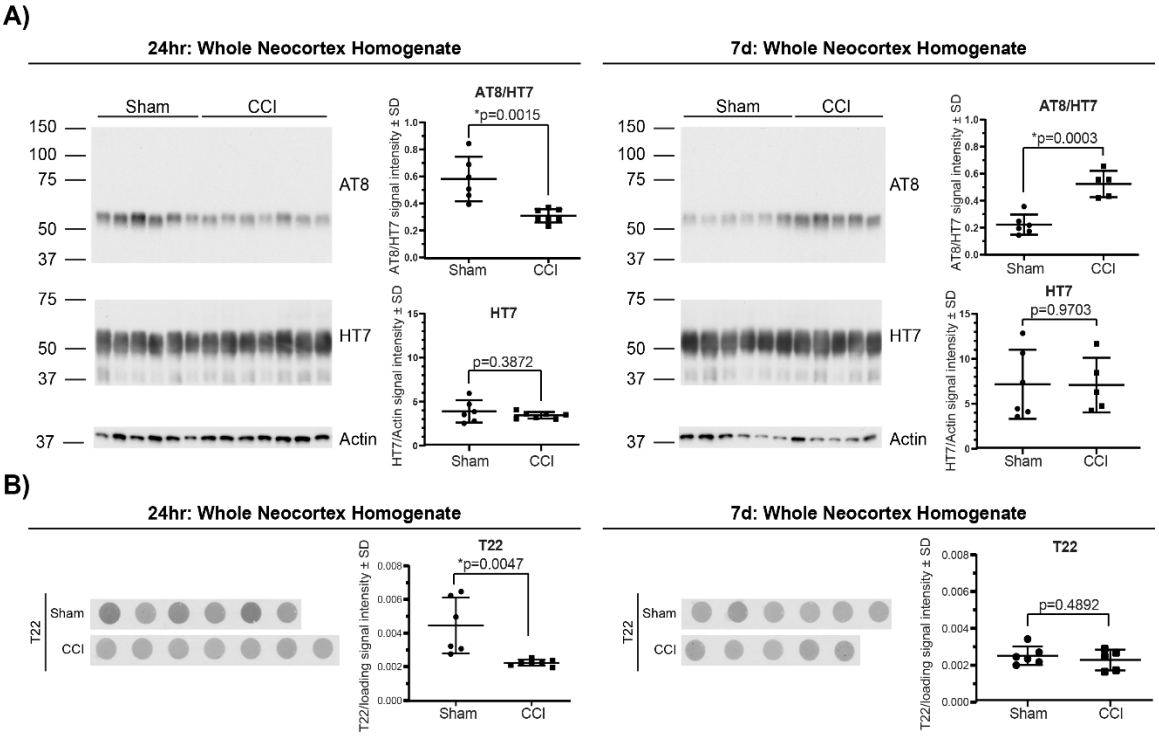

Figure 3.2: Prior to overt tangle formation CCI alters tau phosphorylation at both 24 hours and 7 days post-injury, but only alters oligomerization at 24 hours post-injury. (A) Western blots and quantification on 24 hour and 7 day whole neocortex homogenates of sham and CCI injured mice. AT8 levels are significantly decreased in injured mice compared to shams at 24 hours (p=0.0015, Student's t-test) and significantly increased in injured mice compared to shams at 7 days (p=0.0003, Student's t-test). Total tau levels are not significantly different between sham and CCI injured mice at either time point (24 hours: p=0.3872, 7 days: p=0.9703, Student's t-test). (B) Dot blots and quantification on 24 hour and 7 day whole neocortex homogenates of sham and CCI injured mice. T22 levels are significantly decreased in injured mice compared to shams at 24 hours (p=0.0047, Student's t-test) but not significantly different between sham and injured mice at 7 days (p=0.4892, Student's t-test).

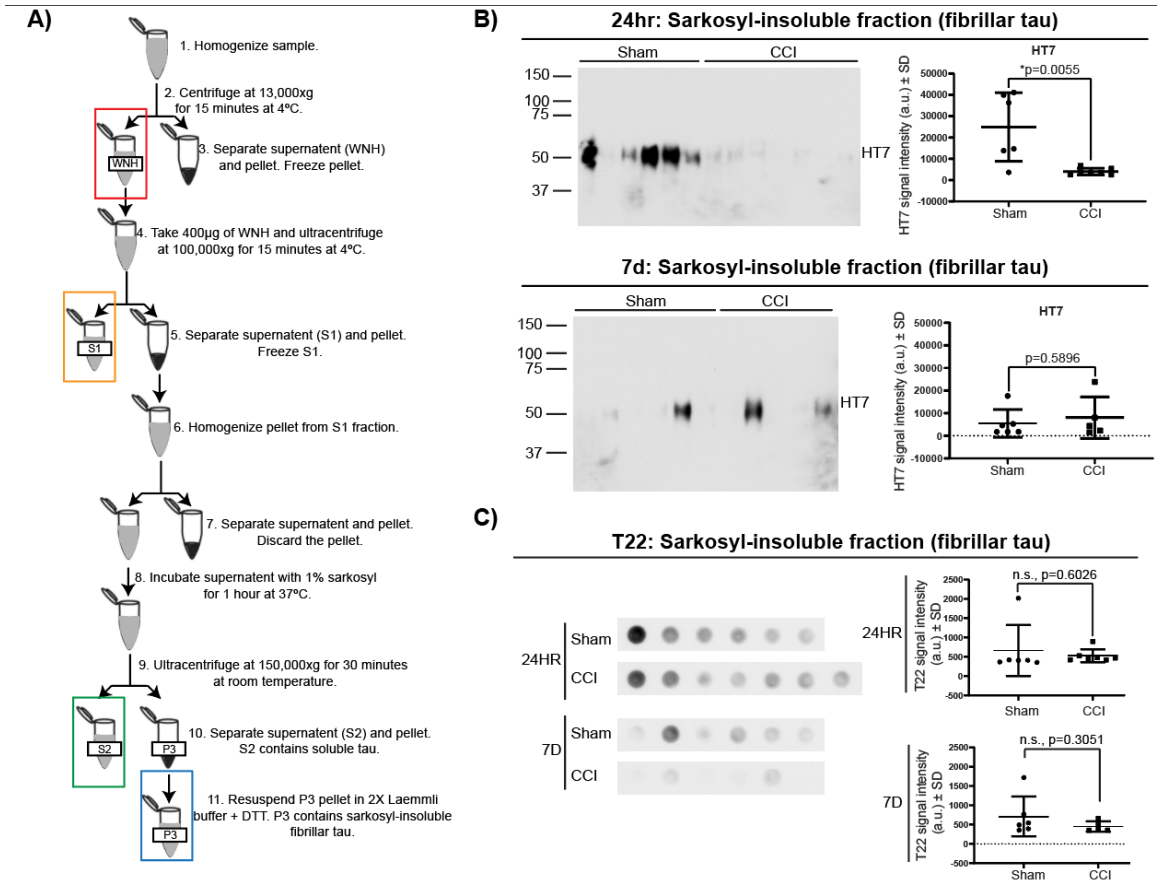

Figure 3.3: Prior to overt tangle formation, CCI does not increase tau fibrillization at 24 hours or 7 days post-injury. (A) Diagram showing each step in the biochemical isolation of fibrillar tau using centrifugation and the detergent sarkosyl. Whole neocortex homogenate in the red box, TBS-soluble cytosolic fraction in the orange box, sarkosyl soluble fraction in the green box, and sarkosyl-insoluble fraction is the final fraction within the blue box. (B) Western blots and quantification of 24 hour and 7 day sarkosyl-insoluble fractions of sham and CCI injured mice. Total tau levels are significantly decreased in injured mice compared to shams at 24 hours (p=0.0055, Student's t-test) but not significantly different between sham and injured mice at 7 days (p=0.5896, Student's t-test). (C) Dot blot and quantification of sarkosyl-insoluble oligomeric tau from sham and injured mice at 24 hours and 7 days post-injury.

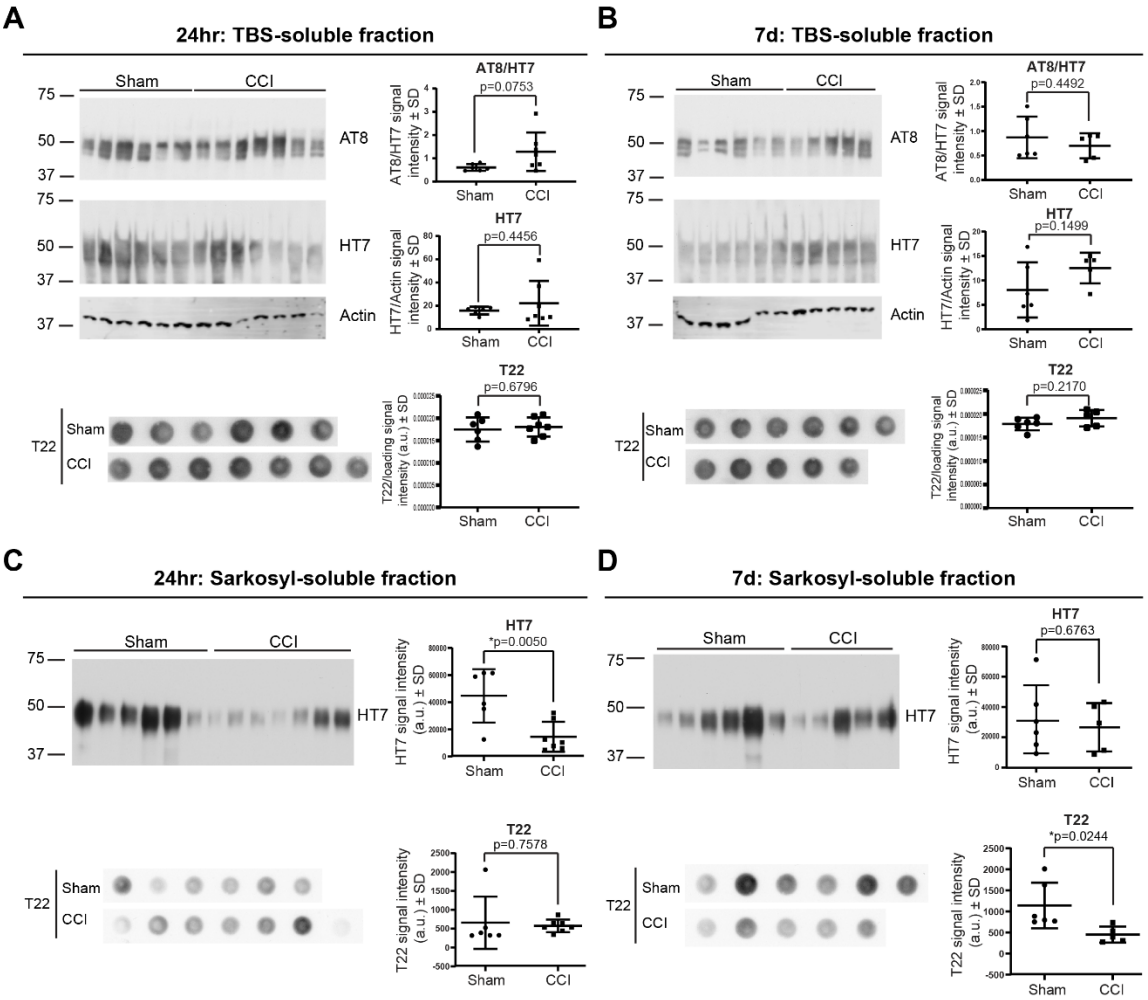

Figure 3.4: Effects of TBI on TBS-soluble and sarkosyl-soluble fractions. (A) Western blot and dot blot showing no significant difference between sham and injured mice in TBS-soluble phosphorylated, total, or oligomeric tau at 24 hours post-injury (Student's t-test performed on all). (B) Western blot and dot blot showing no significant difference between sham and injured mice in TBS-soluble phosphorylated, total, or oligomeric tau at 7 days post-injury (Student's t-test performed on all). (C) Western blot showing a significant decrease in sarkosyl-soluble total tau levels of injured mice compared to shams at 24 hours post-injury (p=0.0050, Student's t-test). Dot blot showing no significant difference between sham and injured mice in TBS-soluble oligomeric tau at 24 hours post-injury (p=0.7578, Student's t-test). (D) Western blot showing no significant difference in sarkosyl-soluble total tau levels between sham and injured mice at 7 days post-injury (p=0.6763, Student's t-test). Dot blot showing a significant decrease in sarkosyl-soluble oligomeric tau in injured mice compared to sham at 7 days post-injury (p=0.0244, Student's t-test).

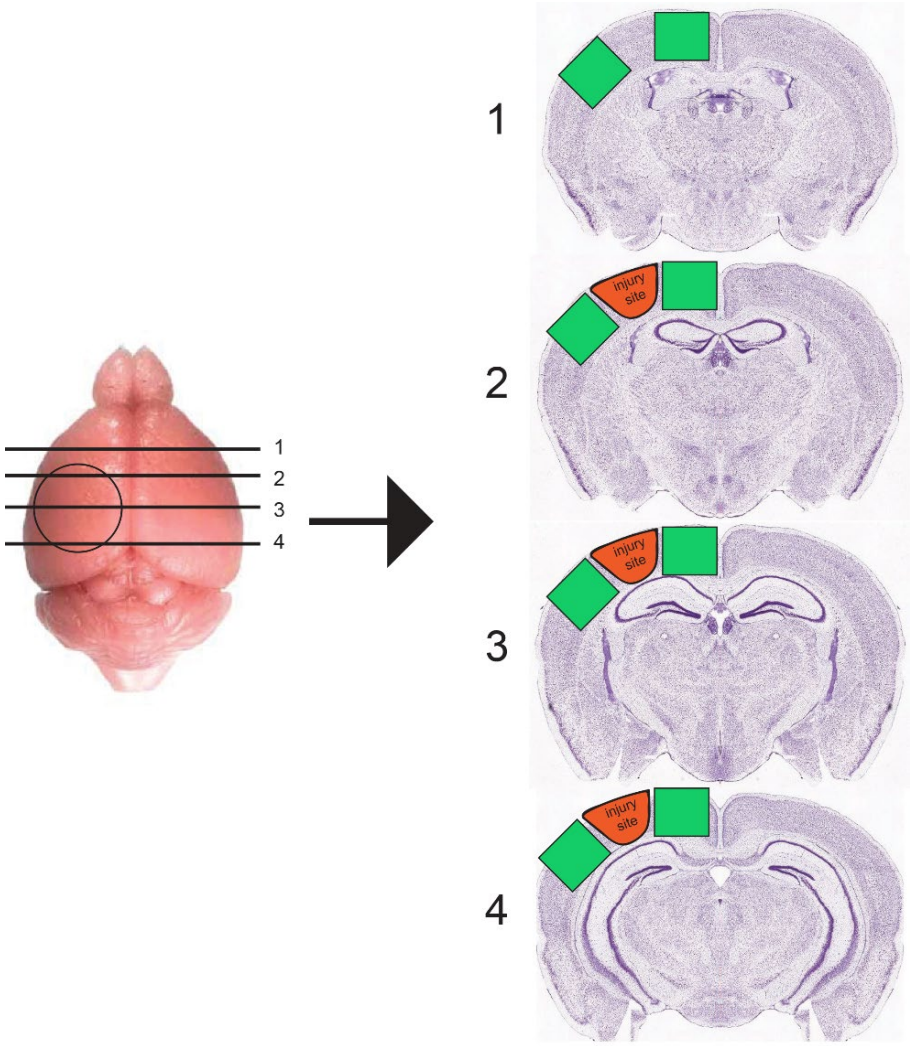

Figure 3.5: Sectioning and tissue selection for staining and quantification of neurofibrillary tangles by FSB. Rostral to caudal sections taken for staining by FSB. Green boxes indicate regions where images were taken for quantification. One image was taken per green box per section (8 images total per mouse). Images were not taken directly within the injury site. For each green box the average tangle count was calculated across all four slices, and then the two green boxes were averaged together.

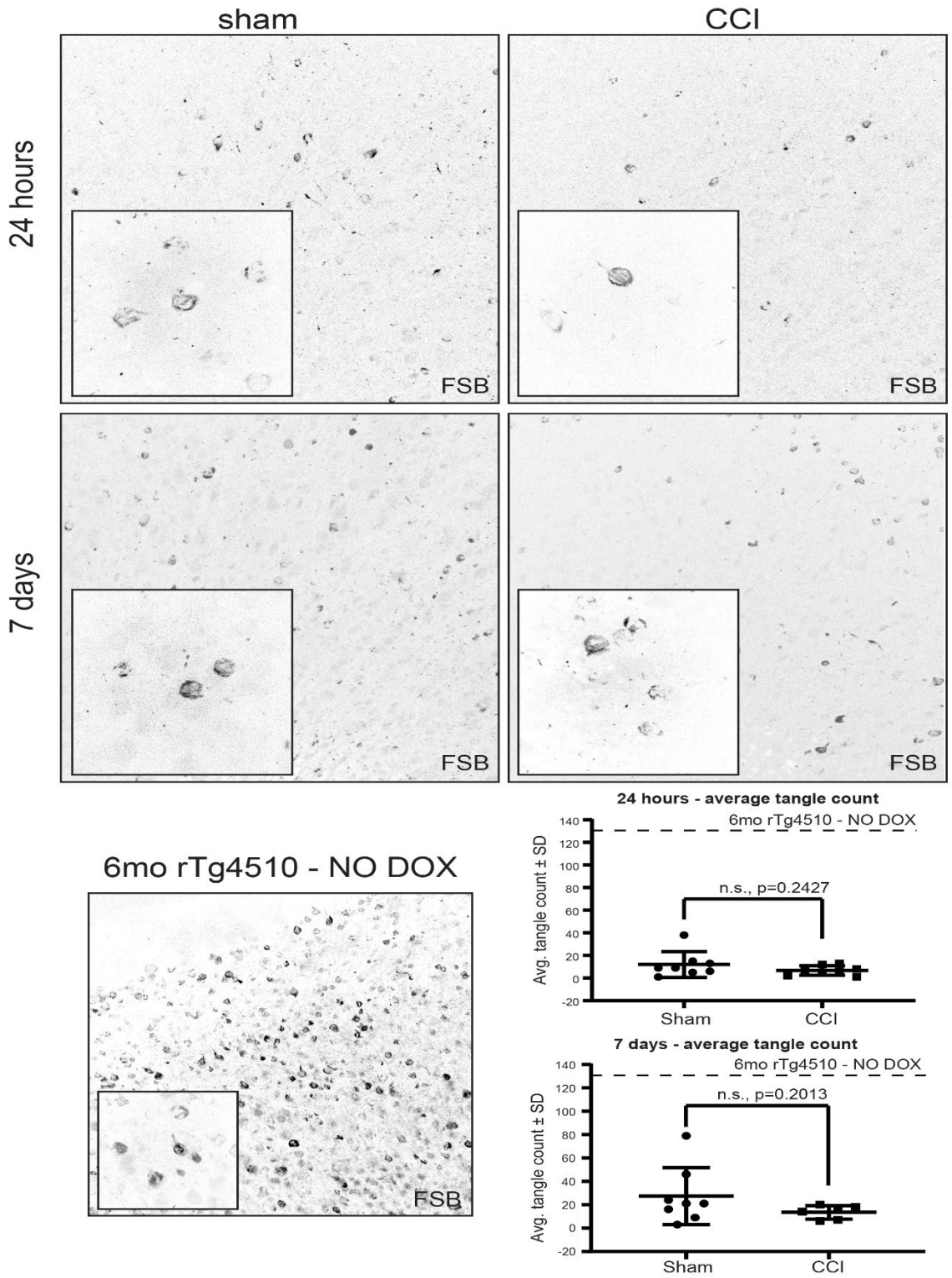

Figure 3.6: At 4.5 months of age, and with mature tangle deposition, CCI does not significantly increase or decrease tangle counts at 24 hours and 7 days post-injury but it does reduce variability observed. Representative images of FSB staining in 24

hour and 7 day sham and CCI injured cortical tissue, as well as 6 month old rTg4510 not on doxycycline. Quantification of these images showed no significant difference between sham and injured mice at either time point (24 hours: p=0.2427, 7 days: p=0.2013, Student's t-test). Inset images are 100X images of FSB positive tangles.

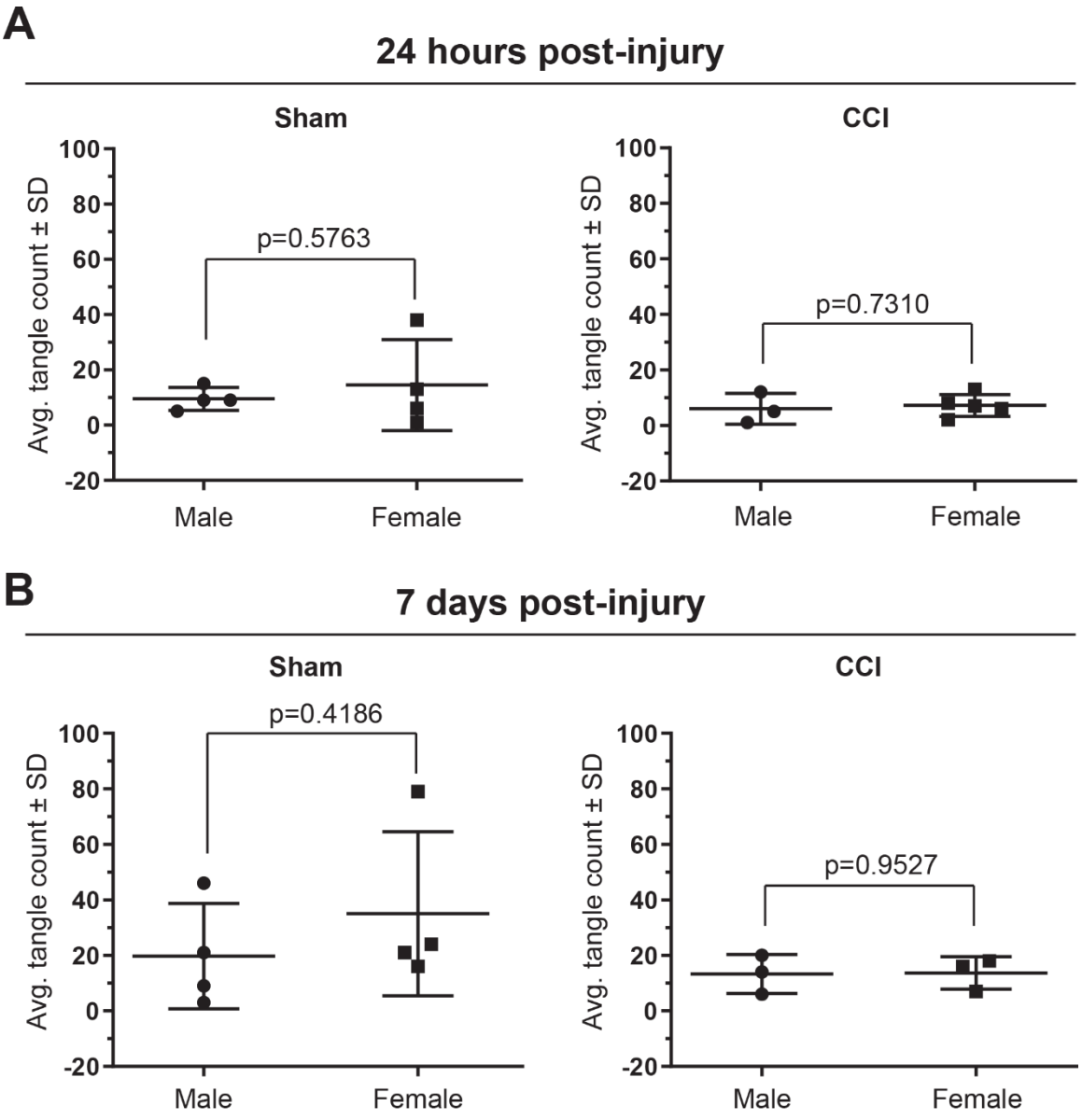

Figure 3.7: Comparison of male and female tangle counts in sham and injured mice. (A) Quantification of tangle counts show no significant difference between male and female mice, in both sham and injured groups at 24 hours post-injury. (B) Quantification of tangle counts show no significant difference between male and female mice, in both sham and injured groups at 7 days post-injury. Student's t-test performed on all.

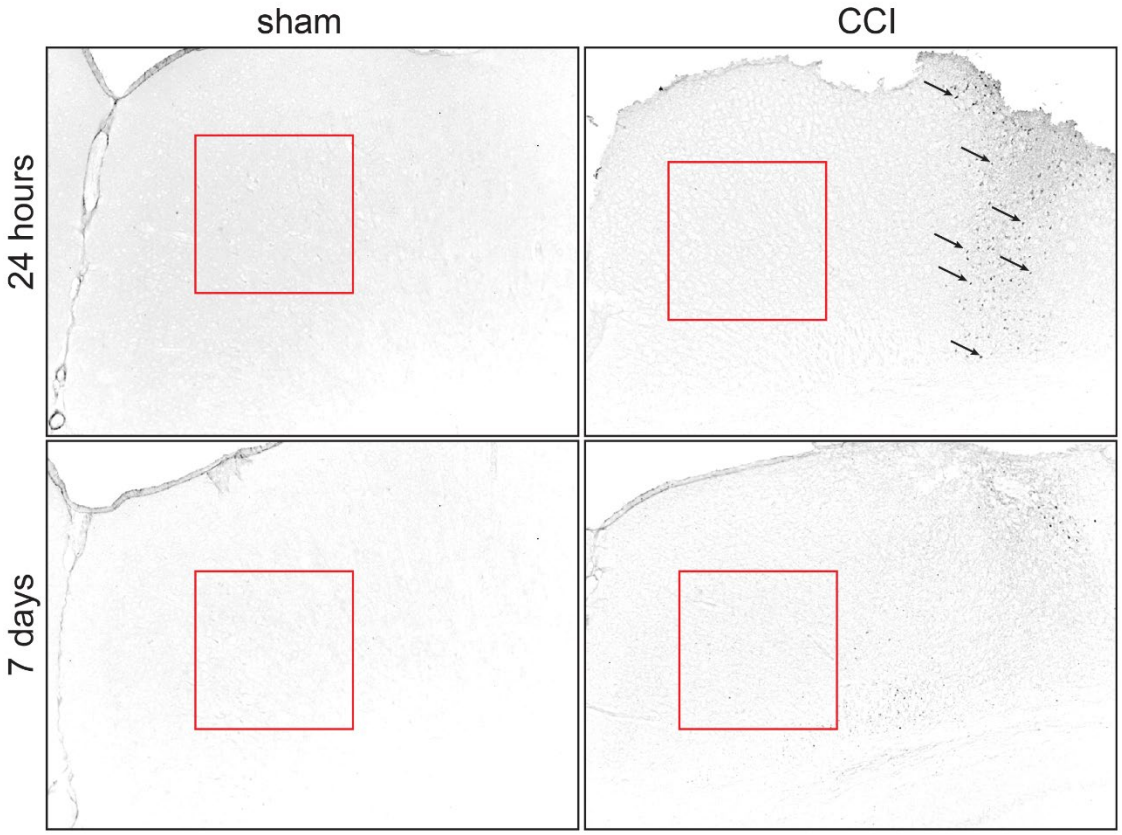

Figure 3.8: Fluorojade C staining shows cell death did not affect tangle counts performed. Representative 10X images of 24 hours and 7 day sham and injured mice with FJC staining. Black arrows point to examples of positive signal from FJC stain (note that not all positive signal has an arrow, but the arrows are provided to aide in demonstrating what was considered a positive signal). Red boxes represent the region where the 20X images were taken for the tangle counts performed.

CHAPTER 4. DISCUSSION

4.1 Summary

The goal of this dissertation was to investigate the role of tau in contributing to cellular dysfunction, as well as the specific consequences of cellular dysfunction in development of tau pathology. This discussion will be divided into three sections. The first will be a brief summary of Chapters 2 and 3. The second will provide insight on how the findings from Chapters 2 and 3 fit into the current literature and important questions still unanswered by this project. The third will outline the limitations of Chapters 2 and 3 and discuss future directions of this study.

Chapter 2 investigated how tau contributes to cellular dysfunction by studying the association of tau with ribosomes. We hypothesized that the interaction between tau and ribosomes would lead to a decrease in protein synthesis. To confirm and further identify specific tau-ribosome interactions we used co-immunoprecipitation followed by liquid chromatography tandem mass spectrometry and immunofluorescent staining in human Alzheimer's disease (AD) and control brains. We found specific interactions of tau with ribosomal proteins in AD and control brains, and found that oligomeric tau is observed in close proximity to ribosomal protein S6. To determine the consequence of this interaction we applied a puromycin-based assay called SUnSET to *in vitro* and *in vivo* models of tauopathy. We found that increased levels of tau led to a decrease in protein translation, and that mutant tau did not reduce protein translation more than wild type tau.

Chapter 3 investigated how cellular dysfunction contributes to development of tau pathology by using a model of traumatic brain injury. We hypothesized that injury would increase tau fibrillization but reduce tangle counts (as we believed that TBI would cause a

breakdown in NFTs). We injured 2 month old rTg4510 mice prior to tangle deposition to investigate how injury affects the fibrillization of tau, a key part in development of tangle pathology. We injured 4.5 month old rTg4510 mice with predominantly tangle pathology (but minimal non-fibrillar tau due to doxycycline administration) to investigate how injury affects neurofibrillary tangles. In mice without tangle pathology we saw an increase in tau phosphorylation after 7 days, but we did not observe an increase in tau fibrillization. In mice with predominantly tangle pathology, we did not see any significant difference in tangle counts after injury.

4.2 Overall analysis of findings

As described in Chapter 1 tauopathic brains demonstrate a cycle of cellular dysfunction and development of tau pathology that feed back onto each other. In humans, tau pathology can develop over decades or in a more acute time frame. Understanding the differences observed in chronic disease states compared to more acute ones is critical to providing accurate treatment in the future. In this work, I chose to look at each arm of that cycle separately to better understand their different contributions toward disease states (Figure 4.1).

In chronic tauopathies, extensive tau pathology develops over decades. As pathology worsens, so does the cellular dysfunction. Development of tau pathology directly leads to or is associated with a variety of types of cellular dysfunction including synaptic dysfunction [164-167, 170-173, 175-178, 377-380], mitochondrial dysfunction [179, 180, 195, 381], impaired protein clearance [334, 382, 383], calcium dyshomeostasis [172, 184-186], and impaired axonal transport [187-194]. Additionally, the association between pathological tau and ribosomes was established well before this study was

performed, with reports being published as early at 1987 [129, 206, 384-386]. The effect of this association, however, remained unknown. Our work in chapter 2 demonstrates a novel mechanism of cellular dysfunction in tauopathies through impairment of protein translation.

While the major purpose of this project was to elucidate the effect of the association of pathological tau with ribosomes, we also identified seven unique RNA-binding proteins that associated with tau in a human non-tauopathic brain. Of those seven, six are ribosomal proteins (Figure 2.1C). While this was only one brain, it would be enough evidence to further explore these associations as it could identify a novel role for non-pathological tau. For example one of the proteins, ribosomal protein L26 (RPL26), controls the binding of the 5' untranslated region (5'-UTR) of p53 mRNA to the ribosome [387]. The binding of RPL26 to the 5'-UTR of p53 increases protein expression [387]. As tau is canonically known as a microtubule stabilizing protein, it is possible that tau acts as a stabilizer of the RPL26-5'UTR interaction to increase translation of p53. As p53 plays a large role in genomic DNA repair and stability (reviewed in [388]), this could very broadly add an indirect role to tau of DNA repair.

In acutely induced tauopathies, such as TBI, a sudden event triggers a cascade of cellular mechanisms that leads to post-translational modifications to tau. As increased phosphorylation of tau after injury is frequently observed, the cause of this could be due to abnormal kinase and phosphatase activity after injury. The activity of one tau kinase, calcium calmodulin-dependent protein kinase 2 (CaMKII) [389, 390], is increased after TBI [391] while the activity of a major tau phosphatases, protein phosphatase 2A (PP2A) and 2B (PP2B) are decreased [373-375]. Interestingly, inhibition of PP2A in causes an

increase in CaMKII activation that directly results in increased tau phosphorylation [392]. This imbalance between kinase and phosphatase activity could directly be contributing to the increased phosphorylation observed after injury. Additionally, imbalance in other kinases and phosphatases (as described in the discussion of chapter 3) could cause the decrease in phosphorylation we observed at 24 hours post-injury.

4.3 Limitations of these studies

In chapter 2, I investigated the effects of tau's association with ribosomes. We utilized co-immunoprecipitation of tau and LC-MS/MS to identify the ribosomal proteins with which tau interacted. As previously stated, we utilized cortical tissue from one AD and one non-AD brain for this experiment. While this does offer novel insight, it does limit the extrapolation of our results to all Alzheimer's diseased brains. We do not know if pathological staging, sex, age, co-morbidities, or lifestyle factors that affect AD can impact the tau-ribosome interaction. Additionally, we do not know if tau binds to the same ribosomal proteins in different regions of the brain. Co-immunoprecipitation/LC-MS/MS experiments using additional AD and non-AD human brain tissue, from cortical and non-cortical regions, would need to be repeated to more accurately describe which ribosomal proteins tau interact with in AD.

We utilized the cell-free *in vitro* translation assay to investigate the effect of oligomeric proteins on translational output as measured by GFP fluorescence. While our research investigated the effects of tau compared to other disease associated oligomeric proteins (α-synuclein, insulin) we did not report on the effects of Aβ oligomers. In the context of AD, Aβ composes the other major neuropathological hallmark of plaques. Although Aβ deposits are traditionally thought of as extracellular, accumulation can also

occur intraneuronally [393-395]. Additional experiments using the cell free assay incubated with Aβ oligomers would need to be performed to confirm that this was a tau specific phenomenon in AD.

In the neuronal lineage HEK cell line, we investigated the effects of mutant tau compared to wild-type tau on protein translation. These experiments investigated 2 mutants of the 107 experimentally studied mutants discussed in chapter 1. This limits our interpretation of these data in two ways. First, while many of the other mutations are substitution mutations like P301L we do not know the effect other amino acid substitutions could have on the interaction between tau and ribosomes. For example, proline is a ringed amino acid while leucine is not. This basic change in amino acid structure can allow or prohibit additional interactions. Without testing all the known tau mutants we don't know how each one affects protein translation. Secondly, many of the tau mutations affect exon 10 splicing (which thereby affects the number of microtubule binding domains in the protein – 3R vs 4R). Since we don't know which region of tau binds to ribosomes, we do not know how these mutants would affect tau's interaction with ribosomes.

In chapter 3, I investigated how a single injury affected tau pathology development in a relatively acute time frame. This paradigm offers insight into a single injury event, but it does not offer new knowledge on how a single injury affects tau pathology development over time or how multiple injuries effect tau pathology development. In CTE, a primary tauopathy for which TBI is a risk factor, both time and number of injuries seem to play a role in disease development [37]. Additionally, there is a unique folding pattern to tau found in CTE compared to tau found in AD or PSP [212] as discussed in

chapter 1. The repeat head trauma exposure or the amount of time after injury could play a role in that folding pattern.

In these experiments we did not investigate any specific mechanistic contribution of cellular dysfunction caused by TBI to the changes we observed in tau, which leaves room to speculate. One possibly important mechanism for changes observed in tau pathology is neuroinflammation. Minutes to hours after TBI pro-inflammatory cytokine production in increased and activation of the inflammasome occurs in injured tissue [396-398] and microglial activation can persist one year after injury [399]. In chronic tauopathies, the neuroinflammation observed contributes to pathology development and propagation of pathology [74, 271-277, 356, 357]. In fact, microglia are a key component to the spreading of tau throughout the brain in AD [400, 401]. This leaves an open pathway to explore the role of neuroinflammation in pathology development after TBI.

Following TBI, mechanical and inertial forces cause tissue deformation throughout the brain [402] that are experienced differentially by region [310, 403, 404]. In CTE, early tau pathology is described at the levels of the cortical sulci but is observed in the gyri at mid-late stages [36]. Additionally, the tau-positive pathology is limited to the more superficial/outer layers of the brain [36, 37]. The development of pathology in these regions could be due to individual primary injuries occurring during deformation of the sulci and gyri. As such, another limitation to this project was the use of mice to investigate the formation of tau pathology after TBI as mouse brains do not have folds. To better understand the effect of sulci on development of tau pathology after TBI, a porcine model could be used as they are gyrencephalic [405]. One model of TBI in pigs

does show tau phosphorylation after injury [406]; however, it has yet to be reported if true NFTs can form in pig brains.

In this study we utilized the rTg4510 mouse model that expressed human mutant P301L tau. We utilized this model due to the early onset and abundance of pathology observed, as well as its ability to be controlled by doxycycline [70]. However, a caveat to using this model is that this mutation is not widely expressed in the general population. In fact, in the disease most associated with this mutation (frontotemporal dementia with parkinsonism-17, FTDP-17) [127, 147] this mutation occurs in less than a third of the patients with familial FTDP-17 [26]. In sporadic cases, there are no mutations observed [407]. While this mutation was vitally important for studying NFT development after TBI (as endogenous mouse tau does not form NFTs), it does limit the interpretation of these studies.

An additional shortcoming in this model is the recent discovery that the insertion of the tetO-MAPT*P301L transgene by random transgenesis caused a null mutation of the FGF14 gene [408]. The null mutation in this gene contributes heavily to the disease phenotype observed in the rTg4510 line [409]. In fact, mutations to FGF14 impact many molecular mechanisms of neurobiology such as synaptic plasticity and neurogenesis [410]. Additionally, the random transgenesis of the Camk2a-tTA gene causes a functional deletion of five other genes (VIPR2, WDR60, ESYT2, NCAPG2, and PTPRN2) [408]. Further studies will need to be completed to understand the full effects of the genes being knocked out. The use of the rTg4510 model for studying phenotypic effects of tauopathies is still being debated, but using the rTg4510 model for studying effects on tau (and not disease mechanism) is still widely accepted.

4.4 Impact of these data on the field(s)

The data presented in chapter 2 demonstrate a novel role for a tau in disease as an inhibitor of protein translation. Before these experiments we knew that tau associated with ribosomes [201, 206, 338, 385] but we did not know any functional consequence of this interaction. We showed that this interaction between tau and ribosomes reduced protein translation. These findings answered our original inquiries, but also created more questions. We still do not know where exactly tau binds to ribosomes or if tau selectively alters the types of proteins that are being made. Not knowing where tau binds to ribosomes limits our ability to understand exactly how tau is inhibiting translation. A recent study by Koren *et al.* from Dr. Joe Abisambra's lab expanded upon the tau-affected transcriptome and translatome. They reported on a interaction between the ribosomal protein S6 (a major regulator of protein translation) and tau that decreases protein translation [411]. This study suggests that tau may play an active role in reducing protein translation by interacting with ribosomal protein S6, rather than a passive one by simply blocking the protein exit site on the ribosome.

The data presented in chapter 3 expand on the role of TBI in tau phosphorylation and fibrillization. We found that TBI decreased tau phosphorylation at 24 hours post-injury but then increased tau phosphorylation at 7 days post-injury. Fibril formation within 7 days of injury was not increased. This created more unanswered questions, and allows us to speculate on what could be happening after TBI that contributes to pathology development in diseases like CTE. As mentioned in chapter 3, the only other study to look at true NFTs after injury does not support a direct causative link between TBI and increased NFT development [268]. One additional study, published in July of 2019,

shows “not statistically significantly” increased levels of tau phosphorylated at S199 in a formic acid insoluble fraction of tau in injured tau transgenic mice compared to sham at 24 hours post-injury [412]. This study did not report on tau fibrillization after the 24 hour time point. Both of these studies, as well as our own data, did not find a robust link between tau fibrillization and TBI at either short or long time points. This leads me to believe that TBI-induced tau pathology could be more of a secondary pathology rather than a primary one. In thinking about tau pathology development as a secondary pathology of TBI, we have to think about other protein pathologies observed after TBI. For example, amyloid beta deposition is another protein abnormality observed after TBI in both animal models [413] and in CTE [414]. In AD models, amyloid beta has been shown to induce tau pathology development [415]. As such, its possible that NFT development is an indirect result of TBI causing amyloid beta deposition rather than a direct result of TBI.

The data in chapters 2 and 3 also present a unique opportunity to speculate on the role of tau pathology impacting protein translation in TBI. Protein translation is altered following TBI [416], with many regulatory pathways that inhibit protein translation being activated [417, 418]. In chapter 2 we showed that increased tau phosphorylation and aggregation cause a decrease in protein translation, and in chapter 3 we showed that TBI increased tau phosphorylation. It is possible that hyperphosphorylated tau created by TBI would interact with ribosomes after TBI and contribute to further inhibit protein synthesis. While we did not explicitly test if TBI-induced phospho-tau contribute to altered protein synthesis after TBI in this dissertation, I have proposed experiments to test this in the future directions section.

4.5 Future directions

One of the major questions still left unanswered after this project is whether tau interacts with other proteins the same way after injury as it does during chronic disease development. In chapter 2 we showed that phosphorylated tau interacts with ribosomes and impedes translation in models that did not undergo any type of injury. In chapter 3, we also observed an increase in tau phosphorylation at 7 days post injury but we did not assess the ability of tau to impede translation in this experiment. To test this, we could administer puromycin to sham and injured tau knockout mice [419] and rTg4510 mice. Administering puromycin to sham and injured tau knockout mice would allow us to observe the isolated effects of TBI on protein translation, while administering puromycin to sham and injured rTg4510 mice would allow us to observe the combined effects of TBI and tau pathology. I would hypothesize that TBI decreases protein translation in tau knockout mice but that when pathological tau is added (using the rTg4510 model) the decrease is even more pronounced. Additional experiments could also investigate which ribosomal proteins TBI-induced tau associates with using the co-IP and LC-MS/MS methodology explained in chapter 2 using the brains of injured rTg4510 mice compared to sham rTg4510 mice. Comparisons could also be made between CTE brains and AD brains to explore similarities and differences in associations with ribosomal proteins.

Another characteristic of tau observed in chronic disease is its ability to propagate and spread throughout the brain. Tau pathology induced in a rodent brain following TBI has the ability to spread when immunoprecipitated tau from injured brains is injected into non-injured mouse brains [265, 420] or cultured with HEK293T cells [421]. We still do not know, however, if TBI-induced tau pathology is the result of individual injuries (as

discussed in regards to gyrencephalic models) or if it is the result of a propagation mechanism. The closest evidence available is a study that showed increased tau phosphorylation on the contralateral hemisphere at 12 months after a single CCI injury [420]. While these data support further investigation into a possible spreading mechanism, presence of phosphorylated tau in the contralateral hemisphere is not necessarily indicative of tau spreading. In fact, contralateral hemispheres experience delayed but significant neurodegeneration after severe TBI like the one modeled in this study [422]. From this we can infer that the contralateral hemisphere is susceptible to experiencing cellular response mechanisms that could modify tau phosphorylation observed in the ipsilateral hemisphere, albeit at a reduced intensity.

To investigate the ability of tau to propagate after TBI, His-tagged recombinant tau could be injected into the cortex of tau knockout mice. These mice could then be injured and their brains could be harvested at similar time points to the findings of the previously mentioned report (3 months and 12 months [420]). Control mice that only receive the injection of His-tagged tau and no other surgery would be used to confirm the cellular uptake of tau. Cellular uptake would be expected following injection based on previous studies performed with injection of recombinant and brain derived tau fibrils and oligomers [265, 423, 424]. Using a commercially available His-tag antibody and immunostaining the final location of the His-tagged tau could be isolated and then the distance travelled from the injection site could be measured. While this would have limitations of its own (such as using a tagged protein, which could affect the native structure of the protein) it would offer more direct insight into the spreading ability of tau.

Our finding that tau fibrillization did not occur at 24 hours or 7 days post-injury was interesting and contrary to our initial hypothesis stated in chapter 3. As CTE is neuropathologically defined by NFT deposition, understanding the mechanism by which tau fibrils form after TBI is still vitally important. In chapter 3, we used a single injury model. To further investigate the effect of a single injury model on NFT development over time we could repeat the experiments outline in chapter 3 and extend the analysis out to longer time points (for example 2 weeks, 1 month, 6 months, 12 months post-injury). I would expect to find tau fibrillization in sham and injured mice at these longer time points as tangle deposition begins between 2.5 and 3 months of age without injury [330]. However, if TBI accelerated fibril formation I would expect to see increased levels of total tau in the sarkosyl-insoluble fraction in injured mice compared to shams. As this is the first study performed looking at tau fibrillization after injury, there are many options to look at in the future including effects of model type (ex: blast vs CCI vs CHI), effects of repeat head injury, and/or the effect of repeat head injury over time on tau fibrillization.

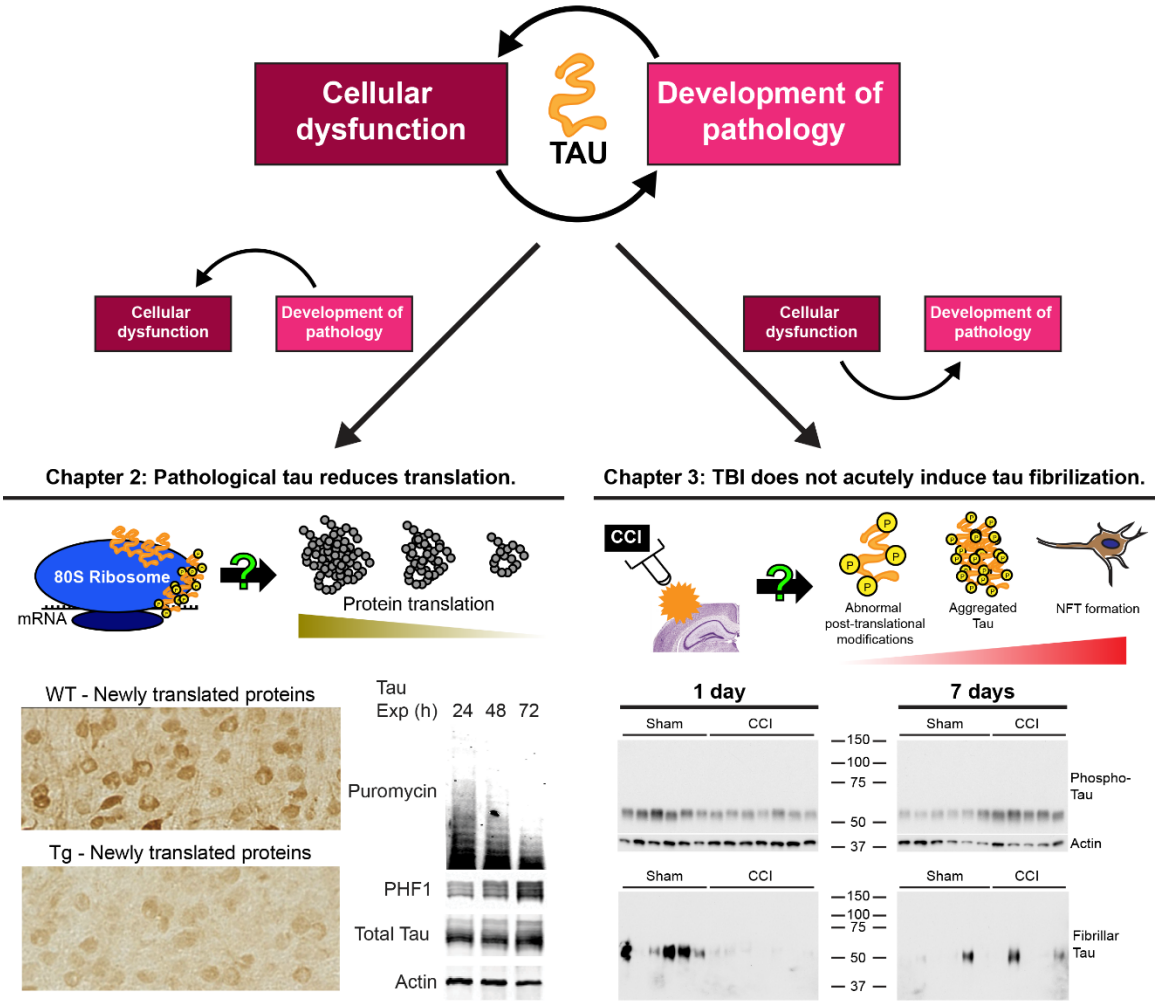

Figure 4.1: Summary of findings presented in this dissertation. Tauopathic brains demonstrate a cycle of cellular dysfunction and development of pathology that feedback on each other. In this dissertation we examined each arm of that cycle individually. In chapter 2 we investigated the effect of pathology on cellular dysfunction and in chapter 3 we investigated the effect of cellular dysfunction on the development of pathology.

REFERENCES

1. Weingarten, M.D., et al., *A protein factor essential for microtubule assembly.* Proc Natl Acad Sci U S A, 1975. **72**(5): p. 1858-62.
2. Chen, J., et al., *Projection domains of MAP2 and tau determine spacings between microtubules in dendrites and axons.* Nature, 1992. **360**(6405): p. 674-7.
3. Frappier, T.F., et al., *tau Regulation of microtubule-microtubule spacing and bundling.* J Neurochem, 1994. **63**(6): p. 2288-94.
4. Wang, Y. and E. Mandelkow, *Tau in physiology and pathology.* Nat Rev Neurosci, 2016. **17**(1): p. 5-21.
5. Andreadis, A., *Misregulation of tau alternative splicing in neurodegeneration and dementia.* Prog Mol Subcell Biol, 2006. **44**: p. 89-107.
6. Goedert, M., et al., *Multiple isoforms of human microtubule-associated protein tau: sequences and localization in neurofibrillary tangles of Alzheimer's disease.* Neuron, 1989. **3**(4): p. 519-26.
7. Mukrasch, M.D., et al., *Structural polymorphism of 441-residue tau at single residue resolution.* PLoS Biol, 2009. **7**(2): p. e34.
8. Kadavath, H., et al., *Tau stabilizes microtubules by binding at the interface between tubulin heterodimers.* Proc Natl Acad Sci U S A, 2015. **112**(24): p. 7501-6.
9. Gruning, C.S., et al., *Alternative conformations of the Tau repeat domain in complex with an engineered binding protein.* J Biol Chem, 2014. **289**(33): p. 23209-18.
10. Jeganathan, S., et al., *Global hairpin folding of tau in solution.* Biochemistry, 2006. **45**(7): p. 2283-93.
11. Guo, T., W. Noble, and D.P. Hanger, *Roles of tau protein in health and disease.* Acta Neuropathol, 2017. **133**(5): p. 665-704.
12. Kanaan, N.M., et al., *Pathogenic forms of tau inhibit kinesin-dependent axonal transport through a mechanism involving activation of axonal phosphotransferases.* J Neurosci, 2011. **31**(27): p. 9858-68.
13. Paholikova, K., et al., *N-terminal truncation of microtubule associated protein tau dysregulates its cellular localization.* J Alzheimers Dis, 2015. **43**(3): p. 915-26.
14. Liu, C. and J. Gotz, *Profiling murine tau with 0N, 1N and 2N isoform-specific antibodies in brain and peripheral organs reveals distinct subcellular localization, with the 1N isoform being enriched in the nucleus.* PLoS One, 2013. **8**(12): p. e84849.
15. Brandt, R., J. Leger, and G. Lee, *Interaction of tau with the neural plasma membrane mediated by tau's amino-terminal projection domain.* J Cell Biol, 1995. **131**(5): p. 1327-40.
16. Magnani, E., et al., *Interaction of tau protein with the dynactin complex.* EMBO J, 2007. **26**(21): p. 4546-54.
17. Connell, J.W., et al., *Effects of FTDP-17 mutations on the in vitro phosphorylation of tau by glycogen synthase kinase 3beta identified by mass spectrometry demonstrate certain mutations exert long-range conformational changes.* FEBS Lett, 2001. **493**(1): p. 40-4.
18. Kovacs, G.G., *Tauopathies.* Handb Clin Neurol, 2017. **145**: p. 355-368.

19. Williams, D.R., *Tauopathies: classification and clinical update on neurodegenerative diseases associated with microtubule-associated protein tau.* Intern Med J, 2006. **36**(10): p. 652-60.
20. Revesz, T. and J.L. Holton, *Anatamopathological spectrum of tauopathies.* Mov Disord, 2003. **18 Suppl 6**: p. S13-20.
21. Leyns, C.E.G. and D.M. Holtzman, *Glial contributions to neurodegeneration in tauopathies.* Mol Neurodegener, 2017. **12**(1): p. 50.
22. Bolos, M., et al., *Direct Evidence of Internalization of Tau by Microglia In Vitro and In Vivo.* J Alzheimers Dis, 2016. **50**(1): p. 77-87.
23. LoPresti, P., *Tau in Oligodendrocytes Takes Neurons in Sickness and in Health.* Int J Mol Sci, 2018. **19**(8).
24. Forrest, S.L., et al., *Retiring the term FTDP-17 as MAPT mutations are genetic forms of sporadic frontotemporal tauopathies.* Brain, 2018. **141**(2): p. 521-534.
25. Forrest, S.L., et al., *Heritability in frontotemporal tauopathies.* Alzheimers Dement (Amst), 2019. **11**: p. 115-124.
26. Woollacott, I.O. and J.D. Rohrer, *The clinical spectrum of sporadic and familial forms of frontotemporal dementia.* J Neurochem, 2016. **138 Suppl 1**: p. 6-31.
27. Association, A.s., *2018 Alzheimer's disease facts and figures.* Alzheimer's & Dementia, 2018. **14**: p. 367-429.
28. Braak, H. and E. Braak, *Neuropathological stageing of Alzheimer-related changes.* Acta Neuropathol, 1991. **82**(4): p. 239-59.
29. Pini, L., et al., *Brain atrophy in Alzheimer's Disease and aging.* Ageing Res Rev, 2016. **30**: p. 25-48.
30. M., C., *Punch-drunk syndromes: The chronic traumatic encephalopathy of boxers.* 1949.
31. JA., M., *Dementia pugilistica.* . US Naval Medicine Bulletin. , 1937. **35**: p. 297–303.
32. McKee, A.C., et al., *The first NINDS/NIBIB consensus meeting to define neuropathological criteria for the diagnosis of chronic traumatic encephalopathy.* Acta Neuropathol, 2016. **131**(1): p. 75-86.
33. Corsellis, J.A., C.J. Bruton, and D. Freeman-Browne, *The aftermath of boxing.* Psychol Med, 1973. **3**(3): p. 270-303.
34. Roberts, G.W., D. Allsop, and C. Bruton, *The occult aftermath of boxing.* J Neurol Neurosurg Psychiatry, 1990. **53**(5): p. 373-8.
35. McKee, A.C., B. Abdolmohammadi, and T.D. Stein, *The neuropathology of chronic traumatic encephalopathy.* Handb Clin Neurol, 2018. **158**: p. 297-307.
36. McKee, A.C., et al., *The spectrum of disease in chronic traumatic encephalopathy.* Brain, 2013. **136**(Pt 1): p. 43-64.
37. McKee, A.C., et al., *The neuropathology of chronic traumatic encephalopathy.* Brain Pathol, 2015. **25**(3): p. 350-64.
38. Mandelkow, E.M. and E. Mandelkow, *Biochemistry and cell biology of tau protein in neurofibrillary degeneration.* Cold Spring Harb Perspect Med, 2012. **2**(7): p. a006247.
39. Mirbaha, H., et al., *Inert and seed-competent tau monomers suggest structural origins of aggregation.* Elife, 2018. **7**.

40. Friedhoff, P., et al., *A nucleated assembly mechanism of Alzheimer paired helical filaments.* Proc Natl Acad Sci U S A, 1998. **95**(26): p. 15712-7.
41. Shammas, S.L., et al., *A mechanistic model of tau amyloid aggregation based on direct observation of oligomers.* Nat Commun, 2015. **6**: p. 7025.
42. Kampers, T., et al., *RNA stimulates aggregation of microtubule-associated protein tau into Alzheimer-like paired helical filaments.* FEBS Lett, 1996. **399**(3): p. 344-9.
43. Goedert, M., et al., *Assembly of microtubule-associated protein tau into Alzheimer-like filaments induced by sulphated glycosaminoglycans.* Nature, 1996. **383**(6600): p. 550-3.
44. Wille, H., et al., *Alzheimer-like paired helical filaments and antiparallel dimers formed from microtubule-associated protein tau in vitro.* J Cell Biol, 1992. **118**(3): p. 573-84.
45. Hernandez, F., R. Cuadros, and J. Avila, *Zeta 14-3-3 protein favours the formation of human tau fibrillar polymers.* Neurosci Lett, 2004. **357**(2): p. 143-6.
46. Giustiniani, J., et al., *Immunophilin FKBP52 induces Tau-P301L filamentous assembly in vitro and modulates its activity in a model of tauopathy.* Proc Natl Acad Sci U S A, 2014. **111**(12): p. 4584-9.
47. Berriman, J., et al., *Tau filaments from human brain and from in vitro assembly of recombinant protein show cross-beta structure.* Proc Natl Acad Sci U S A, 2003. **100**(15): p. 9034-8.
48. von Bergen, M., et al., *Tau aggregation is driven by a transition from random coil to beta sheet structure.* Biochim Biophys Acta, 2005. **1739**(2-3): p. 158-66.
49. Mocanu, M.M., et al., *The potential for beta-structure in the repeat domain of tau protein determines aggregation, synaptic decay, neuronal loss, and coassembly with endogenous Tau in inducible mouse models of tauopathy.* J Neurosci, 2008. **28**(3): p. 737-48.
50. von Bergen, M., et al., *Assembly of tau protein into Alzheimer paired helical filaments depends on a local sequence motif ((306)VQIVYK(311)) forming beta structure.* Proc Natl Acad Sci U S A, 2000. **97**(10): p. 5129-34.
51. Sawaya, M.R., et al., *Atomic structures of amyloid cross-beta spines reveal varied steric zippers.* Nature, 2007. **447**(7143): p. 453-7.
52. Andronesi, O.C., et al., *Characterization of Alzheimer's-like paired helical filaments from the core domain of tau protein using solid-state NMR spectroscopy.* J Am Chem Soc, 2008. **130**(18): p. 5922-8.
53. Inouye, H., et al., *Structure of core domain of fibril-forming PHF/Tau fragments.* Biophys J, 2006. **90**(5): p. 1774-89.
54. Khlistunova, I., et al., *Inducible expression of Tau repeat domain in cell models of tauopathy: aggregation is toxic to cells but can be reversed by inhibitor drugs.* J Biol Chem, 2006. **281**(2): p. 1205-14.
55. Nelson, P.T., et al., *Correlation of Alzheimer disease neuropathologic changes with cognitive status: a review of the literature.* J Neuropathol Exp Neurol, 2012. **71**(5): p. 362-81.
56. Arriagada, P.V., et al., *Neurofibrillary tangles but not senile plaques parallel duration and severity of Alzheimer's disease.* Neurology, 1992. **42**(3 Pt 1): p. 631-9.

57. Giannakopoulos, P., et al., *Tangle and neuron numbers, but not amyloid load, predict cognitive status in Alzheimer's disease.* Neurology, 2003. **60**(9): p. 1495-500.
58. Katsuse, O., et al., *Neurofibrillary tangle-related synaptic alterations of spinal motor neurons of P301L tau transgenic mice.* Neurosci Lett, 2006. **409**(2): p. 95-9.
59. Callahan, L.M., W.A. Vaules, and P.D. Coleman, *Quantitative decrease in synaptophysin message expression and increase in cathepsin D message expression in Alzheimer disease neurons containing neurofibrillary tangles.* J Neuropathol Exp Neurol, 1999. **58**(3): p. 275-87.
60. Ginsberg, S.D., et al., *Expression profile of transcripts in Alzheimer's disease tangle-bearing CA1 neurons.* Ann Neurol, 2000. **48**(1): p. 77-87.
61. Lin, W.L., et al., *Ultrastructural neuronal pathology in transgenic mice expressing mutant (P301L) human tau.* J Neurocytol, 2003. **32**(9): p. 1091-105.
62. LaPointe, N.E., et al., *The amino terminus of tau inhibits kinesin-dependent axonal transport: implications for filament toxicity.* J Neurosci Res, 2009. **87**(2): p. 440-51.
63. Bondareff, W., et al., *Immunohistochemical staging of neurofibrillary degeneration in Alzheimer's disease.* J Neuropathol Exp Neurol, 1994. **53**(2): p. 158-64.
64. Gomez-Isla, T., et al., *Neuronal loss correlates with but exceeds neurofibrillary tangles in Alzheimer's disease.* Ann Neurol, 1997. **41**(1): p. 17-24.
65. Vogt, B.A., et al., *Multivariate analysis of laminar patterns of neurodegeneration in posterior cingulate cortex in Alzheimer's disease.* Exp Neurol, 1998. **153**(1): p. 8-22.
66. Spires, T.L., et al., *Region-specific dissociation of neuronal loss and neurofibrillary pathology in a mouse model of tauopathy.* Am J Pathol, 2006. **168**(5): p. 1598-607.
67. Kopeikina, K.J., B.T. Hyman, and T.L. Spires-Jones, *Soluble forms of tau are toxic in Alzheimer's disease.* Transl Neurosci, 2012. **3**(3): p. 223-233.
68. Berger, Z., et al., *Accumulation of pathological tau species and memory loss in a conditional model of tauopathy.* J Neurosci, 2007. **27**(14): p. 3650-62.
69. Hoover, B.R., et al., *Tau mislocalization to dendritic spines mediates synaptic dysfunction independently of neurodegeneration.* Neuron, 2010. **68**(6): p. 1067-81.
70. Santacruz, K., et al., *Tau suppression in a neurodegenerative mouse model improves memory function.* Science, 2005. **309**(5733): p. 476-81.
71. Lasagna-Reeves, C.A., et al., *Tau oligomers impair memory and induce synaptic and mitochondrial dysfunction in wild-type mice.* Mol Neurodegener, 2011. **6**: p. 39.
72. Quintanilla, R.A., et al., *Caspase-cleaved tau expression induces mitochondrial dysfunction in immortalized cortical neurons: implications for the pathogenesis of Alzheimer disease.* J Biol Chem, 2009. **284**(28): p. 18754-66.
73. Wittmann, C.W., et al., *Tauopathy in Drosophila: neurodegeneration without neurofibrillary tangles.* Science, 2001. **293**(5530): p. 711-4.

74. Yoshiyama, Y., et al., *Synapse loss and microglial activation precede tangles in a P301S tauopathy mouse model.* Neuron, 2007. **53**(3): p. 337-51.
75. Eckermann, K., et al., *The beta-propensity of Tau determines aggregation and synaptic loss in inducible mouse models of tauopathy.* J Biol Chem, 2007. **282**(43): p. 31755-65.
76. Fox, L.M., et al., *Soluble tau species, not neurofibrillary aggregates, disrupt neural system integration in a tau transgenic model.* J Neuropathol Exp Neurol, 2011. **70**(7): p. 588-95.
77. Polydoro, M., et al., *Soluble pathological tau in the entorhinal cortex leads to presynaptic deficits in an early Alzheimer's disease model.* Acta Neuropathol, 2014. **127**(2): p. 257-70.
78. Lasagna-Reeves, C.A., et al., *Alzheimer brain-derived tau oligomers propagate pathology from endogenous tau.* Sci Rep, 2012. **2**: p. 700.
79. Chai, X., J.L. Dage, and M. Citron, *Constitutive secretion of tau protein by an unconventional mechanism.* Neurobiol Dis, 2012. **48**(3): p. 356-66.
80. Perez, M., et al., *Secretion of full-length tau or tau fragments in a cell culture model.* Neurosci Lett, 2016. **634**: p. 63-69.
81. Katsinelos, T., et al., *Unconventional Secretion Mediates the Trans-cellular Spreading of Tau.* Cell Rep, 2018. **23**(7): p. 2039-2055.
82. Kim, W., S. Lee, and G.F. Hall, *Secretion of human tau fragments resembling CSF-tau in Alzheimer's disease is modulated by the presence of the exon 2 insert.* FEBS Lett, 2010. **584**(14): p. 3085-8.
83. Saman, S., et al., *Exosome-associated tau is secreted in tauopathy models and is selectively phosphorylated in cerebrospinal fluid in early Alzheimer disease.* J Biol Chem, 2012. **287**(6): p. 3842-9.
84. Gomez-Ramos, A., et al., *Extracellular tau is toxic to neuronal cells.* FEBS Lett, 2006. **580**(20): p. 4842-50.
85. Fiandaca, M.S., et al., *Identification of preclinical Alzheimer's disease by a profile of pathogenic proteins in neurally derived blood exosomes: A case-control study.* Alzheimers Dement, 2015. **11**(6): p. 600-7 e1.
86. Wang, Y., et al., *The release and trans-synaptic transmission of Tau via exosomes.* Mol Neurodegener, 2017. **12**(1): p. 5.
87. Dujardin, S., et al., *Ectosomes: a new mechanism for non-exosomal secretion of tau protein.* PLoS One, 2014. **9**(6): p. e100760.
88. Tardivel, M., et al., *Tunneling nanotube (TNT)-mediated neuron-to neuron transfer of pathological Tau protein assemblies.* Acta Neuropathol Commun, 2016. **4**(1): p. 117.
89. Fontaine, S.N., et al., *DnaJ/Hsc70 chaperone complexes control the extracellular release of neurodegenerative-associated proteins.* EMBO J, 2016. **35**(14): p. 1537-49.
90. Rodriguez, L., et al., *Rab7A regulates tau secretion.* J Neurochem, 2017. **141**(4): p. 592-605.
91. Mohamed, N.V., A. Desjardins, and N. Leclerc, *Tau secretion is correlated to an increase of Golgi dynamics.* PLoS One, 2017. **12**(5): p. e0178288.

92. Karch, C.M., A.T. Jeng, and A.M. Goate, *Extracellular Tau levels are influenced by variability in Tau that is associated with tauopathies.* J Biol Chem, 2012. **287**(51): p. 42751-62.
93. Holmes, B.B., et al., *Heparan sulfate proteoglycans mediate internalization and propagation of specific proteopathic seeds.* Proc Natl Acad Sci U S A, 2013. **110**(33): p. E3138-47.
94. Greenberg, S.G. and P. Davies, *A preparation of Alzheimer paired helical filaments that displays distinct tau proteins by polyacrylamide gel electrophoresis.* Proc Natl Acad Sci U S A, 1990. **87**(15): p. 5827-31.
95. Lee, V.M., J. Wang, and J.Q. Trojanowski, *Purification of paired helical filament tau and normal tau from human brain tissue.* Methods Enzymol, 1999. **309**: p. 81-9.
96. Julien, C., A. Bretteville, and E. Planel, *Biochemical isolation of insoluble tau in transgenic mouse models of tauopathies.* Methods Mol Biol, 2012. **849**: p. 473-91.
97. de Calignon, A., et al., *Propagation of tau pathology in a model of early Alzheimer's disease.* Neuron, 2012. **73**(4): p. 685-97.
98. Sahara, N., et al., *Characteristics of TBS-extractable hyperphosphorylated tau species: aggregation intermediates in rTg4510 mouse brain.* J Alzheimers Dis, 2013. **33**(1): p. 249-63.
99. Lewis, J., et al., *Neurofibrillary tangles, amyotrophy and progressive motor disturbance in mice expressing mutant (P301L) tau protein.* Nat Genet, 2000. **25**(4): p. 402-5.
100. Martin, L., X. Latypova, and F. Terro, *Post-translational modifications of tau protein: implications for Alzheimer's disease.* Neurochem Int, 2011. **58**(4): p. 458-71.
101. Dickey, C.A., et al., *The high-affinity HSP90-CHIP complex recognizes and selectively degrades phosphorylated tau client proteins.* J Clin Invest, 2007. **117**(3): p. 648-58.
102. Drewes, G., et al., *Microtubule-associated protein/microtubule affinity-regulating kinase (p110mark). A novel protein kinase that regulates tau-microtubule interactions and dynamic instability by phosphorylation at the Alzheimer-specific site serine 262.* J Biol Chem, 1995. **270**(13): p. 7679-88.
103. Sengupta, A., et al., *Phosphorylation of tau at both Thr 231 and Ser 262 is required for maximal inhibition of its binding to microtubules.* Arch Biochem Biophys, 1998. **357**(2): p. 299-309.
104. Cavallini, A., et al., *An unbiased approach to identifying tau kinases that phosphorylate tau at sites associated with Alzheimer disease.* J Biol Chem, 2013. **288**(32): p. 23331-47.
105. Martin, L., et al., *Tau protein phosphatases in Alzheimer's disease: the leading role of PP2A.* Ageing Res Rev, 2013. **12**(1): p. 39-49.
106. Tian, Q., et al., *Injection of okadaic acid into the meynert nucleus basalis of rat brain induces decreased acetylcholine level and spatial memory deficit.* Neuroscience, 2004. **126**(2): p. 277-84.

107. Sun, L., et al., *Inhibition of protein phosphatase 2A- and protein phosphatase 1-induced tau hyperphosphorylation and impairment of spatial memory retention in rats.* Neuroscience, 2003. **118**(4): p. 1175-82.
108. Kopke, E., et al., *Microtubule-associated protein tau. Abnormal phosphorylation of a non-paired helical filament pool in Alzheimer disease.* J Biol Chem, 1993. **268**(32): p. 24374-84.
109. Guillozet-Bongaarts, A.L., et al., *Pseudophosphorylation of tau at serine 422 inhibits caspase cleavage: in vitro evidence and implications for tangle formation in vivo.* J Neurochem, 2006. **97**(4): p. 1005-14.
110. Ittner, L.M., Y.D. Ke, and J. Gotz, *Phosphorylated Tau interacts with c-Jun N-terminal kinase-interacting protein 1 (JIP1) in Alzheimer disease.* J Biol Chem, 2009. **284**(31): p. 20909-16.
111. Thies, E. and E.M. Mandelkow, *Missorting of tau in neurons causes degeneration of synapses that can be rescued by the kinase MARK2/Par-1.* J Neurosci, 2007. **27**(11): p. 2896-907.
112. Braak, E., H. Braak, and E.M. Mandelkow, *A sequence of cytoskeleton changes related to the formation of neurofibrillary tangles and neuropil threads.* Acta Neuropathol, 1994. **87**(6): p. 554-67.
113. Schneider, A., et al., *Phosphorylation that detaches tau protein from microtubules (Ser262, Ser214) also protects it against aggregation into Alzheimer paired helical filaments.* Biochemistry, 1999. **38**(12): p. 3549-58.
114. Yuzwa, S.A., et al., *A potent mechanism-inspired O-GlcNAcase inhibitor that blocks phosphorylation of tau in vivo.* Nat Chem Biol, 2008. **4**(8): p. 483-90.
115. Lefebvre, T., et al., *Evidence of a balance between phosphorylation and O-GlcNAc glycosylation of Tau proteins--a role in nuclear localization.* Biochim Biophys Acta, 2003. **1619**(2): p. 167-76.
116. Robertson, L.A., K.L. Moya, and K.C. Breen, *The potential role of tau protein O-glycosylation in Alzheimer's disease.* J Alzheimers Dis, 2004. **6**(5): p. 489-95.
117. Liu, F., et al., *Reduced O-GlcNAcylation links lower brain glucose metabolism and tau pathology in Alzheimer's disease.* Brain, 2009. **132**(Pt 7): p. 1820-32.
118. Lu, P.J., et al., *The prolyl isomerase Pin1 restores the function of Alzheimer-associated phosphorylated tau protein.* Nature, 1999. **399**(6738): p. 784-8.
119. Zhou, X.Z., et al., *Pin1-dependent prolyl isomerization regulates dephosphorylation of Cdc25C and tau proteins.* Mol Cell, 2000. **6**(4): p. 873-83.
120. Bulbarelli, A., et al., *Pin1 affects Tau phosphorylation in response to Abeta oligomers.* Mol Cell Neurosci, 2009. **42**(1): p. 75-80.
121. Hamdane, M., et al., *Pin1 allows for differential Tau dephosphorylation in neuronal cells.* Mol Cell Neurosci, 2006. **32**(1-2): p. 155-60.
122. Lavoie, S.B., A.L. Albert, and M. Vincent, *[Unexpected roles of the peptidyl-prolyl cis/trans isomerase Pin1].* Med Sci (Paris), 2003. **19**(12): p. 1251-8.
123. Arendt, T., et al., *Reversible paired helical filament-like phosphorylation of tau is an adaptive process associated with neuronal plasticity in hibernating animals.* J Neurosci, 2003. **23**(18): p. 6972-81.
124. Planel, E., et al., *Anesthesia leads to tau hyperphosphorylation through inhibition of phosphatase activity by hypothermia.* J Neurosci, 2007. **27**(12): p. 3090-7.

125. Goedert, M., *Relevance of Mutations in Tau for Understanding the Tauopathies.* Current Medicinal Chemistry - Immunology, Endocrine & Metabolic Agents, 2003. **3**(4): p. 341-348.
126. Wolfe, M.S., *Tau mutations in neurodegenerative diseases.* J Biol Chem, 2009. **284**(10): p. 6021-5.
127. Hutton, M., et al., *Association of missense and 5'-splice-site mutations in tau with the inherited dementia FTDP-17.* Nature, 1998. **393**(6686): p. 702-5.
128. Spillantini, M.G., et al., *Mutation in the tau gene in familial multiple system tauopathy with presenile dementia.* Proc Natl Acad Sci U S A, 1998. **95**(13): p. 7737-41.
129. Iseki, E., et al., *Familial frontotemporal dementia and parkinsonism with a novel N296H mutation in exon 10 of the tau gene and a widespread tau accumulation in the glial cells.* Acta Neuropathol, 2001. **102**(3): p. 285-92.
130. D'Souza, I., et al., *Missense and silent tau gene mutations cause frontotemporal dementia with parkinsonism-chromosome 17 type, by affecting multiple alternative RNA splicing regulatory elements.* Proc Natl Acad Sci U S A, 1999. **96**(10): p. 5598-603.
131. Spillantini, M.G., et al., *A novel tau mutation (N296N) in familial dementia with swollen achromatic neurons and corticobasal inclusion bodies.* Ann Neurol, 2000. **48**(6): p. 939-43.
132. Yasuda, M., et al., *A novel mutation at position +12 in the intron following exon 10 of the tau gene in familial frontotemporal dementia (FTD-Kumamoto).* Ann Neurol, 2000. **47**(4): p. 422-9.
133. Miyamoto, K., et al., *Familial frontotemporal dementia and parkinsonism with a novel mutation at an intron 10+11-splice site in the tau gene.* Ann Neurol, 2001. **50**(1): p. 117-20.
134. Yoshida, H., R.A. Crowther, and M. Goedert, *Functional effects of tau gene mutations deltaN296 and N296H.* J Neurochem, 2002. **80**(3): p. 548-51.
135. Grover, A., et al., *Effects on splicing and protein function of three mutations in codon N296 of tau in vitro.* Neurosci Lett, 2002. **323**(1): p. 33-6.
136. Hasegawa, M., et al., *FTDP-17 mutations N279K and S305N in tau produce increased splicing of exon 10.* FEBS Lett, 1999. **443**(2): p. 93-6.
137. Goedert, M., et al., *Tau gene mutation in familial progressive subcortical gliosis.* Nat Med, 1999. **5**(4): p. 454-7.
138. Stanford, P.M., et al., *Mutations in the tau gene that cause an increase in three repeat tau and frontotemporal dementia.* Brain, 2003. **126**(Pt 4): p. 814-26.
139. Hong, M., et al., *Mutation-specific functional impairments in distinct tau isoforms of hereditary FTDP-17.* Science, 1998. **282**(5395): p. 1914-7.
140. Hasegawa, M., M.J. Smith, and M. Goedert, *Tau proteins with FTDP-17 mutations have a reduced ability to promote microtubule assembly.* FEBS Lett, 1998. **437**(3): p. 207-10.
141. Pickering-Brown, S.M., et al., *Frontotemporal dementia with Pick-type histology associated with Q336R mutation in the tau gene.* Brain, 2004. **127**(Pt 6): p. 1415-26.
142. Hayashi, S., et al., *Late-onset frontotemporal dementia with a novel exon 1 (Arg5His) tau gene mutation.* Ann Neurol, 2002. **51**(4): p. 525-30.

143. Kovacs, G.G., et al., *Unclassifiable tauopathy associated with an A152T variation in MAPT exon 7.* Clin Neuropathol, 2011. **30**(1): p. 3-10.
144. Coppola, G., et al., *Evidence for a role of the rare p.A152T variant in MAPT in increasing the risk for FTD-spectrum and Alzheimer's diseases.* Hum Mol Genet, 2012. **21**(15): p. 3500-12.
145. Grover, A., et al., *A novel tau mutation in exon 9 (1260V) causes a four-repeat tauopathy.* Exp Neurol, 2003. **184**(1): p. 131-40.
146. Pastor, P., et al., *Familial atypical progressive supranuclear palsy associated with homozigosity for the delN296 mutation in the tau gene.* Ann Neurol, 2001. **49**(2): p. 263-7.
147. Dumanchin, C., et al., *Segregation of a missense mutation in the microtubule-associated protein tau gene with familial frontotemporal dementia and parkinsonism.* Hum Mol Genet, 1998. **7**(11): p. 1825-9.
148. Clark, L.N., et al., *Pathogenic implications of mutations in the tau gene in pallido-ponto-nigral degeneration and related neurodegenerative disorders linked to chromosome 17.* Proc Natl Acad Sci U S A, 1998. **95**(22): p. 13103-7.
149. Spillantini, M.G., et al., *Tau pathology in two Dutch families with mutations in the microtubule-binding region of tau.* Am J Pathol, 1998. **153**(5): p. 1359-63.
150. Tacik, P., et al., *A Novel Tau Mutation in Exon 12, p.Q336H, Causes Hereditary Pick Disease.* J Neuropathol Exp Neurol, 2015. **74**(11): p. 1042-52.
151. Poorkaj, P., et al., *Tau is a candidate gene for chromosome 17 frontotemporal dementia.* Ann Neurol, 1998. **43**(6): p. 815-25.
152. Sumi, S.M., et al., *Familial presenile dementia with psychosis associated with cortical neurofibrillary tangles and degeneration of the amygdala.* Neurology, 1992. **42**(1): p. 120-7.
153. Nicholl, D.J., et al., *An English kindred with a novel recessive tauopathy and respiratory failure.* Ann Neurol, 2003. **54**(5): p. 682-6.
154. Rossi, G., et al., *New mutations in MAPT gene causing frontotemporal lobar degeneration: biochemical and structural characterization.* Neurobiol Aging, 2012. **33**(4): p. 834 e1-6.
155. Kouri, N., et al., *Novel mutation in MAPT exon 13 (p.N410H) causes corticobasal degeneration.* Acta Neuropathol, 2014. **127**(2): p. 271-82.
156. Cowan, C.M. and A. Mudher, *Are tau aggregates toxic or protective in tauopathies?* Front Neurol, 2013. **4**: p. 114.
157. Ballatore, C., V.M. Lee, and J.Q. Trojanowski, *Tau-mediated neurodegeneration in Alzheimer's disease and related disorders.* Nat Rev Neurosci, 2007. **8**(9): p. 663-72.
158. Guo, J.L. and V.M. Lee, *Seeding of normal Tau by pathological Tau conformers drives pathogenesis of Alzheimer-like tangles.* J Biol Chem, 2011. **286**(17): p. 15317-31.
159. Musi, N., et al., *Tau protein aggregation is associated with cellular senescence in the brain.* Aging Cell, 2018. **17**(6): p. e12840.
160. Yosef, R., et al., *Directed elimination of senescent cells by inhibition of BCL-W and BCL-XL.* Nat Commun, 2016. **7**: p. 11190.

161. de Calignon, A., et al., *Tangle-bearing neurons survive despite disruption of membrane integrity in a mouse model of tauopathy.* J Neuropathol Exp Neurol, 2009. **68**(7): p. 757-61.
162. Coppe, J.P., et al., *The senescence-associated secretory phenotype: the dark side of tumor suppression.* Annu Rev Pathol, 2010. **5**: p. 99-118.
163. Spillantini, M.G. and M. Goedert, *Tau pathology and neurodegeneration.* Lancet Neurol, 2013. **12**(6): p. 609-22.
164. Fein, J.A., et al., *Co-localization of amyloid beta and tau pathology in Alzheimer's disease synaptosomes.* Am J Pathol, 2008. **172**(6): p. 1683-92.
165. Tai, H.C., et al., *The synaptic accumulation of hyperphosphorylated tau oligomers in Alzheimer disease is associated with dysfunction of the ubiquitin-proteasome system.* Am J Pathol, 2012. **181**(4): p. 1426-35.
166. Henkins, K.M., et al., *Extensive p-tau pathology and SDS-stable p-tau oligomers in Alzheimer's cortical synapses.* Brain Pathol, 2012. **22**(6): p. 826-33.
167. Sahara, N., et al., *Biochemical Distribution of Tau Protein in Synaptosomal Fraction of Transgenic Mice Expressing Human P301L Tau.* Front Neurol, 2014. **5**: p. 26.
168. McInnes, J., et al., *Synaptogyrin-3 Mediates Presynaptic Dysfunction Induced by Tau.* Neuron, 2018. **97**(4): p. 823-835 e8.
169. Zhou, L., et al., *Tau association with synaptic vesicles causes presynaptic dysfunction.* Nat Commun, 2017. **8**: p. 15295.
170. Usenovic, M., et al., *Internalized Tau Oligomers Cause Neurodegeneration by Inducing Accumulation of Pathogenic Tau in Human Neurons Derived from Induced Pluripotent Stem Cells.* J Neurosci, 2015. **35**(42): p. 14234-50.
171. Moreno, H., et al., *Blocking Effects of Human Tau on Squid Giant Synapse Transmission and Its Prevention by T-817 MA.* Front Synaptic Neurosci, 2011. **3**: p. 3.
172. Moreno, H., et al., *Tau pathology-mediated presynaptic dysfunction.* Neuroscience, 2016. **325**: p. 30-8.
173. Min, S.W., et al., *Critical role of acetylation in tau-mediated neurodegeneration and cognitive deficits.* Nat Med, 2015. **21**(10): p. 1154-62.
174. Warmus, B.A., et al., *Tau-mediated NMDA receptor impairment underlies dysfunction of a selectively vulnerable network in a mouse model of frontotemporal dementia.* J Neurosci, 2014. **34**(49): p. 16482-95.
175. Vanderweyde, T., et al., *Interaction of tau with the RNA-Binding Protein TIA1 Regulates tau Pathophysiology and Toxicity.* Cell Rep, 2016. **15**(7): p. 1455-1466.
176. Sontag, E., et al., *Regulation of the phosphorylation state and microtubule-binding activity of Tau by protein phosphatase 2A.* Neuron, 1996. **17**(6): p. 1201-7.
177. Agarwal-Mawal, A., et al., *14-3-3 connects glycogen synthase kinase-3 beta to tau within a brain microtubule-associated tau phosphorylation complex.* J Biol Chem, 2003. **278**(15): p. 12722-8.
178. Maurin, H., et al., *Tauopathy differentially affects cell adhesion molecules in mouse brain: early down-regulation of nectin-3 in stratum lacunosum moleculare.* PLoS One, 2013. **8**(5): p. e63589.

179. Manczak, M. and P.H. Reddy, *Abnormal interaction between the mitochondrial fission protein Drp1 and hyperphosphorylated tau in Alzheimer's disease neurons: implications for mitochondrial dysfunction and neuronal damage.* Hum Mol Genet, 2012. **21**(11): p. 2538-47.
180. Schulz, K.L., et al., *A new link to mitochondrial impairment in tauopathies.* Mol Neurobiol, 2012. **46**(1): p. 205-16.
181. Quintanilla, R.A., et al., *Phosphorylated tau potentiates Abeta-induced mitochondrial damage in mature neurons.* Neurobiol Dis, 2014. **71**: p. 260-9.
182. Quintanilla, R.A., et al., *Truncated tau and Abeta cooperatively impair mitochondria in primary neurons.* Neurobiol Aging, 2012. **33**(3): p. 619 e25-35.
183. Rhein, V., et al., *Amyloid-beta and tau synergistically impair the oxidative phosphorylation system in triple transgenic Alzheimer's disease mice.* Proc Natl Acad Sci U S A, 2009. **106**(47): p. 20057-62.
184. Lasagna-Reeves, C.A., et al., *The formation of tau pore-like structures is prevalent and cell specific: possible implications for the disease phenotypes.* Acta Neuropathol Commun, 2014. **2**: p. 56.
185. Patel, N., et al., *Ion Channel Formation by Tau Protein: Implications for Alzheimer's Disease and Tauopathies.* Biochemistry, 2015. **54**(50): p. 7320-5.
186. Christensen, R.A., et al., *Calcium dyshomeostasis in beta-amyloid and tau-bearing skeletal myotubes.* J Biol Chem, 2004. **279**(51): p. 53524-32.
187. Iqbal, K., et al., *Defective brain microtubule assembly in Alzheimer's disease.* Lancet, 1986. **2**(8504): p. 421-6.
188. Grundke-Iqbal, I., et al., *Abnormal phosphorylation of the microtubule-associated protein tau (tau) in Alzheimer cytoskeletal pathology.* Proc Natl Acad Sci U S A, 1986. **83**(13): p. 4913-7.
189. Bramblett, G.T., et al., *Abnormal tau phosphorylation at Ser396 in Alzheimer's disease recapitulates development and contributes to reduced microtubule binding.* Neuron, 1993. **10**(6): p. 1089-99.
190. Dayanandan, R., et al., *Mutations in tau reduce its microtubule binding properties in intact cells and affect its phosphorylation.* FEBS Lett, 1999. **446**(2-3): p. 228-32.
191. Mudher, A., et al., *GSK-3beta inhibition reverses axonal transport defects and behavioural phenotypes in Drosophila.* Mol Psychiatry, 2004. **9**(5): p. 522-30.
192. Seitz, A., et al., *Single-molecule investigation of the interference between kinesin, tau and MAP2c.* EMBO J, 2002. **21**(18): p. 4896-905.
193. Ebneth, A., et al., *Overexpression of tau protein inhibits kinesin-dependent trafficking of vesicles, mitochondria, and endoplasmic reticulum: implications for Alzheimer's disease.* J Cell Biol, 1998. **143**(3): p. 777-94.
194. Chaudhary, A.R., et al., *Tau directs intracellular trafficking by regulating the forces exerted by kinesin and dynein teams.* Traffic, 2018. **19**(2): p. 111-121.
195. Cummins, N., et al., *Disease-associated tau impairs mitophagy by inhibiting Parkin translocation to mitochondria.* EMBO J, 2019. **38**(3).
196. Schweers, O., et al., *Oxidation of cysteine-322 in the repeat domain of microtubule-associated protein tau controls the in vitro assembly of paired helical filaments.* Proc Natl Acad Sci U S A, 1995. **92**(18): p. 8463-7.

197. Dinkel, P.D., et al., *RNA Binds to Tau Fibrils and Sustains Template-Assisted Growth.* Biochemistry, 2015. **54**(30): p. 4731-40.
198. Zhang, X., et al., *RNA stores tau reversibly in complex coacervates.* PLoS Biol, 2017. **15**(7): p. e2002183.
199. Ginsberg, S.D., et al., *Sequestration of RNA in Alzheimer's disease neurofibrillary tangles and senile plaques.* Ann Neurol, 1997. **41**(2): p. 200-9.
200. Ginsberg, S.D., et al., *RNA sequestration to pathological lesions of neurodegenerative diseases.* Acta Neuropathol, 1998. **96**(5): p. 487-94.
201. Meier, S., et al., *Identification of Novel Tau Interactions with Endoplasmic Reticulum Proteins in Alzheimer's Disease Brain.* J Alzheimers Dis, 2015. **48**(3): p. 687-702.
202. Maziuk, B.F., et al., *RNA binding proteins co-localize with small tau inclusions in tauopathy.* Acta Neuropathol Commun, 2018. **6**(1): p. 71.
203. Gilks, N., et al., *Stress granule assembly is mediated by prion-like aggregation of TIA-1.* Mol Biol Cell, 2004. **15**(12): p. 5383-98.
204. Jiang, L., et al., *TIA1 regulates the generation and response to toxic tau oligomers.* Acta Neuropathol, 2019. **137**(2): p. 259-277.
205. Ding, Q., et al., *Ribosome dysfunction is an early event in Alzheimer's disease.* J Neurosci, 2005. **25**(40): p. 9171-5.
206. Papasozomenos, S.C. and L.I. Binder, *Phosphorylation determines two distinct species of Tau in the central nervous system.* Cell Motil Cytoskeleton, 1987. **8**(3): p. 210-26.
207. FW, M., *The effects of high explosives upon the central nervous system, lecture I.* . Lancet, 1916. **48**: p. 331-8.
208. Smith, C., et al., *Tau immunohistochemistry in acute brain injury.* Neuropathol Appl Neurobiol, 2003. **29**(5): p. 496-502.
209. Ikonomovic, M.D., et al., *Alzheimer's pathology in human temporal cortex surgically excised after severe brain injury.* Exp Neurol, 2004. **190**(1): p. 192-203.
210. Liliang, P.C., et al., *Tau proteins in serum predict outcome after severe traumatic brain injury.* J Surg Res, 2010. **160**(2): p. 302-7.
211. Ost, M., et al., *Initial CSF total tau correlates with 1-year outcome in patients with traumatic brain injury.* Neurology, 2006. **67**(9): p. 1600-4.
212. Falcon, B., et al., *Novel tau filament fold in chronic traumatic encephalopathy encloses hydrophobic molecules.* Nature, 2019. **568**(7752): p. 420-423.
213. Mortimer, J.A., et al., *Head injury as a risk factor for Alzheimer's disease.* Neurology, 1985. **35**(2): p. 264-7.
214. Mortimer, J.A., et al., *Head trauma as a risk factor for Alzheimer's disease: a collaborative re-analysis of case-control studies. EURODEM Risk Factors Research Group.* Int J Epidemiol, 1991. **20 Suppl 2**: p. S28-35.
215. Mayeux, R., et al., *Genetic susceptibility and head injury as risk factors for Alzheimer's disease among community-dwelling elderly persons and their first-degree relatives.* Ann Neurol, 1993. **33**(5): p. 494-501.
216. Rasmusson, D.X., et al., *Head injury as a risk factor in Alzheimer's disease.* Brain Inj, 1995. **9**(3): p. 213-9.

217. O'Meara, E.S., et al., *Head injury and risk of Alzheimer's disease by apolipoprotein E genotype.* Am J Epidemiol, 1997. **146**(5): p. 373-84.
218. van Duijn, C.M. and A. Hofman, *Risk factors for Alzheimer's disease: the EURODEM collaborative re-analysis of case-control studies.* Neuroepidemiology, 1992. **11 Suppl 1**: p. 106-13.
219. Schofield, P.W., et al., *Alzheimer's disease after remote head injury: an incidence study.* J Neurol Neurosurg Psychiatry, 1997. **62**(2): p. 119-24.
220. Guo, Z., et al., *Head injury and the risk of AD in the MIRAGE study.* Neurology, 2000. **54**(6): p. 1316-23.
221. Fleminger, S., et al., *Head injury as a risk factor for Alzheimer's disease: the evidence 10 years on; a partial replication.* J Neurol Neurosurg Psychiatry, 2003. **74**(7): p. 857-62.
222. Mendez, M.F., et al., *Prevalence of Traumatic Brain Injury in Early Versus Late-Onset Alzheimer's Disease.* J Alzheimers Dis, 2015. **47**(4): p. 985-93.
223. Plassman, B.L., et al., *Documented head injury in early adulthood and risk of Alzheimer's disease and other dementias.* Neurology, 2000. **55**(8): p. 1158-66.
224. Nemetz, P.N., et al., *Traumatic brain injury and time to onset of Alzheimer's disease: a population-based study.* Am J Epidemiol, 1999. **149**(1): p. 32-40.
225. LoBue, C., et al., *Traumatic brain injury history is associated with earlier age of onset of Alzheimer disease.* Clin Neuropsychol, 2017. **31**(1): p. 85-98.
226. Ryan, D.H., *A Scottish record linkage study of risk factors in medical history and dementia outcome in hospital patients.* Dementia, 1994. **5**(6): p. 339-47.
227. Fratiglinoni L, A.A., Viitanen M, Winblad B., *Risk factors for late-onset Alzheimer's disease: a population based, casecontrol study.* . Ann Neurol, 1993(33): p. 258–266.
228. Williams, D.B., et al., *Brain injury and neurologic sequelae: a cohort study of dementia, parkinsonism, and amyotrophic lateral sclerosis.* Neurology, 1991. **41**(10): p. 1554-7.
229. Launer, L.J., et al., *Rates and risk factors for dementia and Alzheimer's disease: results from EURODEM pooled analyses. EURODEM Incidence Research Group and Work Groups. European Studies of Dementia.* Neurology, 1999. **52**(1): p. 78-84.
230. Tripodis, Y., et al., *The Effect of Traumatic Brain Injury History with Loss of Consciousness on Rate of Cognitive Decline Among Older Adults with Normal Cognition and Alzheimer's Disease Dementia.* J Alzheimers Dis, 2017. **59**(1): p. 251-263.
231. Weiner, M.W., et al., *Effects of traumatic brain injury and posttraumatic stress disorder on development of Alzheimer's disease in Vietnam Veterans using the Alzheimer's Disease Neuroimaging Initiative: Preliminary Report.* Alzheimers Dement (N Y), 2017. **3**(2): p. 177-188.
232. Julien, J., et al., *Association of traumatic brain injury and Alzheimer disease onset: A systematic review.* Ann Phys Rehabil Med, 2017. **60**(5): p. 347-356.
233. Kalkonde, Y.V., et al., *Medical and environmental risk factors associated with frontotemporal dementia: a case-control study in a veteran population.* Alzheimers Dement, 2012. **8**(3): p. 204-10.

234. Rosso, S.M., et al., *Medical and environmental risk factors for sporadic frontotemporal dementia: a retrospective case-control study.* J Neurol Neurosurg Psychiatry, 2003. **74**(11): p. 1574-6.
235. Deutsch, M.B., M.F. Mendez, and E. Teng, *Interactions between traumatic brain injury and frontotemporal degeneration.* Dement Geriatr Cogn Disord, 2015. **39**(3-4): p. 143-53.
236. Bahia, V.S., L.T. Takada, and V. Deramecourt, *Neuropathology of frontotemporal lobar degeneration: a review.* Dement Neuropsychol, 2013. **7**(1): p. 19-26.
237. Xiong, Y., A. Mahmood, and M. Chopp, *Animal models of traumatic brain injury.* Nat Rev Neurosci, 2013. **14**(2): p. 128-42.
238. Marklund, N., *Rodent Models of Traumatic Brain Injury: Methods and Challenges.* Methods Mol Biol, 2016. **1462**: p. 29-46.
239. Liliang, P.C., et al., *Relationship between injury severity and serum tau protein levels in traumatic brain injured rats.* Resuscitation, 2010. **81**(9): p. 1205-8.
240. Rostami, E., et al., *A Model for Mild Traumatic Brain Injury that Induces Limited Transient Memory Impairment and Increased Levels of Axon Related Serum Biomarkers.* Front Neurol, 2012. **3**: p. 115.
241. Tran, H.T., et al., *Distinct temporal and anatomical distributions of amyloid-beta and tau abnormalities following controlled cortical impact in transgenic mice.* PLoS One, 2011. **6**(9): p. e25475.
242. Bennett, R.E., et al., *Human apolipoprotein E4 worsens acute axonal pathology but not amyloid-beta immunoreactivity after traumatic brain injury in 3xTG-AD mice.* J Neuropathol Exp Neurol, 2013. **72**(5): p. 396-403.
243. Rubenstein, R., et al., *A novel, ultrasensitive assay for tau: potential for assessing traumatic brain injury in tissues and biofluids.* J Neurotrauma, 2015. **32**(5): p. 342-52.
244. Kovesdi, E., et al., *The effect of enriched environment on the outcome of traumatic brain injury; a behavioral, proteomics, and histological study.* Front Neurosci, 2011. **5**: p. 42.
245. Arun, P., et al., *Distinct patterns of expression of traumatic brain injury biomarkers after blast exposure: role of compromised cell membrane integrity.* Neurosci Lett, 2013. **552**: p. 87-91.
246. Kane, M.J., et al., *A mouse model of human repetitive mild traumatic brain injury.* J Neurosci Methods, 2012. **203**(1): p. 41-9.
247. Zhang, J., et al., *Inhibition of monoacylglycerol lipase prevents chronic traumatic encephalopathy-like neuropathology in a mouse model of repetitive mild closed head injury.* J Cereb Blood Flow Metab, 2015. **35**(4): p. 706.
248. Huber, B.R., et al., *Blast exposure causes early and persistent aberrant phospho- and cleaved-tau expression in a murine model of mild blast-induced traumatic brain injury.* J Alzheimers Dis, 2013. **37**(2): p. 309-23.
249. Laskowitz, D.T., et al., *Traumatic brain injury exacerbates neurodegenerative pathology: improvement with an apolipoprotein E-based therapeutic.* J Neurotrauma, 2010. **27**(11): p. 1983-95.
250. Petraglia, A.L., et al., *The pathophysiology underlying repetitive mild traumatic brain injury in a novel mouse model of chronic traumatic encephalopathy.* Surg Neurol Int, 2014. **5**: p. 184.

251. Tran, H.T., et al., *Controlled cortical impact traumatic brain injury in 3xTg-AD mice causes acute intra-axonal amyloid-beta accumulation and independently accelerates the development of tau abnormalities.* J Neurosci, 2011. **31**(26): p. 9513-25.
252. Hawkins, B.E., et al., *Rapid accumulation of endogenous tau oligomers in a rat model of traumatic brain injury: possible link between traumatic brain injury and sporadic tauopathies.* J Biol Chem, 2013. **288**(23): p. 17042-50.
253. Goldstein, L.E., et al., *Chronic traumatic encephalopathy in blast-exposed military veterans and a blast neurotrauma mouse model.* Sci Transl Med, 2012. **4**(134): p. 134ra60.
254. Namjoshi, D.R., et al., *Merging pathology with biomechanics using CHIMERA (Closed-Head Impact Model of Engineered Rotational Acceleration): a novel, surgery-free model of traumatic brain injury.* Mol Neurodegener, 2014. **9**: p. 55.
255. Sawmiller, D., et al., *Luteolin reduces Alzheimer's disease pathologies induced by traumatic brain injury.* Int J Mol Sci, 2014. **15**(1): p. 895-904.
256. Yu, F., Y. Zhang, and D.M. Chuang, *Lithium reduces BACE1 overexpression, beta amyloid accumulation, and spatial learning deficits in mice with traumatic brain injury.* J Neurotrauma, 2012. **29**(13): p. 2342-51.
257. Li, Y., et al., *Protective effects of decay-accelerating factor on blast-induced neurotrauma in rats.* Acta Neuropathol Commun, 2013. **1**: p. 52.
258. Kondo, A., et al., *Antibody against early driver of neurodegeneration cis P-tau blocks brain injury and tauopathy.* Nature, 2015. **523**(7561): p. 431-436.
259. Sabbagh, J.J., et al., *Noncontact Rotational Head Injury Produces Transient Cognitive Deficits but Lasting Neuropathological Changes.* J Neurotrauma, 2016. **33**(19): p. 1751-1760.
260. McAteer, K.M., et al., *Short and Long Term Behavioral and Pathological Changes in a Novel Rodent Model of Repetitive Mild Traumatic Brain Injury.* PLoS One, 2016. **11**(8): p. e0160220.
261. Wang, Y., et al., *The tyrosine phosphatase PTPN13/FAP-1 links calpain-2, TBI and tau tyrosine phosphorylation.* Sci Rep, 2017. **7**(1): p. 11771.
262. Mouzon, B.C., et al., *Lifelong behavioral and neuropathological consequences of repetitive mild traumatic brain injury.* Ann Clin Transl Neurol, 2018. **5**(1): p. 64-80.
263. Ojo, J.O., et al., *Repetitive mild traumatic brain injury augments tau pathology and glial activation in aged hTau mice.* J Neuropathol Exp Neurol, 2013. **72**(2): p. 137-51.
264. Lv, Q., et al., *Intranasal nerve growth factor attenuates tau phosphorylation in brain after traumatic brain injury in rats.* J Neurol Sci, 2014. **345**(1-2): p. 48-55.
265. Gerson, J., et al., *Tau Oligomers Derived from Traumatic Brain Injury Cause Cognitive Impairment and Accelerate Onset of Pathology in Htau Mice.* J Neurotrauma, 2016. **33**(22): p. 2034-2043.
266. Ojo, J.O., et al., *Chronic Repetitive Mild Traumatic Brain Injury Results in Reduced Cerebral Blood Flow, Axonal Injury, Gliosis, and Increased T-Tau and Tau Oligomers.* J Neuropathol Exp Neurol, 2016. **75**(7): p. 636-55.
267. Logsdon, A.F., et al., *A mouse Model of Focal Vascular Injury Induces Astrocyte Reactivity, Tau Oligomers, and Aberrant Behavior.* Arch Neurosci, 2017. **4**(2).

268. Yoshiyama, Y., et al., *Enhanced neurofibrillary tangle formation, cerebral atrophy, and cognitive deficits induced by repetitive mild brain injury in a transgenic tauopathy mouse model.* J Neurotrauma, 2005. **22**(10): p. 1134-41.
269. McKee, A.C. and D.H. Daneshvar, *The neuropathology of traumatic brain injury.* Handb Clin Neurol, 2015. **127**: p. 45-66.
270. Cherry, J.D., et al., *Microglial neuroinflammation contributes to tau accumulation in chronic traumatic encephalopathy.* Acta Neuropathol Commun, 2016. **4**(1): p. 112.
271. Laurent, C., et al., *A2A adenosine receptor deletion is protective in a mouse model of Tauopathy.* Mol Psychiatry, 2016. **21**(1): p. 149.
272. Wang, Y., et al., *COX-2 metabolic products, the prostaglandin I2 and F2alpha, mediate the effects of TNF-alpha and Zn(2+) in stimulating the phosphorylation of Tau.* Oncotarget, 2017. **8**(59): p. 99296-99311.
273. Lee, D.C., et al., *LPS- induced inflammation exacerbates phospho-tau pathology in rTg4510 mice.* J Neuroinflammation, 2010. **7**: p. 56.
274. Li, Y., et al., *Interleukin-1 mediates pathological effects of microglia on tau phosphorylation and on synaptophysin synthesis in cortical neurons through a p38-MAPK pathway.* J Neurosci, 2003. **23**(5): p. 1605-11.
275. Kitazawa, M., et al., *Lipopolysaccharide-induced inflammation exacerbates tau pathology by a cyclin-dependent kinase 5-mediated pathway in a transgenic model of Alzheimer's disease.* J Neurosci, 2005. **25**(39): p. 8843-53.
276. Bemiller, S.M., et al., *TREM2 deficiency exacerbates tau pathology through dysregulated kinase signaling in a mouse model of tauopathy.* Mol Neurodegener, 2017. **12**(1): p. 74.
277. Leyns, C.E.G., et al., *TREM2 deficiency attenuates neuroinflammation and protects against neurodegeneration in a mouse model of tauopathy.* Proc Natl Acad Sci U S A, 2017. **114**(43): p. 11524-11529.
278. Kim, B., et al., *Increased tau phosphorylation and cleavage in mouse models of type 1 and type 2 diabetes.* Endocrinology, 2009. **150**(12): p. 5294-301.
279. El Khoury, N.B., et al., *Insulin dysfunction and Tau pathology.* Front Cell Neurosci, 2014. **8**: p. 22.
280. Clodfelder-Miller, B.J., et al., *Tau is hyperphosphorylated at multiple sites in mouse brain in vivo after streptozotocin-induced insulin deficiency.* Diabetes, 2006. **55**(12): p. 3320-5.
281. Planel, E., et al., *Insulin dysfunction induces in vivo tau hyperphosphorylation through distinct mechanisms.* J Neurosci, 2007. **27**(50): p. 13635-48.
282. Li, Z.G., W. Zhang, and A.A. Sima, *Alzheimer-like changes in rat models of spontaneous diabetes.* Diabetes, 2007. **56**(7): p. 1817-24.
283. Schechter, R., D. Beju, and K.E. Miller, *The effect of insulin deficiency on tau and neurofilament in the insulin knockout mouse.* Biochem Biophys Res Commun, 2005. **334**(4): p. 979-86.
284. Hong, M. and V.M. Lee, *Insulin and insulin-like growth factor-1 regulate tau phosphorylation in cultured human neurons.* J Biol Chem, 1997. **272**(31): p. 19547-53.
285. Cheng, C.M., et al., *Tau is hyperphosphorylated in the insulin-like growth factor-I null brain.* Endocrinology, 2005. **146**(12): p. 5086-91.

286. Platt, T.L., et al., *Obesity, diabetes, and leptin resistance promote tau pathology in a mouse model of disease.* Neuroscience, 2016. **315**: p. 162-74.
287. Chatterjee, S. and A. Mudher, *Alzheimer's Disease and Type 2 Diabetes: A Critical Assessment of the Shared Pathological Traits.* Front Neurosci, 2018. **12**: p. 383.
288. Tramutola, A., et al., *Alteration of mTOR signaling occurs early in the progression of Alzheimer disease (AD): analysis of brain from subjects with pre-clinical AD, amnestic mild cognitive impairment and late-stage AD.* J Neurochem, 2015. **133**(5): p. 739-49.
289. Perluigi, M., et al., *Neuropathological role of PI3K/Akt/mTOR axis in Down syndrome brain.* Biochim Biophys Acta, 2014. **1842**(7): p. 1144-53.
290. Kang, E.B. and J.Y. Cho, *Effect of treadmill exercise on PI3K/AKT/mTOR, autophagy, and Tau hyperphosphorylation in the cerebral cortex of NSE/htau23 transgenic mice.* J Exerc Nutrition Biochem, 2015. **19**(3): p. 199-209.
291. Tang, Z., et al., *mTor mediates tau localization and secretion: Implication for Alzheimer's disease.* Biochim Biophys Acta, 2015. **1853**(7): p. 1646-57.
292. Markesbery, W.R., *Oxidative stress hypothesis in Alzheimer's disease.* Free Radic Biol Med, 1997. **23**(1): p. 134-47.
293. Liu, Z., et al., *The Ambiguous Relationship of Oxidative Stress, Tau Hyperphosphorylation, and Autophagy Dysfunction in Alzheimer's Disease.* Oxid Med Cell Longev, 2015. **2015**: p. 352723.
294. Zhu, X., et al., *Activation of p38 kinase links tau phosphorylation, oxidative stress, and cell cycle-related events in Alzheimer disease.* J Neuropathol Exp Neurol, 2000. **59**(10): p. 880-8.
295. Su, B., et al., *Chronic oxidative stress causes increased tau phosphorylation in M17 neuroblastoma cells.* Neurosci Lett, 2010. **468**(3): p. 267-71.
296. Lovell, M.A., et al., *Induction of hyperphosphorylated tau in primary rat cortical neuron cultures mediated by oxidative stress and glycogen synthase kinase-3.* J Alzheimers Dis, 2004. **6**(6): p. 659-71; discussion 673-81.
297. Patil, S. and C. Chan, *Palmitic and stearic fatty acids induce Alzheimer-like hyperphosphorylation of tau in primary rat cortical neurons.* Neurosci Lett, 2005. **384**(3): p. 288-93.
298. Melov, S., et al., *Mitochondrial oxidative stress causes hyperphosphorylation of tau.* PLoS One, 2007. **2**(6): p. e536.
299. Takeda, A., et al., *In Alzheimer's disease, heme oxygenase is coincident with Alz50, an epitope of tau induced by 4-hydroxy-2-nonenal modification.* J Neurochem, 2000. **75**(3): p. 1234-41.
300. Perez, M., et al., *Phosphorylated, but not native, tau protein assembles following reaction with the lipid peroxidation product, 4-hydroxy-2-nonenal.* FEBS Lett, 2000. **486**(3): p. 270-4.
301. Xiong, Y., A. Mahmood, and M. Chopp, *Current understanding of neuroinflammation after traumatic brain injury and cell-based therapeutic opportunities.* Chin J Traumatol, 2018. **21**(3): p. 137-151.
302. Weber, J.T., *Altered calcium signaling following traumatic brain injury.* Front Pharmacol, 2012. **3**: p. 60.

303. Johnson, V.E., W. Stewart, and D.H. Smith, *Axonal pathology in traumatic brain injury.* Exp Neurol, 2013. **246**: p. 35-43.
304. Hill, C.S., M.P. Coleman, and D.K. Menon, *Traumatic Axonal Injury: Mechanisms and Translational Opportunities.* Trends Neurosci, 2016. **39**(5): p. 311-324.
305. Neary, J.T., *Protein kinase signaling cascades in CNS trauma.* IUBMB Life, 2005. **57**(11): p. 711-8.
306. Stoica, B.A. and A.I. Faden, *Cell death mechanisms and modulation in traumatic brain injury.* Neurotherapeutics, 2010. **7**(1): p. 3-12.
307. Lighthall, J.W., *Controlled cortical impact: a new experimental brain injury model.* J Neurotrauma, 1988. **5**(1): p. 1-15.
308. Brody, D.L., et al., *Electromagnetic controlled cortical impact device for precise, graded experimental traumatic brain injury.* J Neurotrauma, 2007. **24**(4): p. 657-73.
309. Chen, Y., et al., *A modified controlled cortical impact technique to model mild traumatic brain injury mechanics in mice.* Front Neurol, 2014. **5**: p. 100.
310. Pleasant, J.M., et al., *Rate of neurodegeneration in the mouse controlled cortical impact model is influenced by impactor tip shape: implications for mechanistic and therapeutic studies.* J Neurotrauma, 2011. **28**(11): p. 2245-62.
311. Mao, H., et al., *Computational neurotrauma--design, simulation, and analysis of controlled cortical impact model.* Biomech Model Mechanobiol, 2010. **9**(6): p. 763-72.
312. Osier, N.D. and C.E. Dixon, *The Controlled Cortical Impact Model: Applications, Considerations for Researchers, and Future Directions.* Front Neurol, 2016. **7**: p. 134.
313. Dixon, C.E., et al., *One-year study of spatial memory performance, brain morphology, and cholinergic markers after moderate controlled cortical impact in rats.* J Neurotrauma, 1999. **16**(2): p. 109-22.
314. Zhou, H., et al., *Moderate traumatic brain injury triggers rapid necrotic death of immature neurons in the hippocampus.* J Neuropathol Exp Neurol, 2012. **71**(4): p. 348-59.
315. Gao, X., et al., *Selective death of newborn neurons in hippocampal dentate gyrus following moderate experimental traumatic brain injury.* J Neurosci Res, 2008. **86**(10): p. 2258-70.
316. Lighthall, J.W., H.G. Goshgarian, and C.R. Pinderski, *Characterization of axonal injury produced by controlled cortical impact.* J Neurotrauma, 1990. **7**(2): p. 65-76.
317. d'Avila, J.C., et al., *Microglial activation induced by brain trauma is suppressed by post-injury treatment with a PARP inhibitor.* J Neuroinflammation, 2012. **9**: p. 31.
318. Colicos, M.A., C.E. Dixon, and P.K. Dash, *Delayed, selective neuronal death following experimental cortical impact injury in rats: possible role in memory deficits.* Brain Res, 1996. **739**(1-2): p. 111-9.
319. Chen, S.F., et al., *Salidroside improves behavioral and histological outcomes and reduces apoptosis via PI3K/Akt signaling after experimental traumatic brain injury.* PLoS One, 2012. **7**(9): p. e45763.

320. Acosta, S.A., et al., *Long-term upregulation of inflammation and suppression of cell proliferation in the brain of adult rats exposed to traumatic brain injury using the controlled cortical impact model.* PLoS One, 2013. **8**(1): p. e53376.
321. Mirzayan, M.J., et al., *Modified calcium accumulation after controlled cortical impact under cyclosporin A treatment: a 45Ca autoradiographic study.* Neurol Res, 2008. **30**(5): p. 476-9.
322. Xiong, Y., et al., *Mitochondrial dysfunction and calcium perturbation induced by traumatic brain injury.* J Neurotrauma, 1997. **14**(1): p. 23-34.
323. Dixon, C.E., et al., *A controlled cortical impact model of traumatic brain injury in the rat.* J Neurosci Methods, 1991. **39**(3): p. 253-62.
324. Smith, D.H., et al., *A model of parasagittal controlled cortical impact in the mouse: cognitive and histopathologic effects.* J Neurotrauma, 1995. **12**(2): p. 169-78.
325. Manley, G.T., et al., *Controlled cortical impact in swine: pathophysiology and biomechanics.* J Neurotrauma, 2006. **23**(2): p. 128-39.
326. King, C., et al., *Brain temperature profiles during epidural cooling with the ChillerPad in a monkey model of traumatic brain injury.* J Neurotrauma, 2010. **27**(10): p. 1895-903.
327. Hall, E.D., T.R. Gibson, and K.M. Pavel, *Lack of a gender difference in post-traumatic neurodegeneration in the mouse controlled cortical impact injury model.* J Neurotrauma, 2005. **22**(6): p. 669-79.
328. Jullienne, A., et al., *Male and Female Mice Exhibit Divergent Responses of the Cortical Vasculature to Traumatic Brain Injury.* J Neurotrauma, 2018. **35**(14): p. 1646-1658.
329. Lee, V.M., T.K. Kenyon, and J.Q. Trojanowski, *Transgenic animal models of tauopathies.* Biochim Biophys Acta, 2005. **1739**(2-3): p. 251-9.
330. Ramsden, M., et al., *Age-dependent neurofibrillary tangle formation, neuron loss, and memory impairment in a mouse model of human tauopathy (P301L).* J Neurosci, 2005. **25**(46): p. 10637-47.
331. Alzheimer's, A., *2014 Alzheimer's disease facts and figures.* Alzheimers Dement, 2014. **10**(2): p. e47-92.
332. Moreno, J.A., et al., *Sustained translational repression by eIF2alpha-P mediates prion neurodegeneration.* Nature, 2012. **485**(7399): p. 507-11.
333. Harding, H.P., Y. Zhang, and D. Ron, *Protein translation and folding are coupled by an endoplasmic-reticulum-resident kinase.* Nature, 1999. **397**(6716): p. 271-4.
334. Abisambra, J.F., et al., *Tau accumulation activates the unfolded protein response by impairing endoplasmic reticulum-associated degradation.* J Neurosci, 2013. **33**(22): p. 9498-507.
335. Ash, P.E., et al., *Pathological stress granules in Alzheimer's disease.* Brain Res, 2014. **1584**: p. 52-8.
336. Vanderweyde, T., et al., *Contrasting pathology of the stress granule proteins TIA-1 and G3BP in tauopathies.* J Neurosci, 2012. **32**(24): p. 8270-83.
337. Duvarci, S., K. Nader, and J.E. LeDoux, *De novo mRNA synthesis is required for both consolidation and reconsolidation of fear memories in the amygdala.* Learn Mem, 2008. **15**(10): p. 747-55.

338. Piao, Y.S., et al., *Cerebellar cortical tau pathology in progressive supranuclear palsy and corticobasal degeneration.* Acta Neuropathol, 2002. **103**(5): p. 469-74.
339. Meier, S.E., et al., *Identification of novel tau interactions with endoplasmic reticulum proteins in Alzheimer's brain.* Journal of Alzheimer's Disease, 2015. **XXX**(XXX): p. XXX.
340. Zhai, J., et al., *Proteomic characterization of lipid raft proteins in amyotrophic lateral sclerosis mouse spinal cord.* FEBS J, 2009. **276**(12): p. 3308-23.
341. Dhar, S.K., et al., *FUsed in sarcoma is a novel regulator of manganese superoxide dismutase gene transcription.* Antioxid Redox Signal, 2014. **20**(10): p. 1550-66.
342. Schmidt, E.K., et al., *SUnSET, a nonradioactive method to monitor protein synthesis.* Nat Methods, 2009. **6**(4): p. 275-7.
343. Greenberg, S.G., et al., *Hydrofluoric acid-treated tau PHF proteins display the same biochemical properties as normal tau.* J Biol Chem, 1992. **267**(1): p. 564-9.
344. Rosso, S.M., et al., *Frontotemporal dementia in The Netherlands: patient characteristics and prevalence estimates from a population-based study.* Brain, 2003. **126**(Pt 9): p. 2016-22.
345. Nelson, P.T., L. Marton, and C.B. Saper, *Alz-50 immunohistochemistry in the normal sheep striatum: a light and electron microscope study.* Brain Res, 1993. **600**(2): p. 285-97.
346. von Jagow, R., H. Kampffmeyer, and M. Kiese, *The preparation of microsomes.* Naunyn Schmiedebergs Arch Exp Pathol Pharmakol, 1965. **251**(1): p. 73-87.
347. Alberts, B.J., Alexander ; Lewis, Julian ; Raff, Martin ; Roberts, Keith ; Walter, Peter, *Molecular Biology of the Cell, 4th Edition - The Endoplasmic Reticulum*. 2002: Garland Science.
348. Kalies, K.U., D. Gorlich, and T.A. Rapoport, *Binding of ribosomes to the rough endoplasmic reticulum mediated by the Sec61p-complex.* J Cell Biol, 1994. **126**(4): p. 925-34.
349. Potter, M.D. and C.V. Nicchitta, *Endoplasmic reticulum-bound ribosomes reside in stable association with the translocon following termination of protein synthesis.* J Biol Chem, 2002. **277**(26): p. 23314-20.
350. Zhang, C.C., et al., *The Role of MAPT in Neurodegenerative Diseases: Genetics, Mechanisms and Therapy.* Mol Neurobiol, 2015.
351. Momeni, P., et al., *Clinical and pathological features of an Alzheimer's disease patient with the MAPT Delta K280 mutation.* Neurobiol Aging, 2009. **30**(3): p. 388-93.
352. Rizzu, P., et al., *High prevalence of mutations in the microtubule-associated protein tau in a population study of frontotemporal dementia in the Netherlands.* Am J Hum Genet, 1999. **64**(2): p. 414-21.
353. Barghorn, S., et al., *Structure, microtubule interactions, and paired helical filament aggregation by tau mutants of frontotemporal dementias.* Biochemistry, 2000. **39**(38): p. 11714-21.
354. Marciniak, S.J., et al., *Activation-dependent substrate recruitment by the eukaryotic translation initiation factor 2 kinase PERK.* J Cell Biol, 2006. **172**(2): p. 201-9.

355. Prevention, C.f.D.C.a., *Surveillance Report of Traumatic Brain Injury-related Emergency Department Visits, Hospitalizations, and Deaths—United States, 2014*. 2019, Centers for Disease Control and Prevention, U.S. Department of Health and Human Services.
356. Takahashi, K., C.D. Rochford, and H. Neumann, *Clearance of apoptotic neurons without inflammation by microglial triggering receptor expressed on myeloid cells-2.* J Exp Med, 2005. **201**(4): p. 647-57.
357. Hamerman, J.A., et al., *Cutting edge: inhibition of TLR and FcR responses in macrophages by triggering receptor expressed on myeloid cells (TREM)-2 and DAP12.* J Immunol, 2006. **177**(4): p. 2051-5.
358. Abisambra, J.F. and S. Scheff, *Brain injury in the context of tauopathies.* J Alzheimers Dis, 2014. **40**(3): p. 495-518.
359. Castellani, R.J. and G. Perry, *Tau Biology, Tauopathy, Traumatic Brain Injury, and Diagnostic Challenges.* J Alzheimers Dis, 2019. **67**(2): p. 447-467.
360. von Bergen, M., et al., *Mutations of tau protein in frontotemporal dementia promote aggregation of paired helical filaments by enhancing local beta-structure.* J Biol Chem, 2001. **276**(51): p. 48165-74.
361. Yue, M., et al., *Sex difference in pathology and memory decline in rTg4510 mouse model of tauopathy.* Neurobiol Aging, 2011. **32**(4): p. 590-603.
362. Madathil, S.K., et al., *Astrocyte-Specific Overexpression of Insulin-Like Growth Factor-1 Protects Hippocampal Neurons and Reduces Behavioral Deficits following Traumatic Brain Injury in Mice.* PLoS One, 2013. **8**(6): p. e67204.
363. Prevention, C.f.D.C.a., *Report to Congress on Traumatic Brain Injury in the United States: Epidemiology and Rehabilitation.* . 2015: National Center for Injury Prevention and Control; Division of Unintentional Injury Prevention. Atlanta, GA.
364. Braak, H. and E. Braak, *Frequency of stages of Alzheimer-related lesions in different age categories.* Neurobiol Aging, 1997. **18**(4): p. 351-7.
365. Tran, H.T., L. Sanchez, and D.L. Brody, *Inhibition of JNK by a peptide inhibitor reduces traumatic brain injury-induced tauopathy in transgenic mice.* J Neuropathol Exp Neurol, 2012. **71**(2): p. 116-29.
366. McKee, A.C., et al., *Chronic traumatic encephalopathy in athletes: progressive tauopathy after repetitive head injury.* J Neuropathol Exp Neurol, 2009. **68**(7): p. 709-35.
367. Cao, J., et al., *ApoE4-associated phospholipid dysregulation contributes to development of Tau hyper-phosphorylation after traumatic brain injury.* Sci Rep, 2017. **7**(1): p. 11372.
368. Du, X., et al., *Ameliorative Effects of Antioxidants on the Hippocampal Accumulation of Pathologic Tau in a Rat Model of Blast-Induced Traumatic Brain Injury.* Oxid Med Cell Longev, 2016. **2016**: p. 4159357.
369. Gyoneva, S., et al., *Ccr2 deletion dissociates cavity size and tau pathology after mild traumatic brain injury.* J Neuroinflammation, 2015. **12**: p. 228.
370. Hooper, C., R. Killick, and S. Lovestone, *The GSK3 hypothesis of Alzheimer's disease.* J Neurochem, 2008. **104**(6): p. 1433-9.
371. Sperber, B.R., et al., *Glycogen synthase kinase-3 beta phosphorylates tau protein at multiple sites in intact cells.* Neurosci Lett, 1995. **197**(2): p. 149-53.

372. Zhao, S., et al., *Activation of Akt/GSK-3beta/beta-catenin signaling pathway is involved in survival of neurons after traumatic brain injury in rats.* Neurol Res, 2012. **34**(4): p. 400-7.
373. Shultz, S.R., et al., *Sodium selenate reduces hyperphosphorylated tau and improves outcomes after traumatic brain injury.* Brain, 2015. **138**(Pt 5): p. 1297-313.
374. Seo, J.S., et al., *Transcriptome analyses of chronic traumatic encephalopathy show alterations in protein phosphatase expression associated with tauopathy.* Exp Mol Med, 2017. **49**(5): p. e333.
375. Yang, W.J., et al., *Involvement of tau phosphorylation in traumatic brain injury patients.* Acta Neurol Scand, 2017. **135**(6): p. 622-627.
376. Kolarova, M., et al., *Tau Oligomers in Sera of Patients with Alzheimer's Disease and Aged Controls.* J Alzheimers Dis, 2017. **58**(2): p. 471-478.
377. Sokolow, S., et al., *Pre-synaptic C-terminal truncated tau is released from cortical synapses in Alzheimer's disease.* J Neurochem, 2015. **133**(3): p. 368-79.
378. Tracy, T.E., et al., *Acetylated Tau Obstructs KIBRA-Mediated Signaling in Synaptic Plasticity and Promotes Tauopathy-Related Memory Loss.* Neuron, 2016. **90**(2): p. 245-60.
379. Roberson, E.D., et al., *Amyloid-beta/Fyn-induced synaptic, network, and cognitive impairments depend on tau levels in multiple mouse models of Alzheimer's disease.* J Neurosci, 2011. **31**(2): p. 700-11.
380. Ittner, L.M., et al., *Dendritic function of tau mediates amyloid-beta toxicity in Alzheimer's disease mouse models.* Cell, 2010. **142**(3): p. 387-97.
381. Hu, Y., et al., *Tau accumulation impairs mitophagy via increasing mitochondrial membrane potential and reducing mitochondrial Parkin.* Oncotarget, 2016. **7**(14): p. 17356-68.
382. Keck, S., et al., *Proteasome inhibition by paired helical filament-tau in brains of patients with Alzheimer's disease.* J Neurochem, 2003. **85**(1): p. 115-22.
383. Myeku, N., et al., *Tau-driven 26S proteasome impairment and cognitive dysfunction can be prevented early in disease by activating cAMP-PKA signaling.* Nat Med, 2016. **22**(1): p. 46-53.
384. Papasozomenos, S.C., *Tau protein immunoreactivity in dementia of the Alzheimer type: II. Electron microscopy and pathogenetic implications. Effects of fixation on the morphology of the Alzheimer's abnormal filaments.* Lab Invest, 1989. **60**(3): p. 375-89.
385. Nelson, P.T. and C.B. Saper, *Ultrastructure of neurofibrillary tangles in the cerebral cortex of sheep.* Neurobiol Aging, 1995. **16**(3): p. 315-23.
386. Tanemura, K., et al., *Neurodegeneration with tau accumulation in a transgenic mouse expressing V337M human tau.* J Neurosci, 2002. **22**(1): p. 133-41.
387. Takagi, M., et al., *Regulation of p53 translation and induction after DNA damage by ribosomal protein L26 and nucleolin.* Cell, 2005. **123**(1): p. 49-63.
388. Brady, C.A. and L.D. Attardi, *p53 at a glance.* J Cell Sci, 2010. **123**(Pt 15): p. 2527-32.
389. Oka, M., et al., *Ca2+/calmodulin-dependent protein kinase II promotes neurodegeneration caused by tau phosphorylated at Ser262/356 in a transgenic Drosophila model of tauopathy.* J Biochem, 2017. **162**(5): p. 335-342.

390. Yoshimura, Y., T. Ichinose, and T. Yamauchi, *Phosphorylation of tau protein to sites found in Alzheimer's disease brain is catalyzed by Ca2+/calmodulin-dependent protein kinase II as demonstrated tandem mass spectrometry.* Neurosci Lett, 2003. **353**(3): p. 185-8.
391. Atkins, C.M., et al., *Activation of calcium/calmodulin-dependent protein kinases after traumatic brain injury.* J Cereb Blood Flow Metab, 2006. **26**(12): p. 1507-18.
392. Bennecib, M., et al., *Inhibition of PP-2A upregulates CaMKII in rat forebrain and induces hyperphosphorylation of tau at Ser 262/356.* FEBS Lett, 2001. **490**(1-2): p. 15-22.
393. LaFerla, F.M., K.N. Green, and S. Oddo, *Intracellular amyloid-beta in Alzheimer's disease.* Nat Rev Neurosci, 2007. **8**(7): p. 499-509.
394. Blair, J.A., et al., *Accumulation of intraneuronal amyloid-beta is common in normal brain.* Curr Alzheimer Res, 2014. **11**(4): p. 317-24.
395. Billings, L.M., et al., *Intraneuronal Abeta causes the onset of early Alzheimer's disease-related cognitive deficits in transgenic mice.* Neuron, 2005. **45**(5): p. 675-88.
396. Frugier, T., et al., *In situ detection of inflammatory mediators in post mortem human brain tissue after traumatic injury.* J Neurotrauma, 2010. **27**(3): p. 497-507.
397. Stefini, R., et al., *Chemokine detection in the cerebral tissue of patients with posttraumatic brain contusions.* J Neurosurg, 2008. **108**(5): p. 958-62.
398. Yan, E.B., et al., *Post-traumatic hypoxia exacerbates neurological deficit, neuroinflammation and cerebral metabolism in rats with diffuse traumatic brain injury.* J Neuroinflammation, 2011. **8**: p. 147.
399. Mouzon, B.C., et al., *Chronic neuropathological and neurobehavioral changes in a repetitive mild traumatic brain injury model.* Ann Neurol, 2014. **75**(2): p. 241-54.
400. Hopp, S.C., et al., *The role of microglia in processing and spreading of bioactive tau seeds in Alzheimer's disease.* J Neuroinflammation, 2018. **15**(1): p. 269.
401. Perea, J.R., et al., *The Role of Microglia in the Spread of Tau: Relevance for Tauopathies.* Front Cell Neurosci, 2018. **12**: p. 172.
402. Margulies, S.S., L.E. Thibault, and T.A. Gennarelli, *Physical model simulations of brain injury in the primate.* J Biomech, 1990. **23**(8): p. 823-36.
403. Meaney, D.F., B. Morrison, and C. Dale Bass, *The mechanics of traumatic brain injury: a review of what we know and what we need to know for reducing its societal burden.* J Biomech Eng, 2014. **136**(2): p. 021008.
404. Meaney, D.F. and D.H. Smith, *Biomechanics of concussion.* Clin Sports Med, 2011. **30**(1): p. 19-31, vii.
405. Gieling, E.T., et al., *The pig as a model animal for studying cognition and neurobehavioral disorders.* Curr Top Behav Neurosci, 2011. **7**: p. 359-83.
406. Smith, D.H., et al., *Accumulation of amyloid beta and tau and the formation of neurofilament inclusions following diffuse brain injury in the pig.* J Neuropathol Exp Neurol, 1999. **58**(9): p. 982-92.
407. Poorkaj, P., et al., *Frequency of tau gene mutations in familial and sporadic cases of non-Alzheimer dementia.* Arch Neurol, 2001. **58**(3): p. 383-7.

408. Goodwin, L., et al., *Large-scale discovery of mouse transgenic integration sites reveals frequent structural variation and insertional mutagenesis.* bioRxiv, 2017.
409. Gamache, J., et al., *Factors other than hTau overexpression that contribute to tauopathy-like phenotype in rTg4510 mice.* Nat Commun, 2019. **10**(1): p. 2479.
410. Di Re, J., P.A. Wadsworth, and F. Laezza, *Intracellular Fibroblast Growth Factor 14: Emerging Risk Factor for Brain Disorders.* Front Cell Neurosci, 2017. **11**: p. 103.
411. Koren, S.A., et al., *Tau drives translational selectivity by interacting with ribosomal proteins.* Acta Neuropathol, 2019. **137**(4): p. 571-583.
412. Edwards Iii, G.A., et al., *Traumatic brain injury induces tau aggregation and spreading.* J Neurotrauma, 2019.
413. Bird, S.M., et al., *Cerebral amyloid-beta accumulation and deposition following traumatic brain injury--A narrative review and meta-analysis of animal studies.* Neurosci Biobehav Rev, 2016. **64**: p. 215-28.
414. Stein, T.D., et al., *Beta-amyloid deposition in chronic traumatic encephalopathy.* Acta Neuropathol, 2015. **130**(1): p. 21-34.
415. Stancu, I.C., et al., *Models of beta-amyloid induced Tau-pathology: the long and "folded" road to understand the mechanism.* Mol Neurodegener, 2014. **9**: p. 51.
416. Abu Hamdeh, S., et al., *Proteomic differences between focal and diffuse traumatic brain injury in human brain tissue.* Sci Rep, 2018. **8**(1): p. 6807.
417. Chou, A., et al., *Inhibition of the integrated stress response reverses cognitive deficits after traumatic brain injury.* Proc Natl Acad Sci U S A, 2017. **114**(31): p. E6420-E6426.
418. Chen, S., et al., *Alterations in mammalian target of rapamycin signaling pathways after traumatic brain injury.* J Cereb Blood Flow Metab, 2007. **27**(5): p. 939-49.
419. Tucker, K.L., M. Meyer, and Y.A. Barde, *Neurotrophins are required for nerve growth during development.* Nat Neurosci, 2001. **4**(1): p. 29-37.
420. Zanier, E.R., et al., *Induction of a transmissible tau pathology by traumatic brain injury.* Brain, 2018. **141**(9): p. 2685-2699.
421. Woerman, A.L., et al., *Tau prions from Alzheimer's disease and chronic traumatic encephalopathy patients propagate in cultured cells.* Proc Natl Acad Sci U S A, 2016. **113**(50): p. E8187-E8196.
422. Hall, E.D., et al., *Spatial and temporal characteristics of neurodegeneration after controlled cortical impact in mice: more than a focal brain injury.* J Neurotrauma, 2005. **22**(2): p. 252-65.
423. Guo, J.L., et al., *Unique pathological tau conformers from Alzheimer's brains transmit tau pathology in nontransgenic mice.* J Exp Med, 2016. **213**(12): p. 2635-2654.
424. Goedert, M., D.S. Eisenberg, and R.A. Crowther, *Propagation of Tau Aggregates and Neurodegeneration.* Annu Rev Neurosci, 2017. **40**: p. 189-210.

VITA

Shelby Meier

I. EDUCATIONAL INSTITUTIONS

2011-2019 **University of Kentucky**
Bachelor of Science – Biology, with Honors
GPA: 3.505
Graduation: May 9, 2015
Doctor of Philosophy – Physiology
GPA (current): 3.432
Advisors: Joe Abisambra, PhD and Kathryn Saatman, PhD
Anticipated Graduation Date: August 2019

2019- **Vanderbilt University**
Post-doctoral Research Fellow

II. AWARDS

2014 UK Undergraduate Summer Research Grant
2015 Alzheimer's Association International Conference Travel Fellowship Award
2016 Alzheimer's Association International Conference 2016 Student Volunteer
2016 Alzheimer's Association International Conference Student Poster Competition Winner
2016 Department of Physiology Annual Retreat – Best Graduate Student Poster Presentation (tied for first)
2017 Alzheimer's Association International Conference Travel Fellowship Award
2017 College of Medicine Fellowship for Excellence in Graduate Research (1year, $12,500)
2017 Department of Physiology Hardin Award – one per year, given to staff or trainee that exhibits dedication and enthusiasm for their work
2018-2019 NIH T32 AG057461 "Training in Translational Research in Alzheimer's and Related Dementias (TRIAD)" – 2-year award

III. RESEARCH AND INTELLECTUAL CONTRIBUTIONS

A. Publications

1. Koren SA, Hamm MJ, **Meier SE**, Weiss BE, Nation GK, Chishti EA, Arango JP, Chen J, Zhu H, Blalock EM, Abisambra JF. *"Tau drives translational selectivity by interacting with ribosomal proteins."* (2019) Acta Neuropathol
2. Lourenco MV, Frozza RL, de Freitas GB, Zhang H, Kincheski GC, Ribeiro FC, Gonçalves RA, Clarke JR, Beckman D, Staniszewski A, Berman H, Guerra LA, Forny-Germano L, **Meier S**, Wilcock DM, de Souza JM, Alves-Leon S, Prado VF, Prado MAM, Abisambra JF, Tovar-Moll F, Mattos P, Arancio O, Ferreira ST, De Felice FG. "*Exercise-linked FNDC5/irisin rescues synaptic plasticity and memory defects in Alzheimer's models."* (2019) Nat Med
3. Gusareva ES, Twizere JC, Sleegers K, Dourlen P, Abisambra JF, **Meier S**, Cloyd R, Weiss B, Dermaut B, Bessonov K, van der Lee SJ, Carrasquillo MM, Katsumata Y, Cherkaoui M, Asselbergh B, Ikram MA, Mayeux R, Farrer LA, Haines JL, Pericak-Vance MA, Schellenberg GD; Genetic and Environmental Risk in Alzheimer's Disease 1 consortium (GERAD1).; Alzheimer's Disease Genetics Consortium (ADGC).; European Alzheimer Disease Initiative Investigators (EADI1 Consortium)., Sims R, Williams J, Amouyel P, van Duijn CM, Ertekin-Taner N, Van Broeckhoven C, Dequiedt F, Fardo DW, Lambert JC, Van Steen K. "*Male-specific epistasis between WWC1 and TLN2 genes is associated with Alzheimer's disease."* (2018) Neurobiol Aging
4. **Meier S,** Gilad AA, Brandon JA, Qian C, Gao E, Abisambra JF, Vandsburger M. "*Non-invasive detection of adeno-associated viral gene transfer using a genetically encoded CEST-MRI reporter gene in the murine heart."* (2018) Sci Rep
5. Lanzillotta C, Tramutola A, **Meier S**, Schmitt F, Barone E, Perluigi M, Di Domenico F, Abisambra JF. *"Early and Selective Activation and Subsequent Alterations to the Unfolded Protein Response in Down Syndrome Mouse Models*." (2018) J Alzheimers Dis.
6. Fontaine SN, Ingram A, Cloyd RA, **Meier SE**, Miller E, Lyons D, Nation GK, Mechas E, Weiss B, Lanzillotta C, Di Domenico F, Schmitt F, Powell DK, Vandsburger M, Abisambra JF. *"Identification of changes in neuronal function as a consequence of aging and tauopathic neurodegeneration using a novel and sensitive magnetic resonance imaging approach*." (2017) Neurobiol Aging.
7. Bachstetter AD, Zhou Z, Rowe RK, Xing B, Goulding DS, Conley AN, Sompol P, **Meier S**, Abisambra JF, Lifshitz J, et al. (2016) "*MW151 Inhibited IL-1β Levels after Traumatic Brain Injury with No Effect on Microglia Physiological Responses*." (2016) PLoS One.
8. **Meier S**, Bell M, Lyons DN, Rodriguez-Rivera J, Ingram A, Fontaine SN, Mechas E, Chen J, Wolozin B, LeVine H, Zhu H, Abisambra JF. *"Pathological tau promotes neuronal damage by impairing ribosomal function and decreasing protein synthesis"* (2016) J Neurosci
9. Bell MC, **Meier SE,** Ingram AL, Abisambra JF. *"PERK-opathies: An Endoplasmic Stress mechanism underlying neurodegeneration"* (2016) Curr Alzheimer Res

10. **Meier S**, Bell M, Lyons DN, Ingram A, Chen J, Gensel JC, Levine H, Zhu H, Nelson P, Kayed R, and Abisambra JF (2015). *"Identification of novel tau interactions with endoplasmic reticulum proteins in Alzheimer's disease brain."* (2015) J Alzheimers Dis

B. Local, National, and International Symposia

2018 **Society for Neuroscience**
Author, *poster*: "Pathological tau shifts translation by modifying rpS6 and 5' TOP RNA protein synthesis"
Author, *oral presentation:* "PERK-Tau coupling causes biphasic consequences to tau pathology and neuronal function *in vitro* and *in vivo*"

2018 **Markesbery Symposium on Aging and Dementia**
Presenting author, *poster:* "Temporal and anatomical effects on tangle count in rTg4510 mice after TBI"

2017 **Markesbery Symposium on Aging and Dementia**
Presenting author, *poster*: "Post-injury PERK inhibition reduces astrocyte reactivity without reducing tissue loss."

2017 **Alzheimer's Association International Conference**
Presenting author, *poster*: "Post-injury PERK inhibition in mouse model of tauopathy"
Author, *poster*: "Novel applications of MRI techniques in the detection of neuronal dysfunction before tangle pathology in rTg4510 mice."

2017 **International Conference on Alzheimer's and Parkinson's Diseases**
Author, *poster*: "PERK inhibition in CCI Model of Traumatic Brain Injury"
Author, *short oral presentation*: "PERK inhibition in CCI Model of Traumatic Brain Injury"
Author, *short oral presentation*: "Association of pathological tau with ribosomal complex impairs protein synthesis"
Author, *short oral presentation:* "Association of pathological tau with ribosomal complex impairs protein synthesis"

2017 **Midwest Stress Response and Molecular Chaperone Meeting**
Presenting author, *poster*: "Characterization of PERK activation following traumatic brain injury by controlled cortical impact"

2016 **Department of Physiology Annual Retreat**
Presenting author, *poster*: ""PERK inhibition in tau transgenic model improves neuronal function in an eIF2α-independent manner"
Presenting author, *data blitz*: "Pathological tau promotes neuronal damage by impairing ribosomal function and decreasing protein synthesis"

2016 **Kentucky Neuroscience Institute Clinical-Translational Research Symposium**
Presenting author, *oral presentation*: "PERK inhibition in rTg4510 mouse model of tauopathy"

2016 **Cold Spring Harbor: Protein Homeostasis in Health and Disease**

Presenting author, *poster*: "PERK inhibition in tau transgenic mouse model improves neuronal function in an eIF2α-independent manner"
Author, *poster*: "Association of pathological tau with ribosomal subunit impairs protein synthesis"

2016 **Alzheimer's Association International Conference**
Presenting author, *poster:* "PERK inhibition in Controlled Cortical Impact Model of Traumatic Brain Injury"
Presenting author, *oral presentation*: "Pathological tau impairs ribosomal function and decreases protein synthesis"

2016 **National Neurotrauma Society National Conference**
Presenting author, *poster:* "Activation of PERK in Controlled Cortical Impact Model of Traumatic Brain Injury"

2016 **Midwest Stress Response and Molecular Chaperone Meeting**
Presenting author, *oral presentation:* "PERK inhibition reduces phosphorylated tau and rescues neuronal function in an eIF2α-independent mechanism"

2015 **Alzheimer's Association International Conference**
Presenting author, *poster*: "Association of pathological tau with the ribosomal complex impairs protein synthesis"

2014 **Alzheimer's Association International Conference**
Author, *poster*: "Identification of novel tau interactions with endoplasmic reticulum proteins in Alzheimer's disease brain"

2014 **National Conference of Undergraduate Research**
Presenting author, *poster*: "PERK-opathies: An Endoplasmic Reticulum Stress Mechanism Underlying Neurodegeneration"

C. Community Outreach

2016 **Neuroscience Night at Lexington Explorium**
Presented information to elementary aged children and their parents about how people hear things.

2016 **Madison Central High School Neuroscience Day**
Presented information to high school biology students about traumatic brain injury, as well as teaching them about the human brain using donated human brain samples.

2017 **Madison Central High School Neuroscience Day**
Invited back to present information to high school biology students about traumatic brain injury, as well as teaching them about the human brain using donated human brain samples.

2017 **University of Kentucky Biology Department Biobonanza**
Organized and recruited volunteers to help present information on Alzheimer's disease and the Sanders-Brown Center on Aging to the Lexington community. Organized and planned memory related activities to tie in the links between memory loss and Alzheimer's disease. Prepared information for adults and children on the disease and what our research focuses on.

2017 **University of Kentucky GEMS**
GEMS is a University of Kentucky and Girl Scouts of America sponsored event allowing girls of all ages to have hands on experience with scientific experiments and careers. Co-organized a session with fellow graduate student Laura Peterson on the Neuromuscular junction for elementary and high school aged girls.

2018 **Madison Central High School Neuroscience Day**
Invited back to present information to high school biology students about traumatic brain injury, as well as teaching them about the human brain using donated human brain samples.